



RESEARCH & DEVELOPMENT

Assessment of Deteriorated Cored Slabs Bridges No.: 150035 and 150039

**Zachary Van Brunt, EIT
Rudolf Seracino, PhD
Gregory Lucier, PhD
Mohammad Pour-Ghaz, PhD**

**Department of Civil, Construction, and Environmental
Engineering
North Carolina State University**

**FHWA/NC/2014-35
February 2016**

FHWA/NC/2014-35

**Assessment of Deteriorated Cored Slabs
Bridges No.: 150035 and 150039**

Research Assistant	Mr. Zachary Van Brunt
Principal Investigator	Dr. Rudolf Seracino
Key Researcher	Dr. Gregory Lucier
Key Researcher	Dr. Mohammad Pour-Ghaz

**Department of Civil, Construction, and Environmental Engineering
North Carolina State University
Raleigh, NC**

Prepared for:
North Carolina Department of Transportation
Research and Development Unit

February, 2016

Technical Report Documentation Page

1. Report No. FHWA/NC/2014-35	2. Government Accession No.	3. Recipient's Catalog No.	
4. Title and Subtitle Assessment of Deteriorated Cored Slabs Bridges No.: 150035 and 150039		5. Report Date February, 2016	
		6. Performing Organization Code	
7. Author(s) Zachary Van Brunt, Rudolf Seracino, Gregory Lucier, Mohammad Pour-Ghaz		8. Performing Organization Report No.	
9. Performing Organization Name and Address North Carolina State University Department of Civil, Construction, and Environmental Engineering Raleigh, NC 27695-7908		10. Work Unit No. (TRAIS)	
		11. Contract or Grant No.	
12. Sponsoring Agency Name and Address North Carolina Department of Transportation Research and Development Unit 104 Fayetteville Street Raleigh, NC 27601		13. Type of Report and Period Covered Draft Report August, 2013 – May, 2015	
		14. Sponsoring Agency Code NCDOT Project No.: 2014-35	
Supplementary Notes:			
16. Abstract <p>Prestressed cored slabs have been used in North Carolina since 1969 for bridges with span lengths of 40 ft to 70 ft. Cored slabs in coastal regions are showing signs of extensive corrosion of reinforcing steel after less than 40 years in service. Extensive patching, rust stains, and widely varying visual conditions has led to uncertainty in how to accurately load rate these prestressed cored slabs. In order to develop guidelines to accurately assess their flexural strength, an experimental program was implemented including field inspection of cored slabs on two in-service coastal bridges, followed by selection of 12 slabs and their transportation to the NCSU Constructed Facilities Laboratory for non-destructive testing and flexural testing to failure.</p> <p>Field inspection included recording the visual condition of the slabs, sounding for delamination, and concrete resistivity testing. Laboratory testing included obtaining concrete cores and samples of prestressing strands, more detailed concrete resistivity testing, half-cell potential testing, and finally flexural testing to failure and demolition of the slabs to examine the extent of corrosion.</p> <p>Test results were used to develop recommendations and guidelines for uniformly interpreting slab conditions based on their visual condition, sounding for regions of delaminated concrete and patching, and records of the depth of spalling. The depth of spalling and presence of longitudinal rust stains were found to be key indicators of corrosion of prestressing strands. Corrosion was limited to the bottom layer of prestressing strands in most slabs, and strands were observed to generally corrode in groups of adjacent strands. The presence of spalling alone does not necessarily indicate loss of strands, nor does the area of a slab that is spalled. Due to the severe and extensive corrosion, concrete resistivity and half-cell potential testing did not seem to provide additional information to the visual inspection.</p>			
17. Key Words Cored Slabs, Corrosion, Prestressed, Bridge Inspection, Load Rating, Resistivity, Half-cell Potential		18. Distribution Statement	
19. Security Classif. (of this report) Unclassified	20. Security Classif. (of this page) Unclassified	21. No. of Pages 233	22. Price

DISCLAIMER

The contents of this report reflect the views of the authors and not necessarily the views of the University. The authors are responsible for the facts and the accuracy of the data presented herein. The contents do not necessarily reflect the official views or policies of either the North Carolina Department of Transportation or the Federal Highway Administration at the time of publication. This report does not constitute a standard, specification, or regulation.

ACKNOWLEDGEMENTS

In addition to the funding provided by the NCDOT to enable this project, the assistance and logistical support provided by many personnel is acknowledged. Griffith Shapack and undergraduate research assistant Steven Thornton provided extensive assistance in the laboratory and in the field. Technicians Johnathan McEntire and Jerry Atkinson at the Constructed Facilities Laboratory were instrumental in supporting the laboratory testing. Tom Barton and the people at Smith-Rowe Contracting were flexible and accommodating in their assistance with transporting and handling the cored slabs.

EXECUTIVE SUMMARY

Prestressed cored slabs have been in use in North Carolina since 1969 for bridges with spans of 40 ft to 70 ft. Slabs on certain bridges in coastal regions are beginning to show substantial spalling and rusting of rebar stirrups and longitudinal prestressing strands, potentially decreasing the strength and service life of the bridges. Some of these bridges, including the two bridges in Carteret County (opened in 1977) that were the specific focus of this research project, have been in service for fewer than 40 years. Extensive patching, rust stains, and widely varying visual conditions has led to uncertainty in how to accurately load rate these prestressed cored slabs. This research gives guidance on methods to effectively examine and analyze their condition.

Research included field inspection of the two bridges by visual inspection, sounding for delaminations with a hammer, and testing for resistivity of concrete using a commercially available resistivity meter. Twelve slabs in varying states of deterioration were then selected to be transported to the laboratory, where half-cell potential tests were performed, along with material tests of strands and concrete cores, and full-scale flexural testing to obtain residual moment capacity of the slabs.

Results of the research suggest several conclusions. Concrete strength, measured in undeteriorated regions of the slab, was higher than the assumed value of 5000 psi, with average compressive strength of 7130 psi, and undamaged prestressing strands retained ductility and

strength, rupturing at 5% strain and 285 ksi, respectively. Half-Cell Potential and Resistivity testing did not provide consistently useful information in a way that added value to the inspection and evaluation process for the prestressed cored slabs, and are not recommended for that use at this time. Visual inspection and sounding for delamination, if analyzed and recorded correctly, can provide sufficient information for estimating the extent of corrosion of prestressing strands, and this data was used to predict the flexural capacity of the 12 slabs tested. Predictions using this data did not perform consistently in regions of delaminated concrete, and delaminated regions were not found to be accurately assessed without removal of the delamination. Analysis procedures were developed to make consistent evaluations when three key observations are made during inspections: the location of spalling, the depth of spalling, and the location and orientation of visible rust stains. Depth of spalling was found to be a particularly important indicator for loss of prestressing strands due to corrosion. Final recommendations are made on how to use this information to make assumptions about loss of strands, so that existing NCDOT load rating programs can be used.

TABLE OF CONTENTS

DISCLAIMER.....	i
ACKNOWLEDGEMENTS	ii
EXECUTIVE SUMMARY	iii
TABLE OF CONTENTS	v
LIST OF FIGURES	viii
LIST OF TABLES	xii
CHAPTER 1 – INTRODUCTION	1
1.1 – Introduction.....	1
1.2 – Historical Background	1
1.3 – Research Purpose and Scope	4
1.4 – Bridge Numbering and Deterioration Vocabulary.....	5
1.4.1 - <i>Numbering</i>	5
1.4.2 – <i>Deterioration Vocabulary</i>	6
1.5 – Layout of Report	7
CHAPTER 2 – LITERATURE REVIEW	8
2.1 – Introduction.....	8
2.2 – Ward Creek and Oyster Creek bridges	8
2.2.1 – <i>Construction Plans</i>	8
2.2.2 – <i>Inspection Reports</i>	10
2.3 – Non-Destructive Evaluation Techniques	16
2.3.1 – <i>Half-Cell Potential Test</i>	16
2.3.2 – <i>Concrete Resistivity Test</i>	19
2.4 – Testing and Evaluation of In-Service Prestressed Girders	22
2.5 – General Bridge Deterioration.....	25
2.6 – Summary of Research Needs	25
CHAPTER 3 – EXPERIMENTAL PROGRAM	27
3.1 – Introduction.....	27
3.2 – Field Inspection.....	27
3.2.1 – <i>Marking Slabs</i>	28
3.2.2 – <i>Logistics of Inspection Trips</i>	29
3.2.3 – <i>Photographing</i>	30
3.2.4 – <i>Sounding</i>	31
3.2.5 – <i>Resistivity</i>	33
3.2.6 – <i>Selection of Slabs for Laboratory Testing</i>	35
3.2.7 – <i>Additional Observations from Field Inspection</i>	37
3.3 – Demolition and Transportation	39
3.4 – Laboratory Testing – Non-Destructive Testing	40

3.4.1 – Preparation of Slabs	40
3.4.2 – Resistivity	42
3.4.3 – Half-Cell Potential.....	43
3.5 – Laboratory Testing – Flexural Testing	44
3.5.1 – 40 ft Slab Setup (Ward Creek Bridge)	45
3.5.2 – 45 ft Slab Setup (Oyster Creek Bridge).....	49
3.5.3 – Instrumentation	52
3.6 – Post-Test Demolition and Inspection	55
3.7 – Materials Testing	56
CHAPTER 4 – RESULTS.....	60
4.1 – Field Data	60
4.1.1 – Photography and Visual Observation.....	60
4.1.2 – Sounding	63
4.1.3 – Resistivity	63
4.2 – Laboratory Data	67
4.2.1 – Resistivity	67
4.2.2 – Half-Cell Potential.....	67
4.2.3 – Moment-Deflection	69
4.2.4 – Strain Data.....	71
4.2.5 – Strand Slip.....	72
4.2.6 – Concrete Cores in Compression	72
4.2.7 – Prestressing Strands in Tension.....	74
4.2.8 – Condition of strands at failed region.....	74
4.3 – Slab Results.....	75
4.3.1 – Ward Creek – Span 1 – Slab 13	76
4.3.2 – Ward Creek – Span 1 – Slab 14.....	81
4.3.3 – Ward Creek – Span 4 – Slab 5.....	85
4.3.4 – Ward Creek – Span 4 – Slab 6.....	89
4.3.5 – Ward Creek – Span 9 – Slab 6.....	93
4.3.6 – Ward Creek – Span 9 – Slab 7	96
4.3.7 – Oyster Creek – Span 1 – Slab 13	101
4.3.8 – Oyster Creek – Span 1 – Slab 14	104
4.3.9 – Oyster Creek – Span 2 – Slab 4	109
4.3.10 – Oyster Creek – Span 2 – Slab 5	112
4.3.11 – Oyster Creek – Span 8 – Slab 12	115
4.3.12 – Oyster Creek – Span 8 – Slab 13	119
CHAPTER 5 – ANALYSIS AND DISCUSSION.....	123
5.1 – General Analysis of Field Observations	123
5.2 – Resistivity and Half-Cell Potential	126
5.2.1 - Resistivity.....	126
5.2.2 – Half-Cell Potential.....	137
5.3 – Structural Analysis to Predict Flexural Response.....	143
5.3.1 – Stress Block Analysis	144
5.3.2 – Layered Sectional Analysis	148

5.4 – Visual Inspection and Sounding	165
5.4.1 – <i>Delaminations</i>	166
5.4.2 – <i>Patched Regions</i>	170
5.4.3 – <i>Analysis Strategies</i>	171
5.4.4 – <i>Discussion of Analysis Strategies</i>	184
5.5 – Observations Not Found to Affect Strength	186
5.5.1 – <i>Red marks on slab soffit</i>	187
5.5.2 – <i>Cracking of Slab Ends</i>	187
5.5.3 – <i>Shear Capacity</i>	188
5.5.4 – <i>Relationships from Literature Review</i>	189
CHAPTER 6 – FINDINGS AND CONCLUSIONS	191
6.1 – Flexural Capacity of Slabs	191
6.2 – Shear Capacity of Slabs	193
6.3 – Load Rating of Slabs.....	193
CHAPTER 7 – RECOMMENDATIONS	194
7.1 – Recommendations for Load Rating Procedures	194
7.1.1 – <i>“Depth of Spall” Strategy</i>	194
7.1.2 – <i>Additional Load Rating Recommendations</i>	196
7.2 – Recommendations for Field Inspection	198
CITED REFERENCES	200
APPENDICES	204
Appendix A – Inspection Report Slab Conditions	205

LIST OF FIGURES

Figure 1.1 - Cored Slab Cross-Sections	2
Figure 1.2 – Severe rust stains on patched slab soffit, Ward Creek Bridge	3
Figure 1.3 - Location of bridges discussed, Carteret County (<i>Maps from USGS, US Census Bureau</i>)	3
Figure 1.4 - Numbering scheme, Ward Creek and Oyster Creek Bridges.....	5
Figure 2.1 - Plan and Elevation Sections from Ward Creek Bridge plans	9
Figure 2.2 - Slab conditions per 2013 report	10
Figure 2.3 - 1997: "Delaminated and/or spalled with rusty exposed steel"	13
Figure 2.4 - 2003: "[...]were delaminated and/or spalled with rusting rebars exposed but are [...] repaired"	13
Figure 2.5 - 2005: "Slabs 6 and 7 are delaminated"	14
Figure 2.6 - 2009: (Description in photograph)	14
Figure 2.7 - 2011: (Description in photograph)	15
Figure 2.8 - 2013: "Delamination at previous patch with heavy longitudinal and transverse rust"	15
Figure 2.9 - Diagram of half-cell potential test (ASTM C876, 2009)	17
Figure 2.10 - Resistivity probe diagram (Proceq SA, 2013).....	20
Figure 2.11 - Strands assumed deteriorated, PennDOT Report on AASHTO Box Beams (Hartle, 2008)	23
Figure 3.1 – Spray-painted orange dots for marking of slabs.....	29
Figure 3.2 - Bipod for photographing slabs	30
Figure 3.3 - Typical photograph with bipod	31
Figure 3.4 - Sounding with hammer	32
Figure 3.5 - Resistivity meter in use in the field.....	33
Figure 3.6 - Varying moisture on slab soffits, Ward Creek Bridge – Span 1	34
Figure 3.7 – Asphaltic overlay thickness near roadway centerline	37
Figure 3.8 - Transverse post-tensioning strand.....	38
Figure 3.9 - Depth of spalling, Ward Creek – Span 1 – Slab 9	38
Figure 3.10 - Slab removal rig	39
Figure 3.11 - Slabs arriving at CFL from Ward Creek – Span 9	40
Figure 3.12 – 1 ft intervals marked on side of slab.....	41
Figure 3.13 - Marking slab soffit	41
Figure 3.14 - Measurement locations for laboratory NDE	42
Figure 3.15 - Half-cell potential testing – electrode and software (Giatec Scientific)	44
Figure 3.16 – 40 ft slab flexural test setup.....	46
Figure 3.17 – Schematic of 40 ft slab flexural test setup.....	47
Figure 3.18 – Supports: pin (left), roller (right).....	48
Figure 3.19 – Loading at third points via four 25-kip hydraulic jacks with 10" stroke.....	48
Figure 3.20 - 45-ft slab flexural test setup	49
Figure 3.21 – Schematic of 45 ft slab flexural test setup.....	50

Figure 3.22 – Supports	51
Figure 3.23 - Loading via 220-kip 40 in. stroke actuator with spreader beam	51
Figure 3.24 – 50 kip load cell	53
Figure 3.25 – 50 in. string potentiometers at midspan.....	53
Figure 3.26 - Linear potentiometers at slab end	54
Figure 3.27 - Pi gauges at midspan (top and bottom)	54
Figure 3.28 – Post-test demolition in laboratory (Oyster Creek – Span 8 – Slab 12)	55
Figure 3.29 - Strands uncovered with jackhammer outside laboratory (Ward Creek – Span 1 – Slab 14)	56
Figure 3.30 - Coring slab end (Ward Creek – Span 9 – Slab 6)	57
Figure 3.31 - Testing core in compression.....	57
Figure 3.32 – Strands exposed near slab end via jackhammer	58
Figure 3.33 - Tension test of prestressing strand	59
Figure 3.34 - Strand failure.....	59
Figure 4.1 - Area surrounding Oyster Creek - Span 8 - Slab 11.....	61
Figure 4.2 - Oyster Creek - Span 8 - Slab 11 at 26 ft, before (left) and after (right) removal of icolastic patch.....	61
Figure 4.3 – Left 3 strands, not visible in Figure 4.2.....	61
Figure 4.4 - Deterioration of slabs above retaining wall blocks	62
Figure 4.5 - Wetting of slabs above retaining wall blocks	62
Figure 4.6 - Presentation of sounding data	63
Figure 4.7 - Color scale, resistivity plots	66
Figure 4.8 - Color scale, Half-Cell Potential plots.....	68
Figure 4.9 - Concrete core from Ward Creek – Span 1 – Slab 13	74
Figure 4.10 - Oyster Creek - Span 1 - Slab 14 - 19 to 21 ft.....	75
Figure 4.11 - Ward Creek - Span 1 - Slab 13 flexural test results	77
Figure 4.12 - Ward Creek - Span 1 - Slab 13, soffit at failed region.....	78
Figure 4.13 - Ward Creek - Span 1 - Slab 13, crushed concrete removed.....	78
Figure 4.14 - Ward Creek - Span 1 - Slab 13, rusted, ruptured strands	79
Figure 4.15 - Ward Creek - Span 1 - Slab 14 flexural test results	82
Figure 4.16 - Ward Creek - Span 1 - Slab 14, strands at failed region	83
Figure 4.17 - Ward Creek - Span 1 - Slab 14, overview of failed region	83
Figure 4.18 - Ward Creek - Span 4 - Slab 5 flexural test results	86
Figure 4.19 - Ward Creek - Span 4 - Slab 5, overview of failed region	87
Figure 4.20 – Ward Creek - Span 4 - Slab 5, typical strands.....	87
Figure 4.21 - Ward Creek - Span 4 - Slab 6 flexural testing results	90
Figure 4.22 - Ward Creek - Span 4 - Slab 6 flexural test results combined	91
Figure 4.23 - Ward Creek - Span 4 - Slab 6, failed region	91
Figure 4.24 - Ward Creek - Span 9 - Slab 6 flexural test results	93
Figure 4.25 - Ward Creek - Span 9 - Slab 6, strands exposed around failure region	94
Figure 4.26 - Ward Creek - Span 9 - Slab 7 flexural test results	96
Figure 4.27 - Ward Creek - Span 9 - Slab 7, delamination visible at failed region.....	97
Figure 4.28 - Ward Creek - Span 9 - Slab 7, bottom layer of strands at failure plane after testing	98

Figure 4.29 - Ward Creek - Span 9 - Slab 7, patching material bonded with strands	98
Figure 4.30 - Ward Creek - Span 9 - Slab 7, heavy rust and pitting extends through patched region	99
Figure 4.31 - Oyster Creek - Span 1 - Slab 13 flexural test results	101
Figure 4.32 - Oyster Creek - Span 1 - Slab 13, slab soffit after failure	102
Figure 4.33 - Oyster Creek - Span 1 - Slab 14 flexural test results	104
Figure 4.34 - Oyster Creek - Span 1 - Slab 14, slab soffit after failure, showing broken stirrup	105
Figure 4.35 - Oyster Creek - Span 1 - Slab 14, failed region	106
Figure 4.36 - Oyster Creek - Span 1 - Slab 14, bottom layer strands from failed region	106
Figure 4.37 - Oyster Creek - Span 1 - Slab 14, second layer strands from failed region	107
Figure 4.38 - Oyster Creek - Span 1 - Slab 14, corroded stirrup from failed region	107
Figure 4.39 - Oyster Creek - Span 2 - Slab 4 flexural test results	109
Figure 4.40 - Oyster Creek - Span 2 - Slab 4, central strands at failed region	110
Figure 4.41 - Oyster Creek - Span 2 - Slab 5 flexural test results	112
Figure 4.42 - Oyster Creek - Span 2 - Slab 5, strands at failed region	113
Figure 4.43 - Oyster Creek - Span 8 - Slab 12 flexural test results	116
Figure 4.44 - Oyster Creek - Span 8 - Slab 12, soffit after testing, formerly covered by icolastic patch	117
Figure 4.45 - Oyster Creek - Span 8 - Slab 12, strand section loss extends full length of icolastic patch	117
Figure 4.46 - Oyster Creek - Span 8 - Slab 13 flexural test results	119
Figure 4.47 - Oyster Creek - Span 8 - Slab 13, moderate rust and pitting of ruptured corner strand	120
Figure 4.48 - Oyster Creek - Span 8 - Slab 13, rust and pitting of strands above (removed) stirrup location	121
Figure 4.49 - Oyster Creek - Span 8 - Slab 13, bottom layer strands removed from failed region	121
Figure 5.1 - Deterioration of slabs above retaining wall blocks	124
Figure 5.2 - Typical intermediate span spalling, Oyster Creek - Span 2 - Slab 4	125
Figure 5.3 - Resistivity Contours, Ward Creek - Span 1 - Slab 14	128
Figure 5.4 - Ward Creek - Span 1 - Slab 14	129
Figure 5.5 - Ward Creek - Span 9 - Slab 6, 17 - 26 ft	131
Figure 5.6 - Honeycombing, Oyster Creek - Span 2 - Slab 5, 9 - 14 ft	132
Figure 5.7 - Hairline cracks, Ward Creek - Span 9 - Slab 7, 3 ft	133
Figure 5.8 - Center strands, Ward Creek - Span 1 - Slab 14, 0 - 1 ft	133
Figure 5.9 - Field data: resistivity vs. total moment capacity	135
Figure 5.10 - Field data: percentage of resistivity values < 30 k Ω -cm vs. total moment capacity	135
Figure 5.11 - Laboratory data: resistivity vs. total moment capacity	136
Figure 5.12 - Laboratory data: percentage of resistivity values < 30 k Ω -cm vs. total moment capacity	136
Figure 5.13 - Moment vs. average half-cell potential, middle third of slabs	140
Figure 5.14 - Moment vs. average half-cell potentials, entire slab	141

Figure 5.15 Moment vs. average half-cell potentials, locations of visible or audible deterioration	142
Figure 5.16 - Moment vs. percentage of half-cell potentials below -0.35 V	142
Figure 5.17 - Stess Block Analysis	145
Figure 5.18 - Layered Sectional Analysis, discretizing into layers	149
Figure 5.19 - Layered Sectional Analysis, determining force components	149
Figure 5.20 - Calculated moment-curvature plot	150
Figure 5.21 - Calculated load-deflection plot	151
Figure 5.22 - Theoretical stress-strain for concrete in compression (Bramblett, 2000)	152
Figure 5.23 – Predicted load-deflection responses, 5000 psi concrete	155
Figure 5.24 – Predicted load-deflection responses, 7000 psi concrete	156
Figure 5.25 – Modified Ramberg-Osgood stress-strain relationship fit to Ward Creek strand tests	157
Figure 5.26 – Predicted load-deflection responses, calibrated steel stress-strain response	158
Figure 5.27 - Calculated load-deflection response fit to experimental results	161
Figure 5.28 - Ward Creek Bridge predicted load-deflection response	162
Figure 5.29 - Oyster Creek Bridge predicted load-deflection response	162
Figure 5.30 – Ruptured wires in strand, Oyster Creek - Span 8 - Slab 13	163
Figure 5.31 - Ward Creek Bridge - Predicted moment capacity vs. number of bottom strands	164
Figure 5.32 - Oyster Creek Bridge - Predicted moment capacity vs. number of bottom strands	164
Figure 5.33 – Delamination, 2007 Inspection, Oyster Creek Bridge	165
Figure 5.34 - Delaminated region, Ward Creek - Span 4 - Slab 6	167
Figure 5.35 - Delaminated region, Ward Creek - Span 1 - Slab 13	168
Figure 5.36 - Delaminated region after testing, Ward Creek - Span 1 - Slab 13	168
Figure 5.37 – Delaminated patched region, Oyster Creek - Span 8 - Slab 12	170
Figure 5.38 - Small patches, Oyster Creek - Span 2 - Slab 4 at 10 ft	171
Figure 5.39 – Ward Creek - Span 9 - Slab 6	173
Figure 5.40 - Ward Creek - Span 9 - Slab 7	173
Figure 5.41 - Oyster Creek - Span 1 - Slab 13	174
Figure 5.42 - Oyster Creek - Span 8 - Slab 12	174
Figure 5.43 - Cored slab cross-section, grouping of strands	178
Figure 5.44 - Deteriorated region, Ward Creek - Span 1 - Slab 14	185
Figure 5.45 - Parallel red marks, Oyster Creek - Span 1 - Slab 13	187
Figure 5.46 - Map-pattern cracking and minor spall at slab end, Oyster Creek - Span 1 - Slab 14	188
Figure 5.47 – Total section loss of bottom of stirrup, Oyster Creek – Span 8 – Slab 14	189
Figure 6.1 - Typical intermediate span spalling, Oyster Creek - Span 2 - Slab 4	192
Figure 7.1 - Cored slab cross-section	195

LIST OF TABLES

Table 2.1 – Permeability Classes for Surface Resistivity (Rupnow, 2011).....	21
Table 3.1 - Slabs selected for laboratory testing.....	36
Table 4.1 - Resistivity Classes.....	64
Table 4.2 - Resistivity statistics, all tests.....	65
Table 4.3 – Maximum and minimum recorded half-cell potentials.....	68
Table 4.4 – Calculated available moment capacities for undamaged slabs.....	69
Table 4.5 - Maximum moment values observed in laboratory testing.....	71
Table 4.6 - Maximum measured top strain, all slabs.....	72
Table 4.7 - Concrete core testing in compression.....	73
Table 4.8 – Ward Creek – Span 1 – Slab 13.....	80
Table 4.9 – Ward Creek – Span 1 – Slab 14.....	84
Table 4.10 – Ward Creek – Span 4 – Slab 5.....	88
Table 4.11 – Ward Creek – Span 4 – Slab 6.....	92
Table 4.12 – Ward Creek – Span 9 – Slab 6.....	95
Table 4.13 – Ward Creek – Span 9 – Slab 7.....	100
Table 4.14 – Oyster Creek – Span 1 – Slab 13.....	103
Table 4.15 – Oyster Creek – Span 1 – Slab 14.....	108
Table 4.16 – Oyster Creek – Span 2 – Slab 4.....	111
Table 4.17 – Oyster Creek – Span 2 – Slab 5.....	114
Table 4.18 – Oyster Creek – Span 8 – Slab 12.....	118
Table 4.19 – Oyster Creek – Span 8 – Slab 13.....	122
Table 5.1 - Distance from support blocks, end-span slabs.....	124
Table 5.2 - Areas of interest, resistivity.....	130
Table 5.3 - Areas of interest, half-cell potential.....	138
Table 5.4 – Calculated moment capacities, Stress Block Analysis.....	147
Table 5.5 – Calculated moment capacities, assumed material properties.....	154
Table 5.6 – Calculated moment capacities, 7000 psi concrete.....	156
Table 5.7 – Calculated moment capacities, calibrated steel stress-strain response.....	158
Table 5.8 – Error as a percentage of experimental applied load.....	159
Table 5.9 - Predicted strength using "Only Visible Corrosion" strategy.....	176
Table 5.10 - Predicted strength using "Depth of Spall" strategy.....	181
Table 5.11 - Predicted strength using “Two-Stirrup Spall” strategy.....	184
Table A-1 - Ward Creek Bridge slab conditions, 1997-2013	206
Table A-2 – Ward Creek Bridge: Select Photos from Inspection Reports - 1997 to 2013	207
Table A-3 – Oyster Creek Bridge Slab Conditions, 1997 - 2013	213
Table A-4 – Oyster Creek Bridge: Select Photos from Inspection Reports - 1997 to 2013	214

CHAPTER 1 – INTRODUCTION

1.1 – Introduction

In 2013 the North Carolina Department of Transportation (NCDOT) initiated a research project to examine inspection and evaluation options for bridges built using prestressed concrete cored slabs. This project was carried out at the Constructed Facilities Laboratory (CFL) at the North Carolina State University Department of Civil, Construction, and Environmental Engineering. It included detailed field inspection of two bridges recorded as entering service in 1977, along with flexural testing to failure at the CFL of select slabs from those bridges. This report details the results and conclusions from that project.

1.2 – Historical Background

Prestressed concrete cored slabs are believed to have first entered service in North Carolina in 1969, and have been used in North Carolina continuously since then with minor modifications (Muller & Malik, 2015). They are currently available in three standard depths: 18 in., 21 in., and 24 in., are 3 ft wide, and are used for spans of 40 ft to 70 ft (NCDOT, 2013). The bridges examined in this project used slabs manufactured in 1974 and 1975. The bridges used a 2 ft - 9 in. wide slab with depths of 17 in. and 20 in. for spans of 40 ft and 45 ft, respectively. These slabs were in service for 37 years in two bridges on US 70 in Carteret County: Ward Creek Bridge (9 - 40 ft spans, also known as No. 150035) and Oyster Creek Bridge (8 - 45 ft spans, also known as No. 150039). The slab cross-sections used in these bridges are shown in

Figure 1.1. Cored slabs are typically used in single or multi-span bridges, with each span composed of 14 to 16 simply supported slabs. Slabs are grouted together and transversely post-tensioned using $\frac{1}{2}$ " strands at third points, then topped with an asphaltic wearing surface.

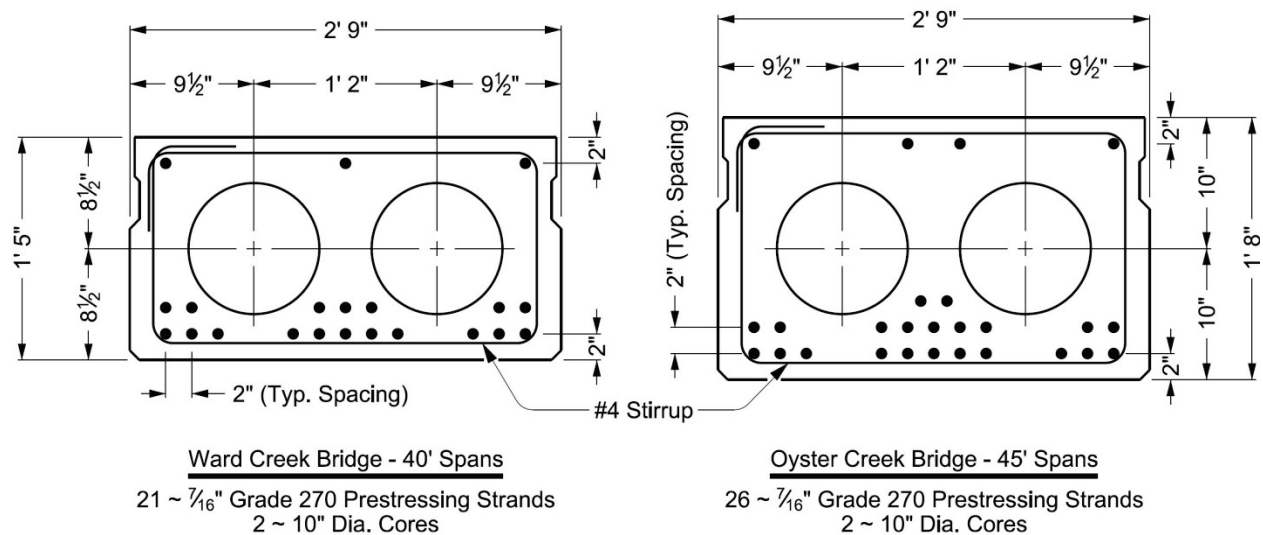


Figure 1.1 - Cored Slab Cross-Sections

This research project on the condition and evaluation of cored slabs was driven initially by the discovery in October, 2012 of visible flexural cracks on Bridge No. 150096 providing access between Harkers Island and the mainland in Carteret County. The severity of the cracks and deterioration prompted immediate load posting of that bridge, reduction of traffic to one lane, and subsequent replacement of all cored slabs (NCDOT, 2012). An evaluation of other cored slab bridges in Carteret County suggested that while Bridge No. 150096 appeared to show the most severe visual deterioration, several other bridges showed similar patterns of longitudinal rust stains and extensive patching, including the two bridges examined as part of this project (Muller & Malik, 2015). Figure 1.2 shows the visual condition of one of the more significantly deteriorated slabs examined in this project. A variety of different patching/repair methods of

varying ages are present on these slabs, complicating consistent analysis of their current condition. The locations of these three bridges are marked in Figure 1.3.



Figure 1.2 – Severe rust stains on patched slab soffit, Ward Creek Bridge

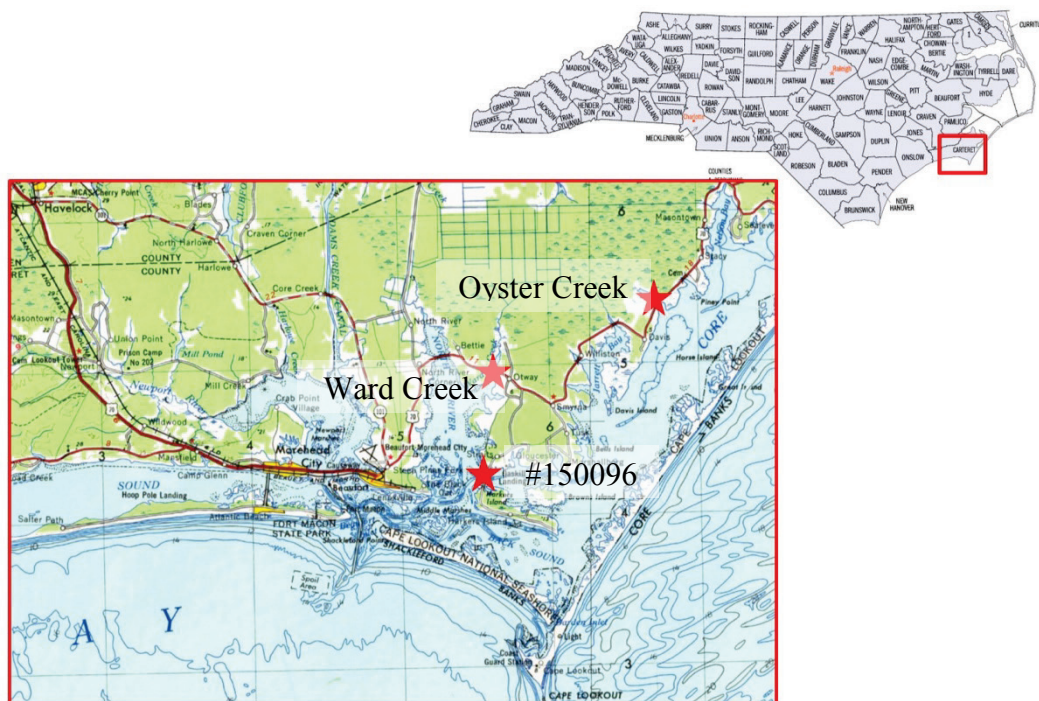


Figure 1.3 - Location of bridges discussed, Carteret County (*Maps from USGS, US Census Bureau*)

In light of the uncertainty in the remaining capacity of the cored slabs in the Oyster Creek and Ward Creek bridges, along with their visual deterioration, a contract was granted for the replacement of the superstructures for both bridges (Muller & Malik, 2015).

1.3 – Research Purpose and Scope

The NCDOT initiated this research project in order to determine how best to evaluate and understand the condition of these existing cored slab bridges. Research was focused on examining different methods of field inspection, with particular attention paid to the practicality of field implementation, and then relating results of field inspection with experimental evaluations of residual strength via destructive testing of cored slabs in the CFL.

Methods of inspection included traditional methods such as visual inspection and sounding for delamination, along with electrically-based non-destructive evaluation methods not in common use for routine NCDOT bridge inspections, specifically Half-Cell Potential and Concrete Resistivity testing. Inspection methods were applied as much as possible in the field, and then results from these methods were used to select 6 slabs each from Ward Creek and Oyster Creek Bridges for further study in the laboratory. Research was coordinated with the contracted demolition and replacement of the superstructure, allowing the 12 selected slabs to be transported intact to the CFL in Raleigh, NC, for more detailed examination and flexural testing. Flexural test results were then used to analyze data collected during inspections and to more accurately define the relationship between non-destructive evaluation methods and flexural strength for the spectrum of deteriorated prestressed concrete cored slabs.

1.4 – Bridge Numbering and Deterioration Vocabulary

1.4.1 - Numbering

Throughout this report, a consistent numbering scheme is used to describe slabs by their location on the bridge. This numbering is based on the initial layout of the road per construction documents, which ran roughly west to east. For Ward Creek Bridge the west span was Span 1 and the east span, Span 9. For Oyster Creek Bridge, the south span was Span 1, and the north span, Span 8. Slabs are numbered left-to-right when looking from the beginning of the bridge to the end. Numbering is shown schematically in Figure 1.4.

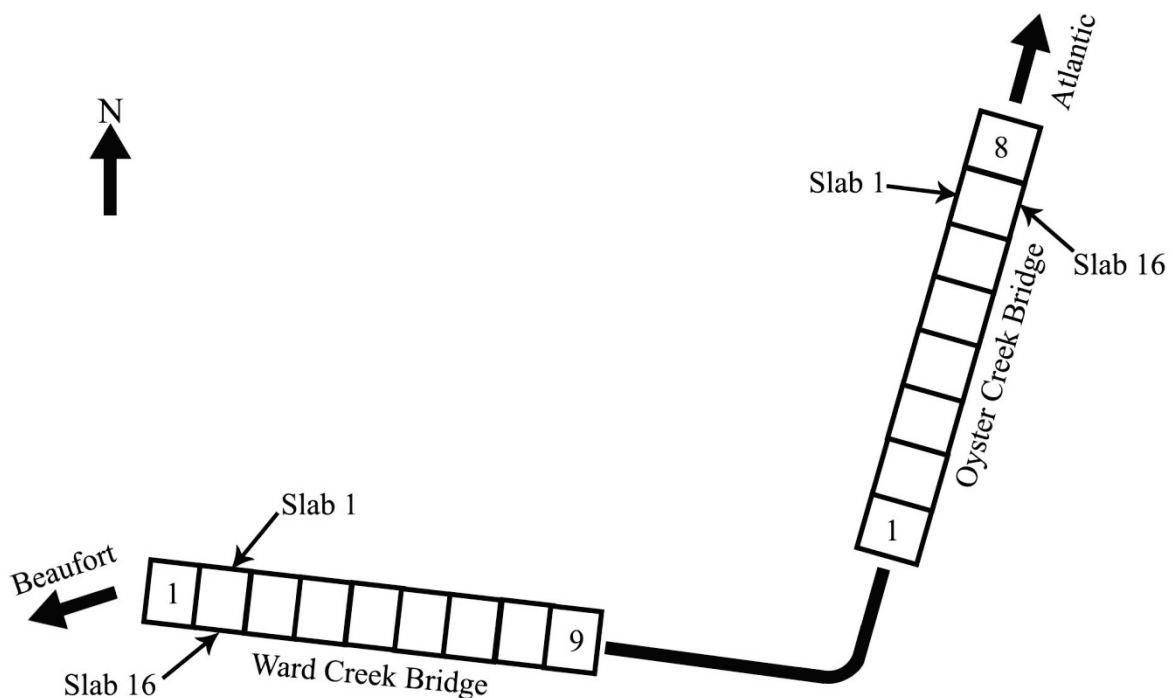


Figure 1.4 - Numbering scheme, Ward Creek and Oyster Creek Bridges

1.4.2 – Deterioration Vocabulary

A variety of vocabulary is used throughout the report to qualitatively describe rust, spalling, delaminations, and other deterioration. Though by no means comprehensive, some of that vocabulary is described here. Words used to describe rusting specifically are as follows:

- **Very light surface rust** – Generally for describing prestressing strands, this presents as a slight discoloration, reddish or brownish, on a few locations of strands. No estimated section loss, and likely no deterioration.
- **Light surface rust** – As above, but more uniformly on strands, and perhaps slightly darker. No estimated section loss.
- **Surface rust** – A widespread, shallow layer of rust.
- **Rust/rusting** – Spread across a strand in the same manner as surface rust, but possibly significant to strength. May be modified by “minor,” “moderate,” or “heavy.”
- **Pitting** – Unlike rust or surface rust, pitting is corrosion at one specific location on a strand. Generally more serious, it is associated with discernible loss of strength in the wire that is pitted.
- **Heavy pitting** – Pitting, but concentrated enough and close enough that the strand is significantly compromised, and may have lost all its strength.

Descriptors for all types of deterioration are as follows:

- **Minor** – Minor is used as the lowest level of deterioration that might warrant noting in the field. Likely not yet significant to the strength of the slab, and likely not widespread, but may have the potential to worsen in the future. Minor spalling might be spalling that does not expose any steel, or exposes steel without significant rust stains. Minor rust

might be a red corroded layer on the outside of strands that represents a small amount of section loss.

- **Moderate** – The next step up from minor, at this point deterioration is felt to have an impact on the overall condition of the bridge, but is not yet clearly hazardous. Moderate spalling might be spalling that is widespread and deeper than “minor” spalling, with some rust stains underneath but no visible deterioration of strands. Moderate rusting of strands is likely affecting the capacity of the slab in some way and may be associated with shallow pitting, while moderate rusting of stirrups likely involves up to 50% section loss on the underside of the stirrup.
- **Heavy/Severe** – Used somewhat interchangeably, these two words indicate the worst level of deterioration, with a severity and extent of deterioration that has certainly had some impact on slab strength, and likely has significantly weakened the slab. Heavy spalling is widespread and deep, likely exposing prestressing strands. Severe corrosion likely means most of the original steel has been turned into rust, and may be brittle and in pieces.

1.5 – Layout of Report

This report begins with a review of existing research and available literature in Chapter 2, and then moves into a discussion of the experimental program (Chapter 3), results of the experimental program (Chapter 4), an analysis of those results (Chapter 5), and finally conclusions (Chapter 6) and recommendations (Chapter 7). Additional materials related to the research are presented in Appendix A.

CHAPTER 2 – LITERATURE REVIEW

2.1 – Introduction

The project began with a review of available information concerning both specific information related to the project and prestressed concrete cored slabs from the NCDOT, and research and available information about more general bridge inspection methods and evaluation. This section begins with a review of pertinent information relating to the Ward Creek and Oyster Creek bridges, NCDOT inspection procedures, and typical load rating procedures. Then it moves into a brief discussion of alternate non-destructive evaluation techniques, specifically half-cell potential and concrete resistivity testing. Finally, similar efforts to examine the capacity of deteriorating prestressed concrete beams are discussed.

2.2 – Ward Creek and Oyster Creek bridges

Construction plans dated 1973 were available for both bridges, along with biennial routine inspection reports from 1997 to 2013. Information pertinent to this research from these documents is discussed here.

2.2.1 – Construction Plans

Construction plans for both bridges show details and construction practices that would be considered typical. Details that are pertinent to this project include:

- Construction plans showed that cored slabs followed the standard sections shown in Figure 1.1.
- Prestressing strands used are noted as 7/16 in. diameter, Grade 270, with an ultimate strength of 31,000 pounds per strand and an applied prestress of 21,700 pounds per strand, which given the nominal cross-sectional area of 0.115 in.² is equal to an initial prestress of 189 ksi.
- Slabs are supported on 4 in. x 2 ft – 7 in. x ½ in. elastomeric bearing pads at each end, inset so that the centers of bearing pads are 4 in. from end faces of the slabs.
- The plan and elevation views of the slabs given in the Ward Creek Bridge plans are shown in Figure 2.1. Tubes surrounded by an 8 in. region of solid concrete are specified at third points for transverse post-tensioning strands. Stirrup spacing is 12 in. for the middle 34 ft of 40 ft long slabs and for the middle 39 ft of 45 ft long slabs.

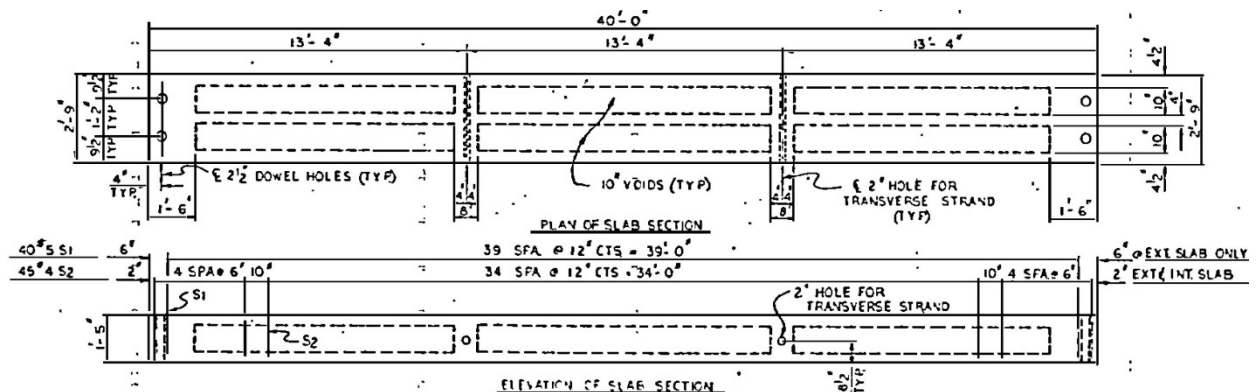


Figure 2.1 - Plan and Elevation Sections from Ward Creek Bridge plans

- Bituminous wearing surface applied directly to the top of the slabs is to be 6 in. at the roadway centerline, and minimum 1 in. at the rails.

2.2.2 – Inspection Reports

Inspection reports from routine biennial inspections were provided by the NCDOT from 1997 to 2013 for both bridges. The condition of slabs from the 2013 report is shown diagrammatically in Figure 2.2, with each row representing one span of the bridge, and each column representing one slab number (1 to 16). In these reports, inspectors stated whether each slab had been patched in the past, and whether it needed “priority maintenance.”

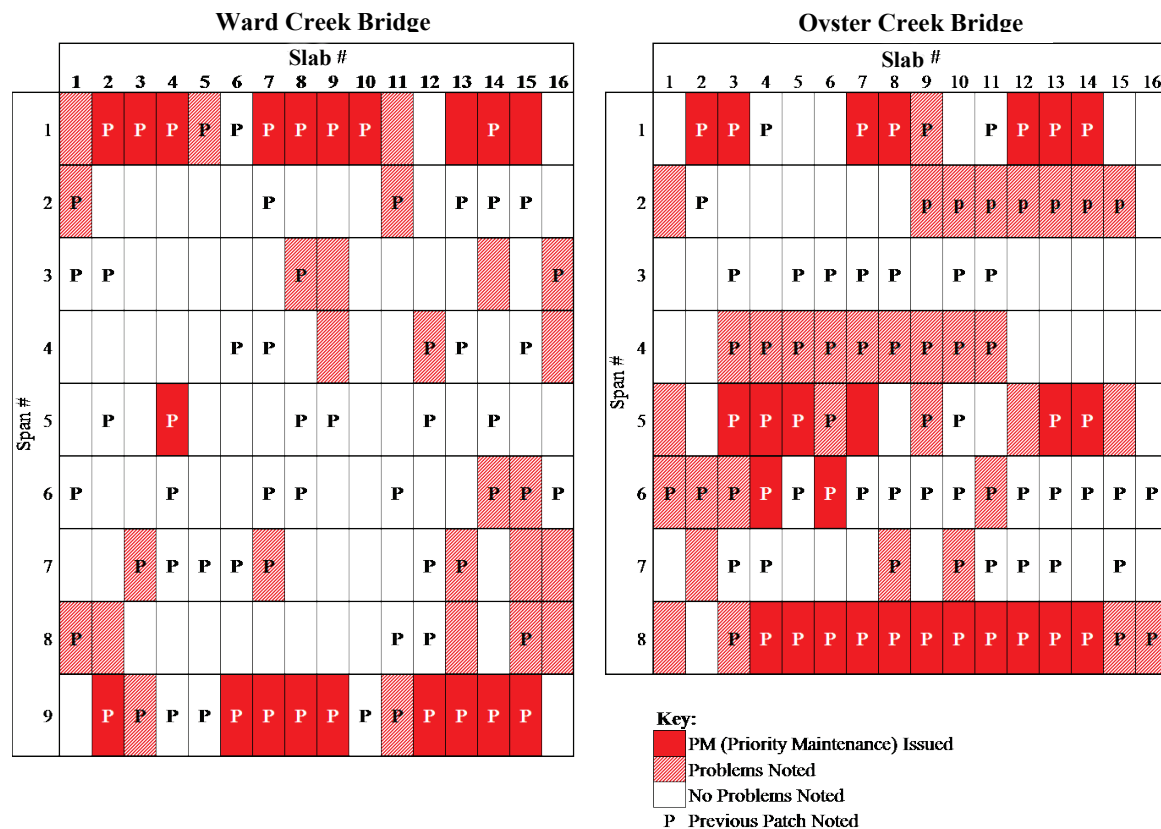



Figure 2.2 - Slab conditions per 2013 report

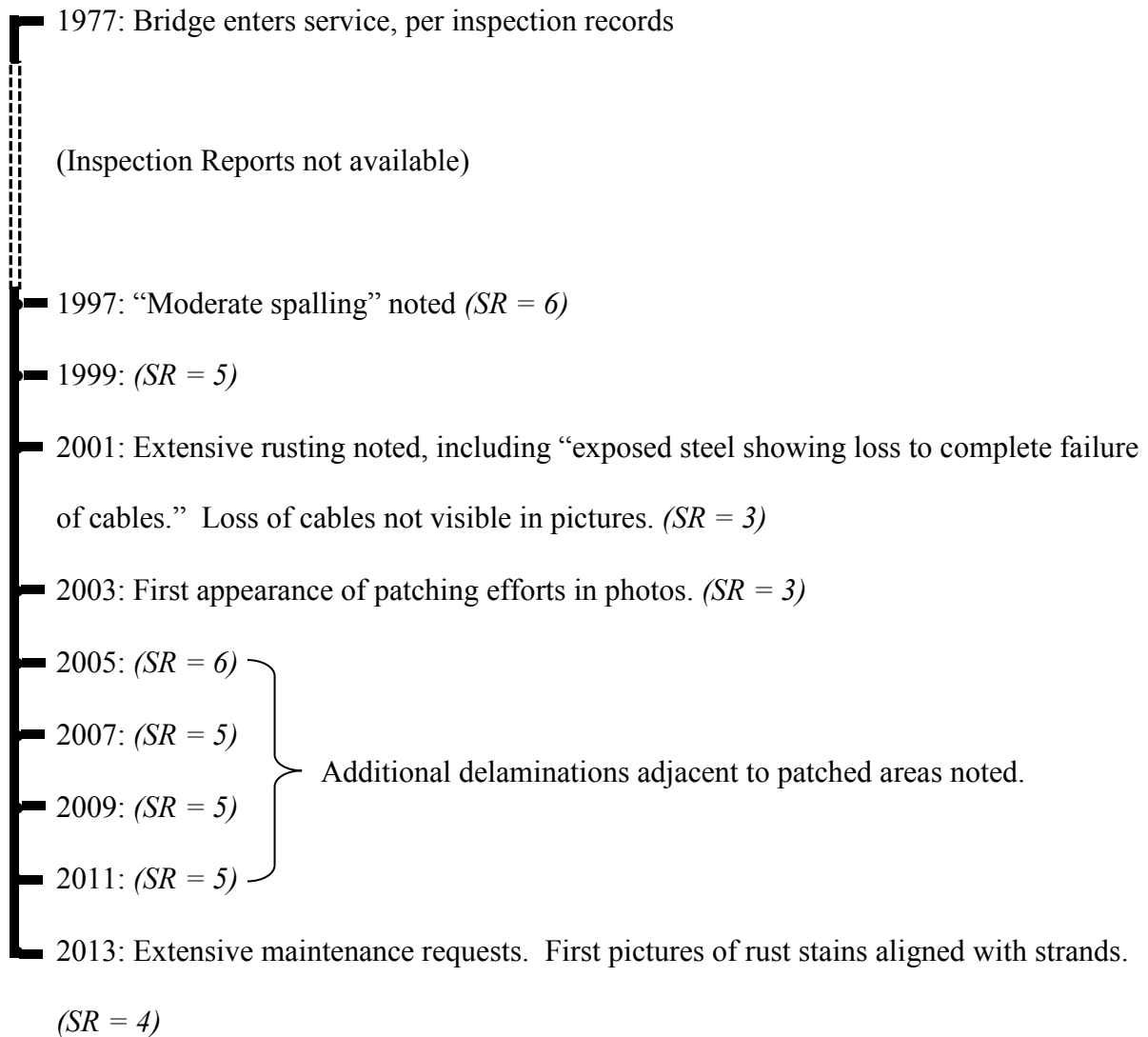
Both bridges showed similar levels of deterioration, with 37 of 64 slabs (58%) in the four end spans needing priority maintenance, and 144 of 272 (53%) having been previously patched.

Inspection reports from 1997 to 2013 were also examined to understand the rate and extent of deterioration over this 15 year time period. Both bridges had been in service for approximately 20 years as of 1997. Pertinent data from inspection reports discussing slab conditions are shown on the following pages. The phrasing and descriptions of deterioration frequently changes from report to report, limiting their usefulness for making comparisons from different time periods. Nevertheless, certain information about the timeline of the deterioration of the bridges can be gleaned from these. Notable events and NBI superstructure rating (SR) are as follows:

Ward Creek Bridge

- 
- 1977: Bridge enters service, per inspection reports
 - (Inspection Reports not available)
 - 1997: Spalling and rusting at stirrups, no visible rusting of strands. (*SR = 6*)
 - 1999: (*SR = 5*)
 - 2001: (*SR = 6*)
 - 2003: First appearance of patching efforts in Span 1, described as “were spalled but are now repaired.” Rust stains visible around patched area in photo. (*SR = 6*)
 - 2005: (*SR = 6*)
 - 2007: (*SR = 5*)
 - 2009: Rust stains noted as bleeding through many patches (*SR = 5*)
 - 2011: New patching noted on Span 9, with “moderate rust bleed thru.” Visible rust stains are aligned with prestressing strands. (*SR = 4*)
 - 2013: Extensive maintenance requests. (*SR = 4*)

Oyster Creek Bridge



Any key pieces of information relating to slab deterioration were noted from each inspection report, and language used to describe deterioration was recorded. Photographs vary in location and description, and language used to describe deterioration varies at times. As a reference, the slab descriptions and photographs from each inspection are presented in Appendix A. With close inspection, the progression of deterioration and patching efforts can be seen on a select number of slabs from both bridges. Only one location is clearly photographed from 1997 to

2013: Ward Creek – Span 9 – Slabs 7 and 8. Photographs and given descriptions of those two slabs are presented below in Figure 2.3 to Figure 2.8, as a means of showing what is believed to be a representative visual timeline of deterioration and patching efforts on the most heavily corroded slabs.



Figure 2.3 - 1997: "Delaminated and/or spalled with rusty exposed steel"



Figure 2.4 - 2003: "[...]were delaminated and/or spalled with rusting rebars exposed but are [...] repaired"



Figure 2.5 - 2005: "Slabs 6 and 7 are delaminated"



Figure 2.6 - 2009: (Description in photograph)



Figure 2.7 - 2011: (Description in photograph)



Figure 2.8 - 2013: "Delamination at previous patch with heavy longitudinal and transverse rust"

2.3 – Non-Destructive Evaluation Techniques

Bridge inspection and evaluation is typically a non-destructive process. As shown in the inspection reports discussed in the previous section, typical inspection methods include noting and photographing visual deterioration, combined with some method to check concrete for delamination, typically by tapping a concrete surface with a small hammer. In addition to using these methods, this research project examined two additional non-destructive evaluation techniques that use electrical methods to quantify or qualify the condition of reinforced concrete structures. These methods, half-cell potential and concrete resistivity, are discussed below.

2.3.1 – Half-Cell Potential Test

Half-Cell Potential testing is the most extensively used electrically-based technique for examining corrosion in mild-steel rebar embedded in concrete (Poursaee, 2011). The half-cell potential test relies on the potential difference (voltage) between a reference half-cell and a steel reinforcing bar embedded in concrete. Steel corrosion is an electrochemical process, whereby electrons are given up by the rusting section of steel (the anode) in the presence of a cathode (frequently a different section of steel not undergoing corrosion (Babaei, 1986). Because of this, when a reference electrode is connected to a piece of steel embedded in concrete, the presence of corrosion at the steel changes the potential difference between them, such that areas of steel displaying greater corrosion coincide with more negative potential differences relative to areas of steel without corrosion. This difference can be measured by a high-impedance voltmeter, and has been used to characterize the corrosion of steel in concrete since the 1970s. It has been approved as ASTM C867 (2009).

ASTM C876 recommends the use of a copper-copper sulfate reference electrode, which is connected to a piece of steel reinforcement through a voltmeter, and is then pushed against a concrete surface at various locations along the steel. A wet sponge provides contact between the reference electrode and the concrete, which must have sufficient moisture to allow for the complete electrical circuit. This is shown in Figure 2.9 (ASTM C876, 2009).

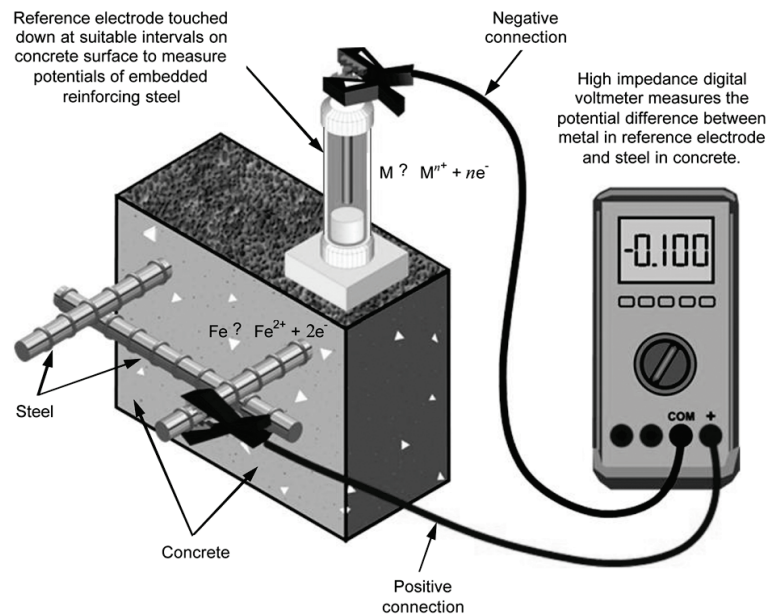


Figure 2.9 - Diagram of half-cell potential test (ASTM C876, 2009)

Half-cell potential tests have become common, particularly for large, horizontal grids of rebar such as are present near the top of a bridge deck (Clemeña, 1992). Materials are typically affordable, results can be interpreted visually via contour plots, and commercial solutions that automate parts of the ASTM measurement process are readily available (Giatec Scientific, 2015). Typical reference electrodes use a liquid electrolyte solution, but gel-based electrodes allow for

measurements to be taken with the cell “upside down,” as required for measurements on a slab soffit.

ASTM C876 discusses two different ways to interpret the results of half-cell potential tests. The first is to look at contour plots of a surface, to show the relative difference in potentials between different areas of a structure. In this case the specific values measured are less important than their variation across the structure. The second option, the “Numeric Magnitude Technique” is to look at the specific values measured. ASTM C876 states that “If potentials over an area are more positive than -0.20 V [relative to a Copper-Copper Sulfate reference electrode] there is a greater than 90% probability that no reinforcing steel corrosion is occurring in that area at the time of measurement,” while potentials more negative than -0.35 V indicate “there is a greater than 90% probability that reinforcing steel corrosion is occurring in that area at the time of measurement” (2009).

Half-cell potential testing has a number of known limitations. Measurements vary with temperature and moisture (and oxygen) content of concrete (Frølund, 2003). The numeric magnitude technique discussed in ASTM C876 is considered to be particularly inaccurate in such conditions, as discussed by Clemeña (1992) and Nakamura (2008). ASTM C876 prescribes a pre-wetting process in order to try and stabilize these values in the event that potential readings fluctuate, and this process slows and complicates measurements. Unlike other measurement techniques examined in this report, half-cell potential testing requires a physical contact with the steel in at least one location, thereby likely requiring some damage to the cover concrete.

Though half-cell potential testing is well-understood, its application to in-service prestressed concrete structures is less common than to structures reinforced with mild steel rebar, and this research presents the opportunity to look at its applicability in the setting of prestressed concrete slab soffits. In a rebar cage such as is present on a bridge deck, there is sufficient contact between all pieces of steel that a physical contact can be made at one point on the cage to allow measurements at all other points. This may not necessarily be true in prestressed cored slabs, since stirrups are typically only tied to certain strands, with the rest being suspended in the formwork during casting due to prestress. The need to make multiple holes to access multiple strands could substantially affect the practicality of this method. Finally, in this research the results of half-cell potential testing of a prestressed concrete cored slab can be compared against the residual full-scale flexural strengths of slabs, so that the structural effects of corrosion can be directly examined.

2.3.2 – Concrete Resistivity Test

The second electrically-based non-destructive evaluation technique examined in this research is concrete resistivity. Unlike the half-cell potential test, concrete resistivity requires no direct contact with reinforcing steel, and is intended to characterize not corrosion specifically, but rather the susceptibility for corrosion based on the porosity of the concrete, which correlates with the susceptibility of the concrete to chloride penetration (Rupnow, 2011). Surface resistivity has become widely accepted as a substitute for the Rapid Chloride Permeability Test of ASTM C1202 (Kessler, 2008).

Concrete resistivity is measured using a 4-point Wenner probe, with two metal outer probes applying a current to the concrete surface, and two metal inner probes measuring the potential (voltage) under the applied current. This setup is shown diagrammatically in Figure 2.10 (Proceq SA, 2013).

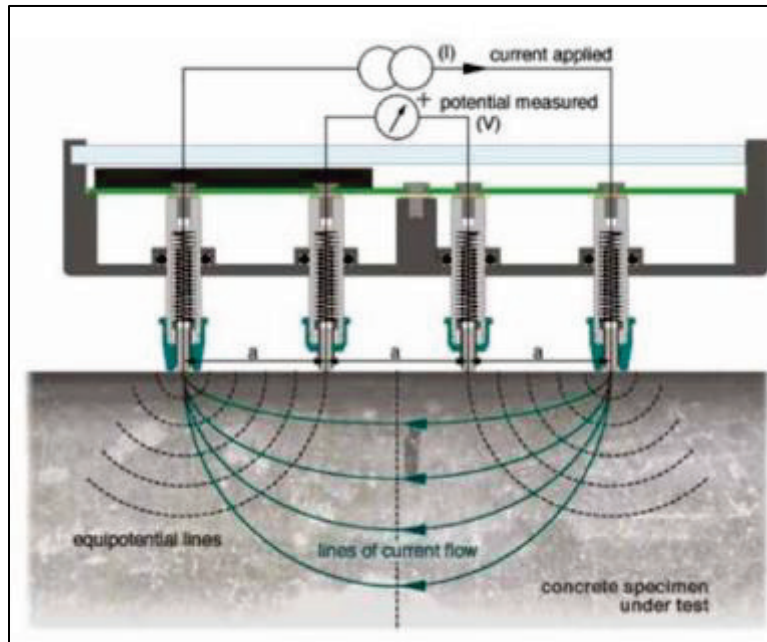


Figure 2.10 - Resistivity probe diagram (Proceq SA, 2013)

Resistance in its simplest form is voltage/current, but such a value varies with the path the current travels and the material through which it travels. If one adjusts for the path that current travels (the distance between the probes), the material property, resistivity, is measured. The equation for this is given by Equation 1 (Liu, 2010).

$$\rho = 2\pi a * \frac{V}{I} \quad \text{Equation 1}$$

Variables are ρ = resistivity, a = distance between probes (same spacing for all probes), V = measured voltage, and I = applied current. Typical units used for resistivity are $\text{k}\Omega\text{-cm}$. Values

obtained from the test are then commonly related to the permeability classes that are used in the Rapid Chloride Permeability Test, reflecting the common use of concrete resistivity as a direct replacement for that test. Rupnow (2011) tested various types of concrete, and recommended that the relationships in Table 2.1 be used when measuring a saturated 4 in. x 8 in. cylinder at 28 days.

Table 2.1 – Permeability Classes for Surface Resistivity (Rupnow, 2011)

Permeability Class	56-Day Rapid Chloride Permeability Charge Passed (Coulombs)	28-Day Surface Resistivity (kΩ-cm)
High	> 4,000	< 12
Moderate	2,000 - 4,000	12 - 21
Low	1,000 - 2,000	21 - 37
Very Low	100 - 1,000	37 - 254
Negligible	< 100	> 254

Use of resistivity measurements to characterize in-service structures appears to be limited. Liu, Suarez, and Presuel-Moreno (2010) conducted research including modeling and field testing on columns at more than 60 coastal bridges in Florida. They found field resistivity values were approximately 3 times the values used in Table 2.1, though they noted substantial variability, primarily relating to varying water saturation of concrete.

This variability is noted in Rupnow (2011) to not only include water saturation, but also the components of the pore solution, the water/cement ratio, the type of cementitious materials used, and the age of the concrete. Due to this, substantial challenges remain in consistent interpretation of resistivity values collected in the field. Recent research on the effects of rebar

and cracks in concrete suggest that the presence of uncoated rebar can additionally affect resistivity results. (Morales, 2015).

Resistivity was chosen for this research due to the clear ability to add to the understanding of its practicality as an inspection method, and also due to its ease of use compared to other electrical inspection methods. Compact, battery-powered water-resistant electricity meters are commonly available and affordable (Proceq SA, 2013), and they can be used anywhere a flat concrete surface can be accessed.

2.4 – Testing and Evaluation of In-Service Prestressed Girders

Research on the performance of prestressed beams is extensive, but that focusing on the evaluation of the capacity of deteriorated in-service beams, and more particularly slab- or box-girder-style sections such as the cored slabs, is limited. A few such research efforts are discussed here.

Research following the failure of a prestressed box beam on a US 70 bridge in Washington County, Pennsylvania (Hartle, 2008) examined the relationship between visual condition and deterioration of strands. The beams examined were not composite with any cast concrete deck, and were not connected to one another transversely. These beams had two layers of 250 ksi prestressing strands in the bottom flange, both layers of which had extensive corrosion at the time of collapse. The researchers determined that a number of issues contributed to the failure of the beam, chief among them “leakage” of water through the spaces between beams from the deck

above, introducing high chloride concentrations that led to corrosion of prestressing strands. Contributing to this was variable concrete thickness for the bottom flange due to quality control during construction which led to reduced cover concrete for strands and stirrups, and clogging of vent holes and drain holes on the bridge superstructure leading to more leakage than would otherwise be anticipated. This study of the US 70 bridge in Pennsylvania showed measured concrete strength and strand strength was not a contributing issue, with compressive strength of concrete and yield strength of an intact strand both exceeding design requirements. Longitudinal cracks were highlighted as a significant indicator of strand deterioration, with cracks running the full depth of the bottom flange of the box beam, from the soffit into the void. Hartle's conclusions present longitudinal cracks as an indicator of loss of 2 strands due to corrosion in locations without stirrups (Figure 2.11, left), and two strands plus adjacent strands on the bottom layer (4 total) in the presence of stirrups (Figure 2.11, right). Hartle (2008) also recommended examining loss of camber as an indication of loss of prestress.

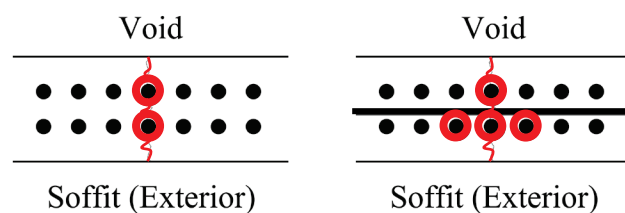


Figure 2.11 - Strands assumed deteriorated, PennDOT Report on AASHTO Box Beams (Hartle, 2008)

Research conducted in Wisconsin similarly looked at methods of assessing the condition of prestressed box beams (Aktan, 2009). This research included removing and testing one 50 year old fascia beam which showed extensive visual deterioration. This research attempted to

calculate remaining prestress from the camber present in the beam, however “it was found that using camber overestimates remaining prestress by 40-50 percent” (Aktan, 2009). The tested beam displayed longitudinal cracks that were again believed to indicate significant deterioration, but flexural testing revealed its capacity exceeded the original design load (Hartle, 2008).

The research conducted in Wisconsin is further discussed in Attanayake & Aktan (2011), which describes the procedure used to remove and test the beam. Testing was done outdoors using a hydraulic jack held by a forklift. This setup did not allow for the ultimate capacity of the jack to be reached, but experimental results showed good agreement with the basic equation to predict the cracking moment given by Equation 2, with results within 5% of the calculated value, suggesting cracking and deterioration did not significantly affect the basic cross-sectional properties of the slab.

$$M_{cr} = \frac{I_g}{y_b} \left[f_r + \frac{P_e}{A_c} \left(1 + \frac{ey_b}{I_g/A_c} \right) \right] \quad \text{Equation 2}$$

In 2002, beams from a 45 year old post-tensioned concrete bridge in Tasmania, Australia, were tested to examine the relationships between corrosion, chloride profiles, and half-cell potential. Two beams were tested, one with little corrosion and one with more extensive corrosion, and it was found that “absolute half-cell potential values, potential gradients, and the location of minima did not provide an indication of the severity of corrosion” (Papè, 2009).

2.5 – General Bridge Deterioration

A limitation inherent in this research project is the focus on the condition of two bridges at a single point in time. Research into statistical prediction of the deterioration of bridges is an active and developing field, but a broad statement characterizing these relationships can be found in the article by Sobanjo et al. (2010) where it is stated that, “all the bridge categories deteriorate faster with age [...], and bridge components located on the interstate roadways are deteriorating faster than similar bridges on noninterstate roadways” (p. 671).

On March 30, 2015, a meeting was held at the NCDOT in Raleigh to obtain background information on the load rating and bridge evaluation process (Muller & Malik, 2015).

Discussion was wide-ranging, but significant challenges in the current process that were identified in this meeting include accurate estimation of asphalt thickness, difficulty assessing deterioration and the significance of rust stains from photos, and uncertainty associated with the condition under audibly delaminated sections.

2.6 – Summary of Research Needs

Though there is a body of research that covers subjects relevant to the deterioration of prestressed cored slabs, the cored slabs used in North Carolina have not been specifically studied in the way that AASHTO standard designs such as box girders have been. In the literature as a whole there are only limited studies that combine field examination of bridges with laboratory testing in a way that reflects routine bridge inspection. This research project is uniquely focused in the experimental program that is described in the following chapter, which combines extensive

field testing with laboratory testing, and is oriented towards the limitations and necessities of bridge inspectors and the accurate analysis of prestressed cored slabs in the environmental conditions of coastal North Carolina.

CHAPTER 3 – EXPERIMENTAL PROGRAM

3.1 – Introduction

The experimental program was categorized into two parts: field inspection and laboratory testing. Field inspection began with initial inspection of the two bridges described in Chapters 1 and 2, followed by a detailed examination of select spans. Information from the 2013 bridge inspection reports for both bridges was used to understand the condition of the bridges prior to going into the field. Field testing included visual inspection, sounding, and resistivity measurement. Twelve slabs (six from each bridge) were selected and transported to the CFL for further testing, which included a more detailed resistivity testing of the selected slabs, half-cell potential testing, and full-scale flexural testing. After flexural testing, concrete was removed near the failed region and the condition of the strands was directly observed visually. Finally, concrete cores and steel prestressing strands were removed from select slabs and tested to obtain material properties. This chapter focuses on the procedures and methods of the experimental program, and only presents limited results as means of illustration. Full results are given in Chapter 4.

3.2 – Field Inspection

Field inspection began with a trip on October 10, 2013 to survey both bridges and gain an initial feel of their condition and the logistical challenges of inspection. In order to match the contractor's demolition schedule, Ward Creek Bridge was chosen to inspect first, with five

inspections taking place between December 9, 2013 and February 8, 2014. Out of the nine 40 ft spans in the bridge, three were chosen for detailed inspection: end Spans 1 & 9, which showed the worst deterioration, and Span 4, which appeared to be representative of the overall state of the intermediate spans. Oyster Creek Bridge was inspected second, with some initial inspection work performed on February 8, 2014, and most inspection tasks completed in three trips between April 12 and May 14, 2014. Detailed inspection again included the two end spans, Spans 1 & 8, and representative intermediate Span 2. Choice of intermediate spans for inspection was partially influenced by ease of access, with Span 2 of Oyster Creek Bridge chosen due to a downstream boat ramp helping to quiet wave action on that side of the bridge. This was not observed to have a significant effect on the overall deterioration, but aided in moving a floating work platform provided by the NCDOT.

3.2.1 – Marking Slabs

Inspection of each span began by marking the slabs in 2 ft intervals. Given the 44 ft width of each span, accurately marking slabs in a uniform way presented challenges. The exterior slabs (fascia slabs) were first marked on the side with a carpenter's crayon, using a nylon 100 ft measuring tape that had been taped to the slabs as a guide. A string was then run across the width of the span and aligned with the marks at 2 ft intervals. Finally, spray-paint and carpenters crayon were used to transfer the 2 ft intervals, marking onto each slab soffit. Later inspection of the marks in the laboratory suggest that the locations as marked using this process rarely varied more than approximately 1 in. from if they had been marked onto each slab directly using a 100

ft tape. Measurements were taken at 1 ft intervals, with mid-point locations between the marked intervals being visually estimated (for example, Figure 3.1 shows a photo taken between marks).



Figure 3.1 – Spray-painted orange dots for marking of slabs

3.2.2 – Logistics of Inspection Trips

Significant inspection tasks for the 2 bridges took place over 8 1-to-2-day trips from December 19, 2013 to May 14, 2014, with three additional trips for the initial site visit, marking of slabs, and examination of demolition. Overall this constituted 16 days of field work, with 2 to 4 people contributing to the inspection process each day. Slabs were accessed via a combination of crawling on concrete riprap, moving in shallow water using waders, and an approximately 10 ft x 20 ft floating work platform supported on pontoons.

3.2.3 – *Photographing*

Photography ideally was taken under bright lighting conditions, but with efforts taken to minimize glare. During the initial site visit and from evaluation of NCDOT inspection reports as discussed in Chapter 2, uniformity of photography was identified as a significant challenge given varying access and lower light underneath the bridge. Because of this, a custom bipod was built and a single camera model was used for all inspection, as seen in Figure 3.2.



Figure 3.2 - Bipod for photographing slabs

The bipod had two legs spaced so that they would approximately align with the joints between slabs, and the legs were cut to length to allow for the full width of a slab to be captured using the camera with its zoom lens at its widest focal length. A typical photograph taken with this setup is shown in Figure 3.3.



Figure 3.3 - Typical photograph with bipod

Despite efforts to minimize camera movement and check focus, variation in picture quality remained, but sufficient overlap between images allows for almost all regions of a slab to be captured by at least two photographs. All recorded photographs used a single type of camera, the Nikon Coolpix P500, with a focal length set to the minimum of 22.5 mm (35 mm equivalent). Lens and perspective distortion were later adjusted as necessary in Adobe Photoshop.

3.2.4 – Sounding

Sounding of slabs was accomplished with a common carpenter's claw hammer, as shown in Figure 3.4. Delamination at any point along the length of the slab can vary in several ways, most notably in its depth and how much of the width of the slab is delaminated, but also in “how hollow” it sounds and how it appears visually. To simplify the inspection process, it was decided that data would be recorded for each foot along the length of the slab, and if any point across the

width of the slab was delaminated, the slab would be considered delaminated at that 1 ft increment.

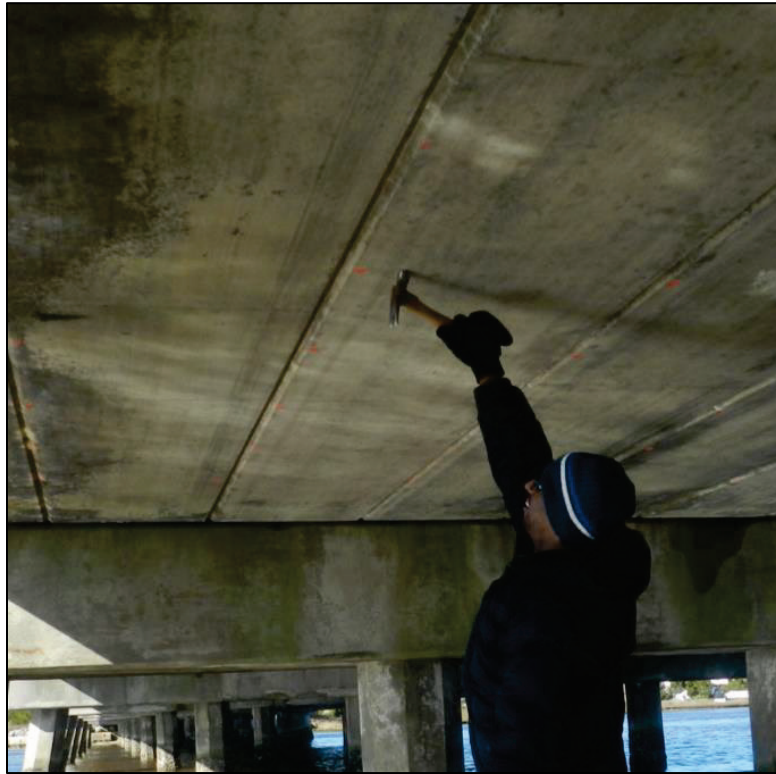


Figure 3.4 - Sounding with hammer

Therefore an inspector would move beneath a 1 ft interval, then tap the hammer a minimum of three times across the width of the slab at that point. If the soffit sounded delaminated at any point in that width, the inspector would confirm this with a second person (typically recording data) and if they agreed that it sounded delaminated, that 1 ft interval would be identified as delaminated. This process was carried out for areas with apparently sound concrete, patched concrete, and spalled concrete.

3.2.5 – Resistivity

As in the photographic record and sounding, resistivity was recorded along the length of each slab in 1 ft increments, with measurements taken in the middle of the slab as seen in Figure 3.5. Concrete resistivity was recorded with the Resipod resistivity meter, manufactured by Proceq.



Figure 3.5 - Resistivity meter in use in the field

The Resipod uses a 4-probe array as discussed in Chapter 2, with two outer probes applying a current to the surface of the concrete, and two inner probes measuring the potential difference. This setup necessitates uniform contact with the concrete surface, and therefore the probe can only be used where the slab soffit is an intact plane. The manufacturer provides small foam tips that are placed onto the ends of the probes and saturated with tap-water to take readings of concrete that is not fully saturated. For field-work, this was modified slightly with more affordable open-cell foam inserts placed into the metal probe and sprayed with tap water after

approximately every 5 to 10 probe readings. This setup proved less prone to being dislodged than the manufacturer-provided foam.

Variable environmental conditions presented a challenge for collecting resistivity data. Based on the literature review and experience, it was known that the ultimate use of the data was to compare resistivity readings within a single span to understand the relative condition of one slab to another. Because resistivity varies with the moisture content and temperature of the slabs, resistivity is ideally measured on days with limited weather and humidity variations. The constraints of field inspection mean these ideal conditions are not always met. A single span typically took 4-6 hours to record resistivity measurements, during which time temperature varied up to 20°F and slabs sometimes transitioned from the soffit appearing completely dry to dripping wet. This can be seen in Figure 3.6, showing photographs taken at varying times on one trip.



Figure 3.6 - Varying moisture on slab soffits, Ward Creek Bridge – Span 1

Resistivity as displayed by the Resipod meter varies as the meter is pressed against the concrete, likely due to moisture from the foam contact pads being absorbed into the concrete. Because of this, readings will vary depend on how soon they are recorded after initial contact. Initial resistivity measurements were made with varying intervals of time between contact and

recording, and it was observed that even when waiting several minutes to record the reading, the values still might not stabilize. Generally the readings fluctuated in the following manner: after applying the probe an initial reading would quickly fluctuate (sometimes trending positive, sometimes trending negative) for anywhere from 3 seconds to over 1 minute, and then after that variation would slow considerably, though it could take as much as 5 minutes of continuous contact for readings to stabilize within 5 k Ω -cm. A combination of expediency in measurement and stability of readings was desired, and the compromise chosen for field readings was to wait beyond the initial fluctuation, until it was felt by the person using the probe that the reading was likely within a 25 k Ω -cm region (for example 150 to 175 k Ω -cm) that it would finally stabilize to. This method is subjective, but the competing priorities of stable individual readings and stable environmental conditions across an entire span necessitated a compromise.

For certain locations on slabs above very shallow water, it was not possible to maneuver the work platform below the slabs, nor to access it within arms-reach. For these locations a 3-ft extension arm was constructed out of PVC pipe. Prior to use on these locations, this extension arm was used on several locations which had been tested with the probe directly applied, and was found to give consistent readings.

3.2.6 – Selection of Slabs for Laboratory Testing

Six slabs from each bridge were selected for flexural testing at the CFL. Partially due to the challenges faced collecting consistent resistivity data, slabs were chosen primarily based on sounding and visual condition. The contractor's demolition schedule placed certain constraints

on the slabs selected: slabs needed to be selected as adjacent pairs, and each pair needed to be from a single half of the bridge (Slabs 1-8 or Slabs 9-16 in a span). Within these constraints, slabs were selected from each bridge to try and capture the full range of deterioration in both extent and variety. A brief summary of the slabs selected is shown in Table 3.1. Language used to describe them is typical of that used in bridge inspection, along with whether they had been selected for Priority Maintenance (PM) in the 2013 NCDOT inspection. Complete photographic records of these slabs are provided in Chapter 4.

Table 3.1 - Slabs selected for laboratory testing

Ward Creek Bridge			
<i>Slab Number</i>		<i>Description</i>	<i>PM Request</i>
Span 1	Slab 13	No spalling, but audible delamination over 6 ft length with parallel longitudinal cracks near midspan	Yes
	Slab 14	Two visible, shallow spalls with rust stains near stirrups, surrounded by audible delamination (no visible cracks)	Yes
Span 4	Slab 5	No apparent deterioration	No
	Slab 6	Six shallow patched spalls underneath stirrups; two isolated areas of delamination; no widespread deterioration.	No
Span 9	Slab 6	Variety of patches, somewhat deeper spalls with rust stains, and visible/audible delamination under stirrups.	Yes
	Slab 7	Deep spalls and patches with extensive longitudinal and transverse rust stains over ~9 ft region.	Yes

Oyster Creek Bridge			
<i>Slab Number</i>		<i>Description</i>	<i>PM Request</i>
Span 1	Slab 13	~11 ft heavily spalled and delaminated region with extensive rust stains	Yes
	Slab 14	Moderate ~5 ft spalled region with longitudinal rust stains	Yes
Span 2	Slab 4	Shallow spalls with rust stains under stirrups	No
	Slab 5	No apparent deterioration	No
Span 8	Slab 12	~11 ft icolastic patch, now delaminated	Yes
	Slab 13	Moderate spalled region with rust stains	Yes

3.2.7 – Additional Observations from Field Inspection

Demolition of the superstructure was phased, with one side (lane) of the bridge replaced prior to the other. This allowed for several observations that are not possible in a typical inspection process. Asphalt thickness could be measured accurately at midspan. Original plans call for the crown of the road to be made of up to 6 in. of asphalt, and it appeared that over 36 years of service two additional wearing surfaces ~1 in. thick each had been applied, leading to a total thickness of approximately 8 in., as is visible in Figure 3.7 (showing asphalt between approximately 1 in. and 9 in. marks, due to perspective of the picture).



Figure 3.7 – Asphaltic overlay thickness near roadway centerline

Transverse post-tensioning strands were cut and removed in the process of demolition, and generally appeared to be undamaged, with no significant corrosion. A strand can be seen extending from the duct in Figure 3.8.



Figure 3.8 - Transverse post-tensioning strand

A crack visible on the side of Ward Creek – Span 1 – Slab 9 shows delaminated concrete extended up to 3 in. into the slab, as visible in Figure 3.9.



Figure 3.9 - Depth of spalling, Ward Creek – Span 1 – Slab 9

3.3 – Demolition and Transportation

After milling of the asphalt and sawing of the grouted shear keys, the selected slabs were lifted off of the bridge using the C-clamp lifting rig shown in Figure 3.10 and placed onto trucks for transportation to the CFL at NCSU.



Figure 3.10 - Slab removal rig

At the CFL the slabs were off-loaded using forklifts (for the 40 ft slabs from Ward Creek Bridge), as shown in Figure 3.11, and the lab's gantry cranes (for the 45 ft long slabs from Oyster Creek Bridge). Slabs were delivered in pairs. Slabs from Ward Creek Bridge were delivered to the lab on March 12 and 31, and May 5, 2014. Slabs from Oyster Creek Bridge were delivered on July 23, August 29, and September 19, 2014. During all transportation overseen by researchers, lifting of slabs was restricted to lifting points within 8 ft of the slab ends in order to prevent cracking of the slabs under self-weight.



Figure 3.11 - Slabs arriving at CFL from Ward Creek – Span 9

3.4 – Laboratory Testing – Non-Destructive Testing

Laboratory testing consisted of four steps: detailed non-destructive evaluation (resistivity and half-cell potential), flexural testing to failure, material testing (concrete cores and prestressing strands), and jackhammering of the tested slabs to visually examine the extent of deterioration.

3.4.1 – Preparation of Slabs

Prior to the laboratory non-destructive evaluation, the slabs were cleaned, with any remaining asphalt and pieces of shear keys removed and the sides wiped down with water to remove cement residue from the cutting of the shear keys. Then the sides of the slabs were marked at 1 ft intervals (Figure 3.12), and marks were placed underneath five strands (Figure 3.13) in preparation for the resistivity and half-cell testing. The environmental stability provided by the laboratory setting allowed for more time to conduct resistivity and half-cell tests relative to what

would be available in the field, so measurements were taken at multiple locations along the width of a slab for each of the 12 slabs chosen for laboratory testing.



Figure 3.12 – 1 ft intervals marked on side of slab



Figure 3.13 - Marking slab soffit

The five marks on the slab soffit are directly underneath five strands (of eleven strands total in the bottom layer for all cored slab standards) as shown in Figure 3.14. These locations were chosen to try and capture possible varying conditions for each cluster of strands in the slab.

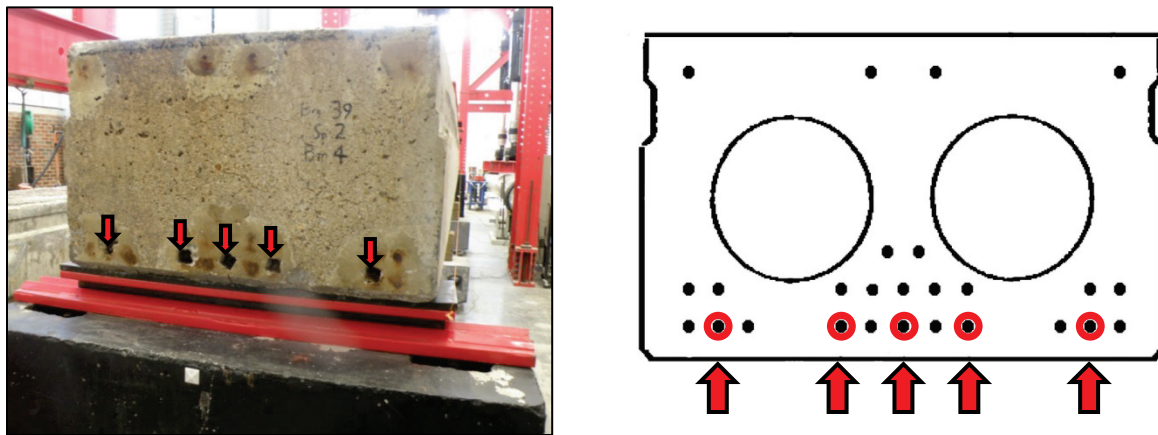


Figure 3.14 - Measurement locations for laboratory NDE

Strand ends were exposed at one end of the slab by drilling out the surrounding grout with a hammer-drill and cleaning with a rotary tool and compressed air. All slabs were left in the laboratory at $72 \pm 3^{\circ}\text{F}$ for a minimum of 24 hours prior to resistivity and half-cell potential testing.

3.4.2 – Resistivity

Resistivity was measured in the laboratory at each point using the same method as that used in the field (Section 3.2.5). Lower saturation of the slab soffit meant that contact sponges needed to be regularly re-wet to maintain consistent readings, and the sponges were soaked approximately once every 25 readings.

3.4.3 – Half-Cell Potential

Unlike resistivity, half-cell potential testing only took place in the laboratory. The necessity of making direct contact with a prestressing strand (drilling into the slab) along with the requirement to run a copper wire along the length of a beam means half-cell is significantly more time-intensive than resistivity, and subjects prestressing strands to additional environmental exposure where concrete is drilled. Therefore unlike all other non-destructive tests, evaluation of half-cell was chosen as a laboratory-only activity, with potential field application to only be attempted given positive results from later data analysis.

Half-cell potential was measured using the procedure outlined in ASTM C876 (2009). This calls for connecting a copper-copper sulfate reference electrode directly to the reinforcing steel via a low-impedance wire, and then making contact with the concrete surface at various points and recording the potential difference measured. This wire needed to be connected to the end of each strand being examined individually, as preliminary measurements suggested that there was not sufficient connection between adjacent strands to allow for an electrical connection at only one point. Limitations on fluctuations of readings and treatment of slabs were followed per ASTM, including pre-wetting the slab with a contact solution (detergent and water) in most situations in order to limit fluctuations when the electrode's contact sponge was placed against the mostly-unsaturated concrete (ASTM C876, 2009). The specific electrode used connected to a tablet via Bluetooth to allow for data recording, recorded data to 0.1 mV, and simultaneously recorded the temperature at the time of each recording in order to correct for temperature fluctuations as

recommended by ASTM C876 (2009) (Giatec Scientific, 2015). The electrode was gel-based, using silver-silver chloride, with potentials converted in software to the copper-copper sulfate standard as suggested by ASTM C876. The gel-based electrode allowed for use upside-down on the slab soffit. A photograph of the electrode and measuring system used is shown in Figure 3.15.



Figure 3.15 - Half-cell potential testing – electrode and software (Giatec Scientific)

With pre-wetting of the beam, values for half-cell potential would generally stabilize within two minutes, and generally did not fluctuate beyond 0.2 mV once they had stabilized. Therefore stable readings were generally recorded. Readings were also generally obtainable on patches and delaminations, and were recorded in these areas when possible. The exception to this is the icolastic patches present on some Oyster Creek slabs, which were electrically insulating.

3.5 – Laboratory Testing – Flexural Testing

Slabs were tested monotonically to failure in four-point bending, with loading at the third-points. The decision to load at third-points was motivated by three factors: a desire to roughly match the

shape of the moment distribution from loading due to a moving truck wheel-load (which is parabolic in shape and may be significantly under-represented by loading applied only near midspan); an interest in applying the load into the cored slabs above the post-tensioning ducts, which are surrounded by regions of solid concrete; and an interest in providing constant applied moment across all points of the substantially deteriorated regions of the selected slabs. The deterioration was generally concentrated near mid-span, and did not substantially extend beyond the third points. The slabs were supported on pin and roller supports, with the width and placement of supports being the same as what was used in the field. Though both the 40 ft and 45 ft slabs shared similar test set-ups, they differed in how the load was applied.

3.5.1 – 40 ft Slab Setup (Ward Creek Bridge)

For the 40-ft slabs from Ward Creek Bridge, load was applied via four hydraulic jacks, one on each side of the slab at each load point. Jacks were connected to the laboratory strong floor via HSS spreader beams, with load distributed to the slab via HSS loading beams. Elastomeric bearing pads and metal shims were used to ensure loading beams applied force to the top of the slab uniformly. An overall view of the as-built 40 ft slab test setup can be seen in Figure 3.16, and a schematic can be seen in Figure 3.17. Details of the setup can be seen in Figure 3.18 and Figure 3.19.



Figure 3.16 – 40 ft slab flexural test setup

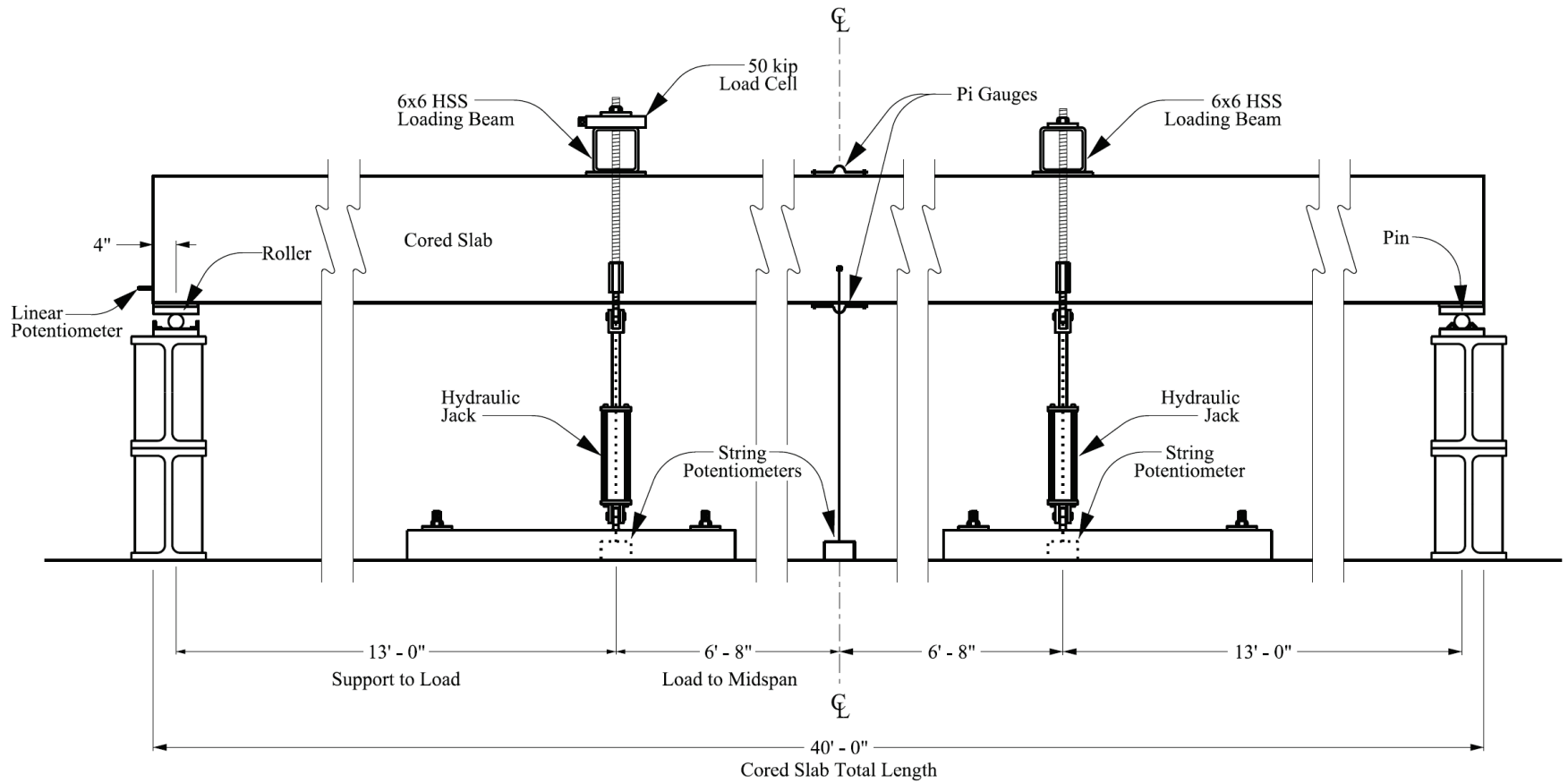


Figure 3.17 – Schematic of 40 ft slab flexural test setup



Figure 3.18 – Supports: pin (left), roller (right)



Figure 3.19 – Loading at third points via four 25-kip hydraulic jacks with 10" stroke

3.5.2 – 45 ft Slab Setup (Oyster Creek Bridge)

For the 45 ft slabs from Oyster Creek Bridge, load was applied by a 220-kip capacity hydraulic actuator, with a 15 ft steel spreader beam distributing the load to the third-points. A reaction frame connected the actuator to the laboratory strong floor. An overall view of the as-built 45 ft slab test setup is shown in Figure 3.20, and a schematic of the test setup can be seen in Figure 3.21. Details of the setup can be seen in Figure 3.22 and Figure 3.23.



Figure 3.20 - 45-ft slab flexural test setup

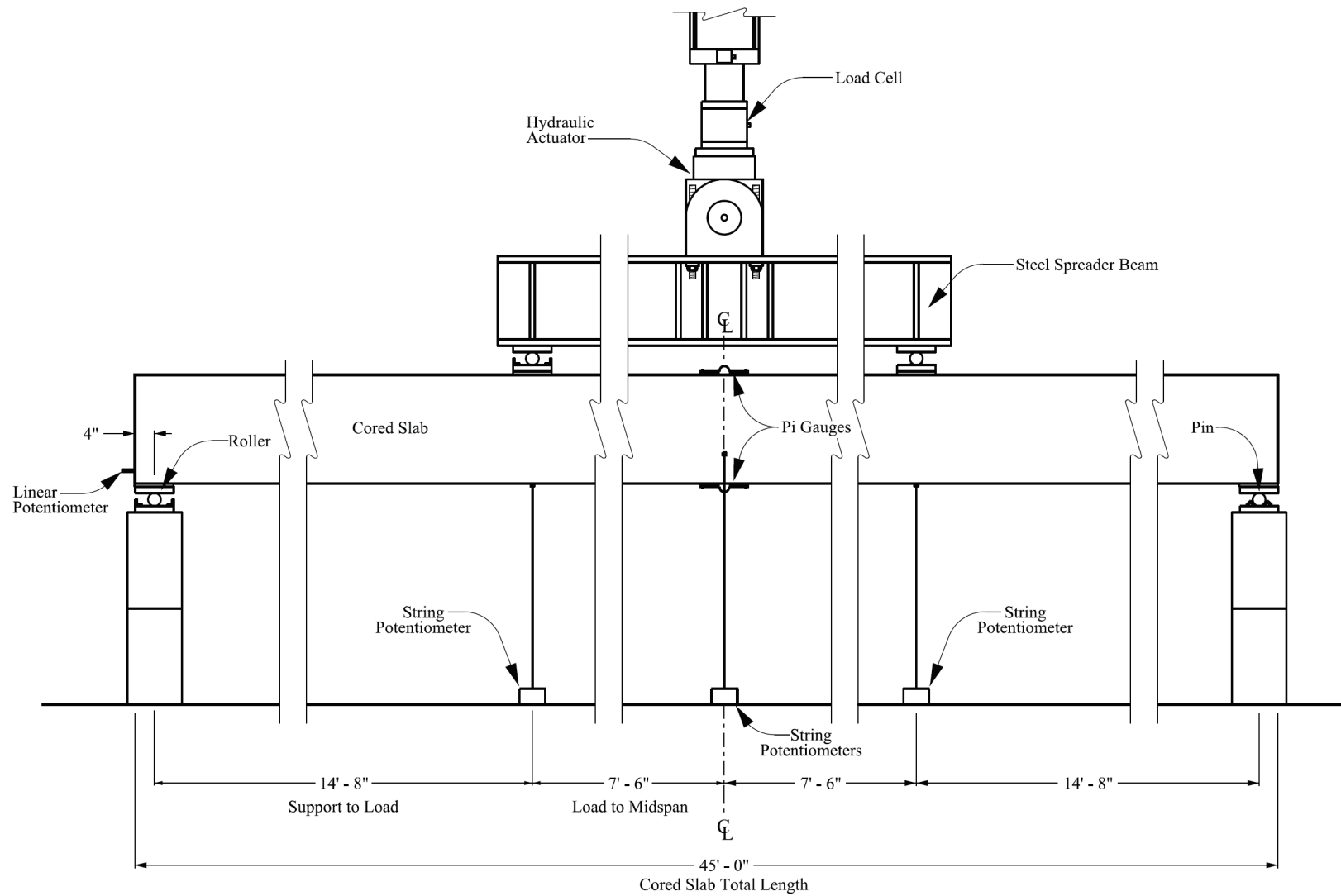


Figure 3.21 – Schematic of 45 ft slab flexural test setup



Figure 3.22 – Supports



Figure 3.23 - Loading via 220-kip 40 in. stroke actuator with spreader beam

3.5.3 – Instrumentation

Critical measurements taken for each test were applied load and deflection at midspan. Also measured were concrete strain on the top and bottom surface of the slab at midspan, deflection at each third-point, and slip of prestressing strands at one slab end. Data was recorded for all instrumentation through a data acquisition system recording at 2 Hz. A summary of the instrumentation is given in the following:

- Applied Load – The 40 ft setup used two 50 kip load cells, one at each load point. The 45 ft setup used a 250 kip load cell integral with the MTS actuator.
- Deflection – Two string potentiometers with a 50 in. maximum capacity were placed to either side of the slab at midspan. One additional string potentiometer with 25 in. maximum capacity was placed at each third point, centered on the slab width.
- Strain – Pi gauges with 100 mm gauge length and deformation capacities of 2 mm or 5 mm were affixed using studs attached with epoxy to the slab surface at the center of the slab width at midspan top and bottom.
- Strand-slip – Linear potentiometers were placed on three strands in the bottom layer of prestressing at one end of the slab. Strands chosen for instrumentation were the two exterior strands and the center strand of the five strands that had been exposed for half-cell potential testing (Figure 3.14).

Locations of instrumentation are shown on the schematics in Figure 3.17 and Figure 3.21.

Photos of the instrumentation are shown in Figure 3.24 to Figure 3.27.



Figure 3.24 – 50 kip load cell



Figure 3.25 – 50 in. string potentiometers at midspan



Figure 3.26 - Linear potentiometers at slab end



Figure 3.27 - Pi gauges at midspan (top and bottom)

3.6 – Post-Test Demolition and Inspection

After flexural testing slabs were broken apart at the failed region, and the extent of deterioration was examined in more detail with full access to all strands. Initial stages of this activity were conducted in the laboratory with hand tools, with more extensive efforts using a hydraulic jackhammer outside the laboratory to determine the full extent of corrosion near the failed region. Photographs from this process can be seen in Figure 3.28 and Figure 3.29.



Figure 3.28 – Post-test demolition in laboratory (Oyster Creek – Span 8 – Slab 12)



Figure 3.29 - Strands uncovered with jackhammer outside laboratory (Ward Creek – Span 1 – Slab 14)

3.7 – Materials Testing

Seven of the 12 slabs were cored to obtain more accurate measurements of concrete strength. Cores were obtained using a 4 in. (nominal) core drill as seen in Figure 3.30, which produced a core with an outer diameter of approximately 3.74 in. Ends of the core were then cut with a masonry saw and were tested in compression per ASTM C42 (2013) and ASTM C39 (2014), seen in Figure 3.31.



Figure 3.30 - Coring slab end (Ward Creek – Span 9 – Slab 6)



Figure 3.31 - Testing core in compression

Three samples of prestressing strand were removed from the ends of one slab (Ward Creek – Span 9 – Slab 7) to test in tension in order to determine the stress-strain curve. Strands were exposed via jackhammering the surrounding concrete, with direct impact of strands avoided in order to minimize damage (Figure 3.32). Strands from this end region displayed typical light

surface rust, and overall appeared to be in good condition with no section loss. Strands were tested in accordance with ASTM A1061 (2009), deviating from recommended test procedures by using standard tensioning chucks to grip the strand. This is not recommended by ASTM 1061 (2009) due to the potential for premature strand failure at the chuck, but was approved here due to ease of testing. Two of three strands tested failed away from the chuck, though indentations caused by chuck grips were evident on all strands tested. Typical strand failure by necking and rupture of wires can be seen in Figure 3.34.



Figure 3.32 – Strands exposed near slab end via jackhammer



Figure 3.33 - Tension test of prestressing strand



Figure 3.34 - Strand failure

After materials testing, the experimental program was complete. Results from all components of the experimental program are presented individually in Chapter 4, with the analysis of relationships between them in Chapter 5.

CHAPTER 4 – RESULTS

Results from laboratory and field tests are presented herein, with discussion following in Chapter 5. Analysis is presented in this chapter to the extent that it is needed to present and contextualize the results. Summaries of each test method and methods of presentation are shown in Sections 4.1 and 4.2, along with results from select tests. Results for each of the 12 slabs brought to the laboratory are then presented in Section 4.3, organized by slab.

4.1 – Field Data

4.1.1 – Photography and Visual Observation

Photographs taken in the field were aligned and merged using Adobe Photoshop in order to present consistent views of the slab soffits for the 12 slabs selected for laboratory testing, presented in Section 4.3. Additional photographs taken in the field are discussed here.

Immediately prior to slab removal by the contractor, patching material from Oyster Creek – Span 8 – Slab 11 was removed to examine the condition of the strands underneath. This slab was not one of the slabs selected for laboratory testing, but it was covered by a large icolastic patch that was fully delaminated (based on hammer tapping) across the full width of the slab. An overview of this region is visible in Figure 4.1. The slab soffit as seen before and after removal of the patch is shown in Figure 4.2. The strands on the left side of the slab not visible in Figure 4.2 are shown in Figure 4.3. All 11 strands in the bottom layer were fully corroded (100% section loss), and delamination extended above the first layer of strands.



Figure 4.1 - Area surrounding Oyster Creek - Span 8 - Slab 11



Figure 4.2 - Oyster Creek - Span 8 - Slab 11 at 26 ft, before (left) and after (right) removal of icolastic patch



Figure 4.3 – Left 3 strands, not visible in Figure 4.2

The most heavily deteriorated regions of the bridge generally coincided with the location of support blocks for the riprap retaining wall near the abutments. A photograph of this region at Ward Creek bridge – Span 9, is shown in Figure 4.4 (taken during slab replacement) and Figure 4.5 (after slab replacement).



Figure 4.4 - Deterioration of slabs above retaining wall blocks



Figure 4.5 - Wetting of slabs above retaining wall blocks

4.1.2 – Sounding

Sounding data is presented in Section 4.3. As discussed in Chapter 3, any region where a delamination was measured across the width of the slab soffit is recorded as delaminated. If a 1 ft region along the length of the slab is colored red, it therefore indicates that some portion of that region is delaminated and does not necessarily indicate that the entire area is delaminated. An example of this is shown in Figure 4.6, showing sounding data from 21 ft to 29 ft for Ward Creek – Span 9 – Slab 6. In this location, delamination was recorded somewhere across the width of the slab at locations marked at 23 ft and 24 ft.



Figure 4.6 - Presentation of sounding data

4.1.3 – Resistivity

Field conditions and practicality at times limited data collection. Resistivity readings were only possible in locations where all four probes of the resistivity meter could make contact with concrete, meaning no data is recorded for certain sections of deteriorated and patched slabs. Repeatability of measurement was identified as a concern early in the field inspection process. Measurements taken at approximately the same location on a slab by the same operator would regularly vary by approximately 10 kΩ-cm when re-measured, even for measurements taken within the same hour. This does not necessarily invalidate the readings, but it strongly suggests that it is inappropriate to compare resistivity values for one span with those of another.

Some discussion of the resistivity data and its analysis is necessary in order to present the results. In Chapter 2, two methods were discussed for interpreting data. One is to look at the resistivity values themselves, and the second is to look at regions of high and low resistivity within a concrete member, and compare them qualitatively. Unknown, varying saturation of concrete during field testing significantly limits the ability to use the first method, but the categories it uses to differentiate resistivity values may nevertheless be significant, due to the relationship between chloride permeability and resistivity being non-linear and captured by the resistivity categories shown in Table 4.1. Research discussed in Chapter 2 suggested values 3 times higher were more suitable for in-service structures (Liu, 2010), but lower values, such as 2 times higher, may be more appropriate for beams in wet conditions.

Table 4.1 - Resistivity Classes

	Concrete Resistivity Values (kΩ-cm)	
Permeability Class	Fully Saturated 4x8 Cylinder	Prior Research (3x Fully Saturated)
High	< 12	< 36
Moderate	12 - 21	36 - 63
Low	21 - 37	63 - 111
Very Low	37 - 254	111 - 762
Negligible	> 254	> 762

Resistivity data is frequently presented using contour plots. Given limited prior research and substantial uncertainty, contour lines must be chosen that allow for the variation in resistivity values to be visually apparent. In order to preliminarily examine the data and determine what intervals are appropriate the minimum, maximum, average, 25th percentile and 75th percentile resistivity values are displayed for each beam in Table 4.2. This was done for information taken from the field, as well as information taken from the laboratory.

Table 4.2 - Resistivity statistics, all tests

			Concrete Resistivity Values (k Ω -cm)				
			Minimum	25%	Average	75%	Maximum
Ward Creek	Span 1 - Slab 13	Field	9.0	36.7	55.0	77.3	91.2
		Laboratory	11.1	29.8	73.1	95.2	328
		<i>Difference</i>	<i>2.1</i>	<i>-6.9</i>	<i>18.1</i>	<i>17.9</i>	<i>236.8</i>
	Span 1 - Slab 14	Field	12.9	60.6	72.4	85.9	132.7
		Laboratory	7.2	36.4	53.1	65.7	346
		<i>Difference</i>	<i>-5.7</i>	<i>-24.2</i>	<i>-19.3</i>	<i>-20.3</i>	<i>213.3</i>
	Span 4 - Slab 5	Field	22.9	38.8	54.1	67.7	109.4
		Laboratory	9.3	37.8	56.2	70.4	205
		<i>Difference</i>	<i>-13.6</i>	<i>-1.0</i>	<i>2.0</i>	<i>2.7</i>	<i>95.6</i>
	Span 4 - Slab 6	Field	22.3	30.2	36.1	41.6	58.0
		Laboratory	9.0	51.2	74.7	87.2	340
		<i>Difference</i>	<i>-13.3</i>	<i>21.0</i>	<i>38.6</i>	<i>45.6</i>	<i>282.0</i>
	Span 9 - Slab 6	Field	7.4	18.9	23.8	29.3	39.0
		Laboratory	3.8	34.7	67.9	75.4	584
		<i>Difference</i>	<i>-3.6</i>	<i>15.8</i>	<i>44.1</i>	<i>46.1</i>	<i>545.0</i>
	Span 9 - Slab 7	Field	8.1	16.6	26.9	30.9	80.5
		Laboratory	1.4	23.3	46.8	64.4	237
		<i>Difference</i>	<i>-6.7</i>	<i>6.7</i>	<i>19.9</i>	<i>33.5</i>	<i>156.5</i>
Oyster Creek	Span 1 - Slab 13	Field	14.5	30.9	34.7	42.3	47.9
		Laboratory	10.1	51.4	76.7	97.6	249
		<i>Difference</i>	<i>-4.4</i>	<i>20.6</i>	<i>42.0</i>	<i>55.4</i>	<i>201.1</i>
	Span 1 - Slab 14	Field	14.0	26.6	35.8	41.0	112.3
		Laboratory	6.0	29.8	45.8	60.1	117.4
		<i>Difference</i>	<i>-8.0</i>	<i>3.3</i>	<i>10.0</i>	<i>19.1</i>	<i>5.1</i>
	Span 2 - Slab 4	Field	10.9	22.1	28.3	34.6	42.8
		Laboratory	7.1	36.0	78.2	73.9	702
		<i>Difference</i>	<i>-3.8</i>	<i>13.9</i>	<i>49.9</i>	<i>39.3</i>	<i>659.2</i>
	Span 2 - Slab 5	Field	8.3	16.3	24.0	29.8	47.3
		Laboratory	11.8	37.5	55.5	67.9	173
		<i>Difference</i>	<i>3.5</i>	<i>21.2</i>	<i>31.5</i>	<i>38.1</i>	<i>125.7</i>
	Span 8 - Slab 12	Field	10.7	23.6	31.6	33.9	135
		Laboratory	12.3	37.2	67.1	77.8	772
		<i>Difference</i>	<i>1.6</i>	<i>13.7</i>	<i>35.5</i>	<i>43.9</i>	<i>637.0</i>
	Span 8 - Slab 13	Field	15.7	32.6	39.1	47.8	59.3
		Laboratory	5.3	48.0	68.6	86.9	271
		<i>Difference</i>	<i>-10.4</i>	<i>15.4</i>	<i>29.5</i>	<i>39.1</i>	<i>211.7</i>
	Averages	Field	13.1	29.5	38.5	46.8	79.6
		Laboratory	7.9	37.8	63.6	76.9	360.4
		<i>Difference</i>	<i>-5.2</i>	<i>8.3</i>	<i>25.1</i>	<i>30.0</i>	<i>280.8</i>

Minimum values ranged from 9 to 22.9 k Ω -cm in the field and 1.4 to 12.3 k Ω -cm in the laboratory. Averages resistivity values for each slab in the field ranged from 23.8 to 72.4 k Ω -cm, while those recorded in the laboratory ranged from 45.8 to 78.2 k Ω -cm. Significantly, the difference between the field average and laboratory average for all slabs was an average of 25.1 k Ω -cm, which is significant relative to the ranges for the permeability classes presented in Table 4.1. It is likely inappropriate to use such classes in order to examine resistivity under unknown, varying moisture conditions, and therefore it is concluded here that resistivity values obtained in the field should only be used *qualitatively* without significant further research. Though the permeability classes are backed by substantial research when used on saturated 4x8 cylinders, resistivity collected here does not support their use for field measurement.

Distribution of the values in all tests suggests that contour intervals of 10 k Ω -cm would provide a minimum of four contour intervals for all tests. 95th percentile values ranged from 38.8 to 131 k Ω -cm for field data, and 80 to 308 k Ω -cm for laboratory data. Based on this, contours ranged from 0 to 120 k Ω -cm, a range which covers 99% of field resistivity measurements and 94% of laboratory resistivity measurements. The color scale used on all contour plots is shown in Figure 4.7, with light grey representing high resistivity values (lower permeability) and green representing low resistivity values (higher permeability).

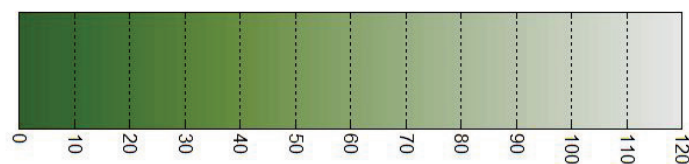


Figure 4.7 - Color scale, resistivity plots

For field data, resistivity values recorded in the middle of the width of the slab are generalized as resistivity for the entire width of the slab at that location.

4.2 – Laboratory Data

4.2.1 – Resistivity

Resistivity values obtained in the laboratory are displayed as contour plots in Section 4.3 in the manner discussed in Section 4.1.3.

4.2.2 – Half-Cell Potential

The favored method of interpreting half-cell potential values is to use contour plots. The “numeric magnitude technique” also presents a relationship between the half-cell potential values themselves and likelihood of corrosion. Using this technique, half-cell potentials more positive than -0.20 V are associated with a greater than 90% probability that corrosion is *not* occurring, while those more negative than -0.35 V are associated with a greater than 90% probability that corrosion *is* occurring (ASTM C876, 2009). It is therefore desirable to include those two values, -0.20 V and -0.35 V, as contours. Contour intervals of 0.05 V were therefore selected in order to allow for sufficient variation within that range.

In order to determine the limits of the contours graphed, maximum and minimum half-cell potential for each slab were examined. These are presented in Table 4.3. Disregarding outlier values of 1.286 V (Oyster Creek – Span 8 – Slab 13) and -1.419 V (Oyster Creek – Span 2 – Slab 4) the average maximum value is -0.029 V, and the average minimum is -0.513 V. Based

on these maxima and minima, displayed contours range from -0.05 V to -0.45 V, with intervals of 0.05 V. Though the range of -0.05 to -0.45 V covers only approximately 85% of all measured half-cell potentials, an additional approximately 9% of measurements fall within 0.05 V of this range, with the remaining 6% of measurements varying considerably. There is an inevitable trade-off when choosing the range of contours between providing clear visual differentiation for typical data (smaller range) and covering all values (larger range). The contours here were chosen to provide clear variation for most values of half-cell, instead of allowing the full range of values to be clearly visible. The standard color scale used on all contour plots is shown in Figure 4.8. Contours for -0.20 V and -0.35 V are labeled on all plots.

Table 4.3 – Maximum and minimum recorded half-cell potentials

		Half-Cell Potentials (V)	
		Minimum	Maximum
Ward Creek	Span 1 - Slab 13	-0.467	-0.014
	Span 1 - Slab 14	-0.447	-0.053
	Span 4 - Slab 5	-0.527	0.096
	Span 4 - Slab 6	-0.274	0.016
	Span 9 - Slab 6	-0.396	-0.066
	Span 9 - Slab 7	-0.648	-0.026
Oyster Creek	Span 1 - Slab 13	-0.943	-0.127
	Span 1 - Slab 14	-0.581	-0.026
	Span 2 - Slab 4	-1.419	-0.052
	Span 2 - Slab 5	-0.437	-0.088
	Span 8 - Slab 12	-0.401	-0.082
	Span 8 - Slab 13	-0.519	1.286

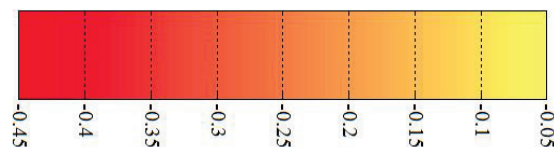


Figure 4.8 - Color scale, Half-Cell Potential plots.

4.2.3 – Moment-Deflection

Applied loads recorded by load cells during testing were converted into applied moments for the middle third of the slab by multiplying the load applied at each third point by the distance from the third point to the supports (13 ft for 40 ft long slabs; 14 ft – 8 in. for 45 ft long slabs).

In order to give context to moments measured during testing, maximum applied moments for each slab as measured in testing are compared to calculated *available moment capacity*, which is defined here as the moment capacity available for applied load on a slab (total moment capacity minus moment due to slab self-weight). This quantity is useful for comparison purposes, as it is the closest number comparable to live load moment capacity without making assumptions about asphalt and rail loading. Details of methods used to calculate moment capacities for prestressed concrete cored slabs are discussed in Chapter 5.

Available moment capacity was calculated using layered sectional analysis (Chapter 5), with assumed material properties (5000 psi concrete, 270 ksi prestressing strands). Moment due to self-weight is calculated with assumed concrete density of 150 pcf and cross-sectional areas as given in plans, with weight applied as a uniform distributed load over the span. Available moments calculated using these assumptions are shown in Table 4.4.

Table 4.4 – Calculated available moment capacities for undamaged slabs

	Moments (kip-ft)		
	Total	Self-Weight	Available
Ward Creek (40 ft)	545	84	461
Oyster Creek (45 ft)	764	133	631

Deflection at midspan was calculated as the average of the two deflection values recorded on each side of the slab at midspan. Deflections measured on the left and right sides of the slabs deviated from one another by a maximum of 0.38 in., in the testing of Oyster Creek – Span 8 – Slab 12, but generally were less than 0.1 in. during testing. Small asymmetries in slab deterioration and small imbalances in loading are likely the cause of these deviations. Applied moment is plotted versus measured deflection for all tested slabs in Section 4.3. In order to provide context to the experimentally measured moment-deflection responses, the calculated maximum moment applied by one wheel-line (one half of the load) of an HS20 truck is shown for reference on all plots. This moment is calculated to be 285 kip-ft (including impact factor of 1.3) for the 40 ft long Ward Creek slabs, and 341 kip-ft (including impact factor of 1.295) for the 45 ft long Oyster Creek slabs.

Results from individual tests are presented in Section 4.3, and are summarized in Table 4.5. The largest measured applied moments were more than 120% of those calculated using assumed material properties, showing these predictions to be conservative. This conservatism is discussed more extensively in Chapter 5.

Table 4.5 - Maximum moment values observed in laboratory testing

		Maximum Moment		
		Applied		Total
		kip-ft	%	kip-ft
Ward Creek	Span 1 - Slab 13	345	75%	429
	Span 1 - Slab 14	367	80%	451
	Span 4 - Slab 5	518	112%	602
	Span 4 - Slab 6	534	116%	618
	Span 9 - Slab 6	484	105%	568
	Span 9 - Slab 7	145	31%	229
Oyster Creek	Span 1 - Slab 13	351	56%	483
	Span 1 - Slab 14	496	79%	628
	Span 2 - Slab 4	767	122%	900
	Span 2 - Slab 5	766	121%	899
	Span 8 - Slab 12	332	53%	465
	Span 8 - Slab 13	613	97%	746

4.2.4 – Strain Data

Pi gauges used to measure strain at midspan gave inconsistent results, with either partial or complete debonding of the epoxy to the concrete surface occurring in at least one of the pi gauges in 5 of 12 tests, and no sufficiently flat surface available to place a pi gauge in an additional 5 of 12 tests. Data from top pi gauges was available for 10 of 12 slabs, and is presented in Table 4.6. Values shown are applied top strains (as measured during testing), and do not include any strain already present in the slab due to self-weight and prestressing. Average maximum applied top strain was 2830 $\mu\epsilon$, with maximum applied top strain of 3430 $\mu\epsilon$.

Table 4.6 - Maximum measured top strain, all slabs

		Applied Top Strain ($\mu\epsilon$)	Applied Moment (kip-ft)
Ward Creek	Span 1 - Slab 13	-3270	345
	Span 1 - Slab 14	-2770	367
	Span 4 - Slab 5	-3430	518
	Span 4 - Slab 6	-	-
	Span 9 - Slab 6	-2120	484
	Span 9 - Slab 7	-1950	145
Oyster Creek	Span 1 - Slab 13	-	-
	Span 1 - Slab 14	-2870	496
	Span 2 - Slab 4	-3100	767
	Span 2 - Slab 5	-3020	766
	Span 8 - Slab 12	-2440	332
	Span 8 - Slab 13	-3320	613

4.2.5 – Strand Slip

Linear potentiometers placed at slab ends during testing did not record any slipping of prestressing strands relative to the concrete in any tests, suggesting that development of prestressing is not a concern with the cored slab standard as produced in the 1970s.

4.2.6 – Concrete Cores in Compression

Concrete cores were drilled from each of the 6 slabs from Ward Creek Bridge. After determining little variation in concrete strength, an additional core was taken from one slab from Oyster Creek Bridge, which displayed strength in the same range as those taken previously. Compressive strengths for all 7 cores are given in Table 4.7.

Table 4.7 - Concrete core testing in compression

Bridge	Span	Slab	Compressive Strength (psi)
Ward Creek	1	13	7620
		14	7560
	4	5	6870
		6	6700
	9	6	10460*
		7	6400
Oyster Creek	1	13	7620
Average Strength (psi):			7130

**Outlier, not included in average strength*

All cores exceeded the assumed concrete strength of 5000 psi used in NCDOT analysis and in the calculation of available moment for an undamaged slab, with measured concrete strengths for 6 of the cores ranged from 6400 to 7620 psi. A typical tested core is shown in Figure 4.9. The core taken from Ward Creek – Span 9 – Slab 6 appeared to include a darker stone aggregate in comparison to the varied river rock present in other cores, and this core was substantially stronger, with a compressive strength of 10,460 psi. Average compressive strength for the cores (excluding Ward Creek – Span 9 – Slab 6, taken as an outlier) was 7130 psi. Including that outlier, the average is 7600 psi. Density of cores varied from 142 to 150 pcf, with median value of 145 pcf.



Figure 4.9 - Concrete core from Ward Creek – Span 1 – Slab 13

4.2.7 – Prestressing Strands in Tension

Of three prestressing strands removed from the end of Ward Creek – Span 9 – Slab 7, two were extracted in good condition, and displayed similar stress-strain response in testing. Both strands exceeded the required rupture strength of 270 ksi, with measured rupture strength f_{pu} as 285 and 289 ksi, at rupture strains of 0.055 and 0.06, respectively.

4.2.8 – Condition of strands at failed region

Though a majority of slabs exhibited some rupturing of strands during testing, loading (displacement control) was continued until ultimate failure by crushing of top compression concrete. Careful demolition of slabs in the vicinity of the failed region after testing allowed for documentation of the condition of all strands in the failed region. Photographs and strand

information are presented for each slab tested. Information about strand corrosion is presented on cross-sections like the one shown in Figure 4.10. Strands that were ruptured during testing are marked with an 'R'. Even after removal of concrete, the precise extent of corrosion for each strand is difficult to determine. Estimated extent of corrosion is represented visually by showing varying amounts of each strand in red. In Figure 4.10, for example, the bottom-left strand had been described as “moderate to heavy rusting & pitting. At least 4 wires ruptured,” while the middle strand was described as, “Heavy Rust. More or less completely gone.” Though depicted as a cross-section, deterioration recorded is anywhere in the failed region, here 19 to 21 ft. All prestressing strands not otherwise noted as deteriorated displayed light to very light surface rust.

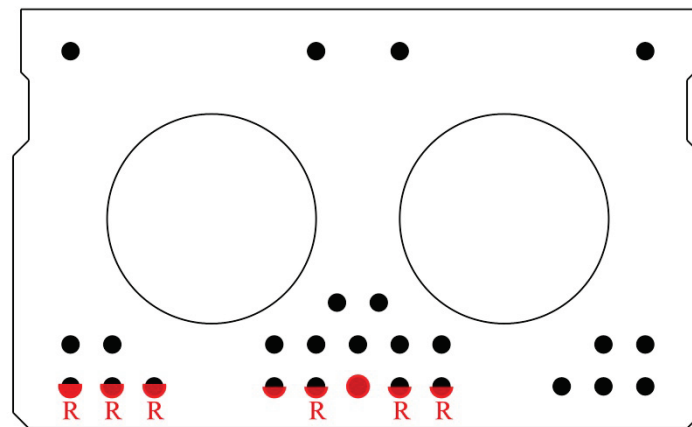


Figure 4.10 - Oyster Creek - Span 1 - Slab 14 - 19 to 21 ft

4.3 – Slab Results

Information from field and laboratory testing is presented slab-by-slab in Sections 4.3.1 to 4.3.12. For each slab, details from flexural testing and moment-deflection response of each slab are presented, along with any specifics relating to non-destructive evaluation that merit

explanation. Most data from testing is brought together into Table 4.8 to Table 4.19, so that comparisons between different data can be made easily in Chapter 5.

4.3.1 – Ward Creek – Span 1 – Slab 13

At the conclusion of field inspection, Ward Creek – Span 1 – Slab 13 was described as having “no spalling, but audible delamination over 6 ft length with parallel longitudinal cracks near midspan.”

Flexural testing produced a total maximum moment of 429 kip-ft, corresponding to an applied moment of 345 kip-ft, 75% of the calculated available moment capacity. Measured applied top strain was 3270 $\mu\epsilon$. The moment-deflection response recorded during testing is shown in Figure 4.11.

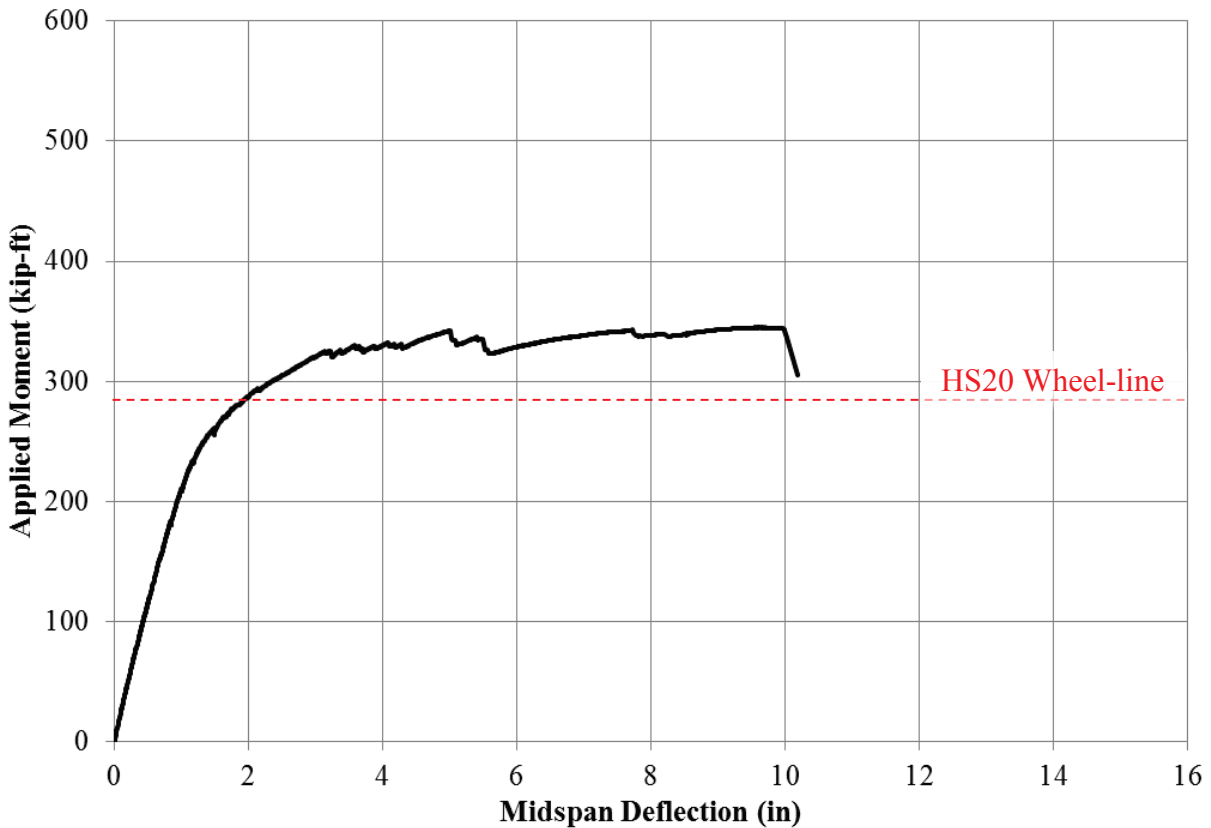


Figure 4.11 - Ward Creek - Span 1 - Slab 13 flexural test results

Examination of the slab after testing revealed the failure region, 17 to 20 ft, was a region of audible delamination. Stirrups showed significant section loss (~50%), with 6 of 11 bottom strands rusty, pitted, and significantly damaged. All strands above the bottom layer were in good condition. Photos of the failed region are shown in Figure 4.12 to Figure 4.14.



Figure 4.12 - Ward Creek - Span 1 - Slab 13, soffit at failed region

Figure 4.12 shows 2 photographs taken immediately after testing. The delaminated concrete had spalled off during testing, revealing moderate to heavy corrosion of strands near several corroded stirrups.



Figure 4.13 - Ward Creek - Span 1 - Slab 13, crushed concrete removed

Figure 4.13 shows the cross-section in the failed region after concrete was removed.



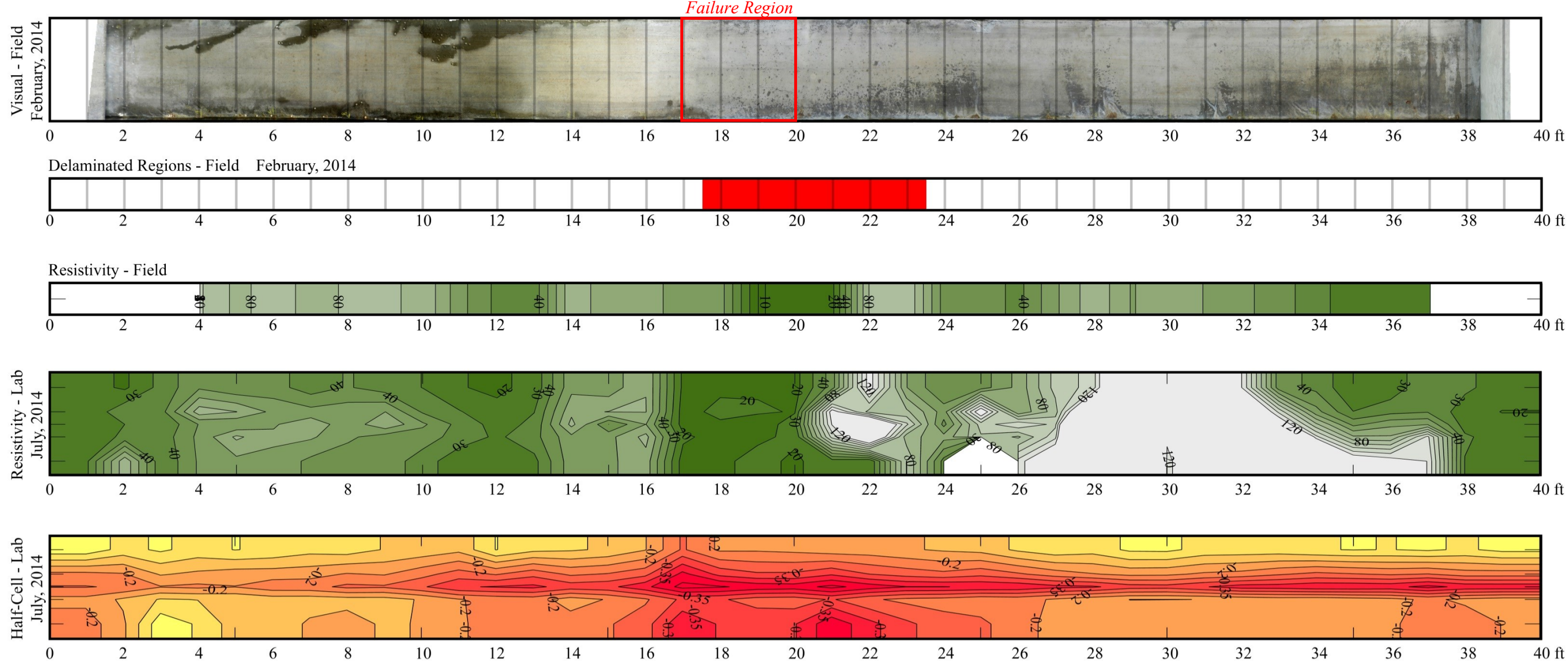
Figure 4.14 - Ward Creek - Span 1 - Slab 13, rusted, ruptured strands

Figure 4.14 shows the condition of several strands in the bottom layer after concrete and stirrups were removed, with rupture and section loss of strands visually apparent.

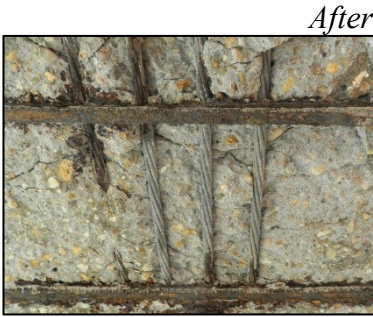
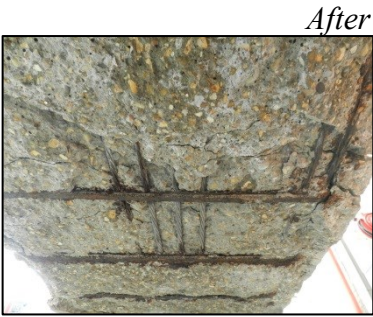
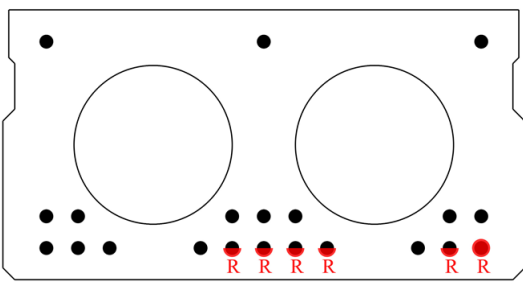
Table 4.8 – Ward Creek – Span 1 – Slab 13

Qualitative Description: No spalling, but audible delamination over 6 ft length with parallel longitudinal cracks near midspan

Priority Maintenance Request: Yes



Region of Failure - 17 to 20 ft



Average Resistivity	73.1 kΩ-cm	Applied Moment	
Average Half-Cell	-0.219 V	345 kip-ft	75%
Cylinder Strength	7620 psi		

4.3.2 – Ward Creek – Span 1 – Slab 14

At the conclusion of field inspection, Ward Creek – Span 1 – Slab 14 was described as having “two visible, shallow spalls with rust stains near stirrups, surrounded by audible delamination (no visible cracks).”

This slab was one of the first on which half-cell potential testing was performed. The electrode used was a liquid-based copper-copper sulfate reference electrode, with a salt bridge used to allow measurements on the slab soffit. This setup proved fragile, and data were only recorded on 2 of 5 strands, leaving an incomplete half-cell potential contour plot in Table 4.9. This electrode was replaced with a more robust gel-based electrode for subsequent tests.

Flexural testing produced a total maximum moment of 451 kip-ft, corresponding to an applied moment of 367 kip-ft, 80% of the calculated available moment capacity. Measured applied top strain was 2770 $\mu\epsilon$. The moment-deflection response recorded during testing is shown in Figure 4.15.

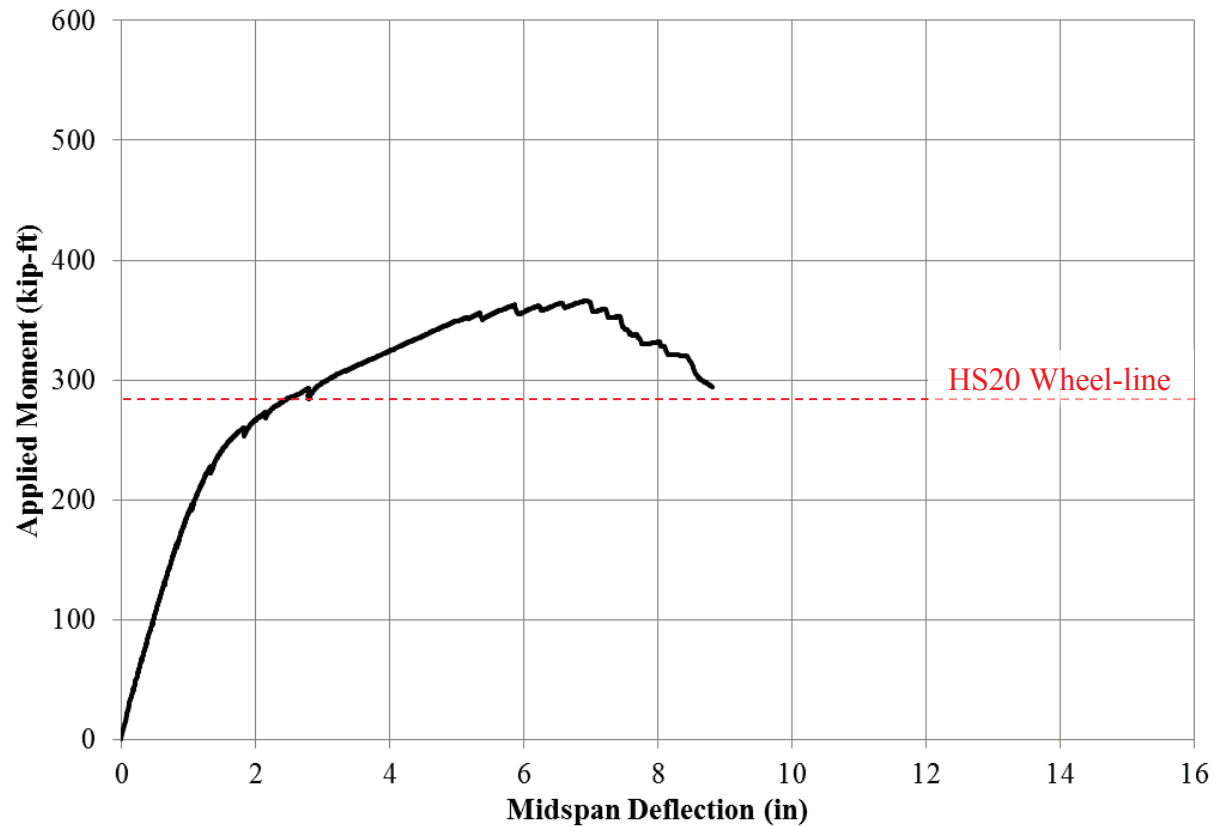


Figure 4.15 - Ward Creek - Span 1 - Slab 14 flexural test results

The failure region, 17 to 21 ft, was a region with a single spall with rust stains surrounded by audible delamination. Stirrups showed some corrosion, with 5 of 11 bottom strands displaying some pitting near the stirrups, and minor rusting of 4 additional strands. All strands above the bottom layer were in good condition. Photos of the failed region are shown in Figure 4.16 and Figure 4.17.



Figure 4.16 - Ward Creek - Span 1 - Slab 14, strands at failed region

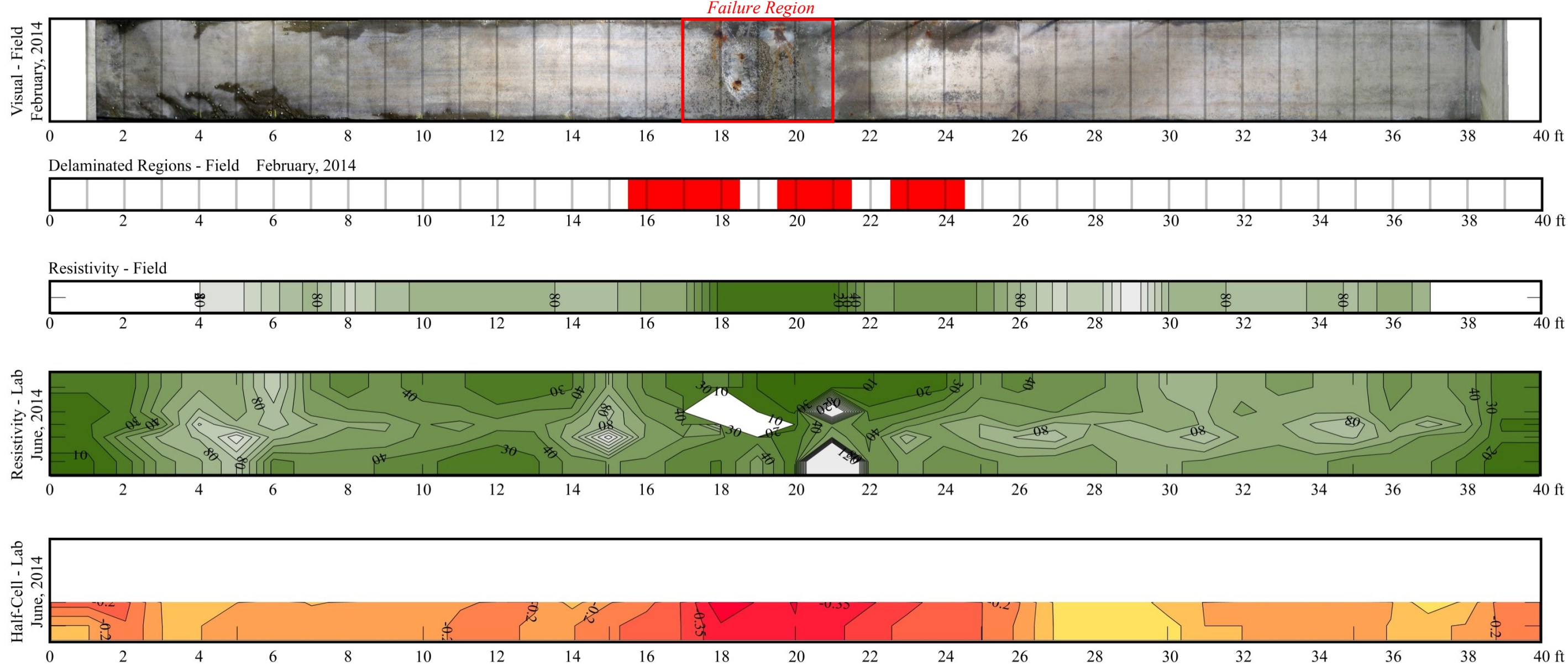


Figure 4.17 - Ward Creek - Span 1 - Slab 14, overview of failed region

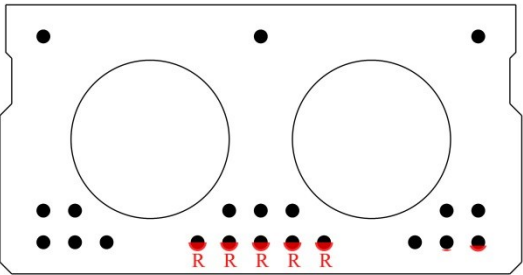
Table 4.9 – Ward Creek – Span 1 – Slab 14

Qualitative Description: Two visible, shallow spalls with rust stains near stirrups, surrounded by audible delamination (no visible cracks)

Priority Maintenance Request: Yes



Region of Failure - 17 to 21 ft



Average Resistivity	53.1 kΩ-cm	Applied Moment	
Average Half-Cell	-0.205 V	367 kip-ft	80%
Cylinder Strength	7560 psi		

4.3.3 – Ward Creek – Span 4 – Slab 5

At the conclusion of field inspection, Ward Creek – Span 4 – Slab 5 was described as having “no apparent deterioration.”

During measurement of half-cell potential, values for the middle strand were observed to diverge noticeably from the values measured in other strands of the same slab. The electrode, connecting wire, and connection to the strand were all examined as possible sources of error, but no obvious issue was found. The contour plot includes this data, though it remains incongruous with that found in all other plots.

Flexural testing produced a total maximum moment of 602 kip-ft, corresponding to an applied moment of 518 kip-ft, 112% of the calculated available moment capacity. Measured applied top strain was 3430 $\mu\epsilon$, the maximum recorded for all slabs. The moment-deflection response recorded during testing is shown in Figure 4.18.

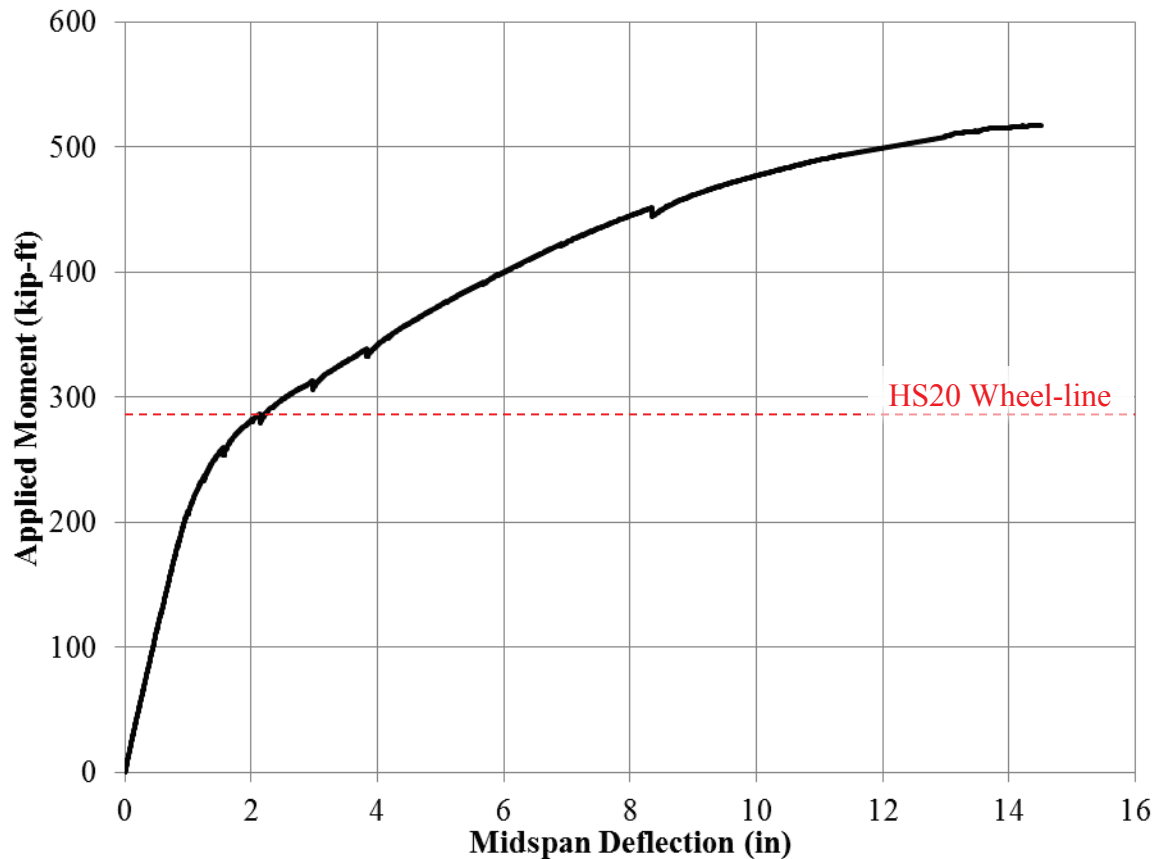


Figure 4.18 - Ward Creek - Span 4 - Slab 5 flexural test results

The failure region, 16 to 18 ft, was a region with no visible deterioration. All strands were in good condition, with only typical light surface rust on some strands. Photos of the failure region are shown in Figure 4.19. Figure 4.20 shows a closer view of a typical group of strands.



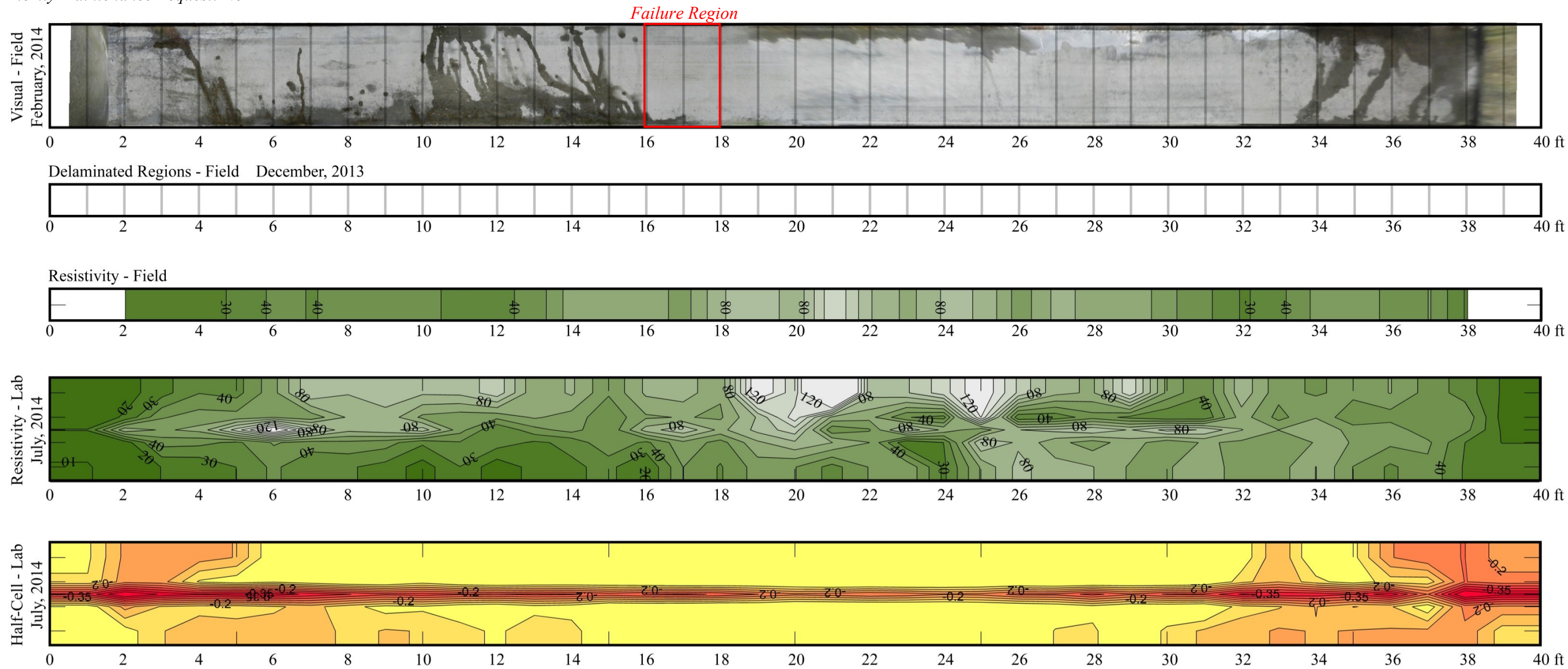
Figure 4.19 - Ward Creek - Span 4 - Slab 5, overview of failed region



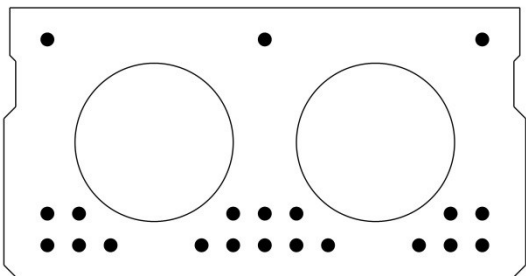
Figure 4.20 – Ward Creek - Span 4 - Slab 5, typical strands

Table 4.10 – Ward Creek – Span 4 – Slab 5

Qualitative Description: No apparent deterioration
Priority Maintenance Request: No



Region of Failure - 16 to 18 ft



Average Resistivity	56.2 kΩ-cm	Applied Moment	
Average Half-Cell	-0.087 V	518 kip-ft	112%
Cylinder Strength	6870 psi		

4.3.4 – Ward Creek – Span 4 – Slab 6

At the conclusion of field inspection, Ward Creek – Span 4 – Slab 6 was described as having “six shallow patched spalls underneath stirrups; two isolated areas of delamination; no widespread deterioration.”

Flexural testing produced a total maximum moment of 618 kip-ft, corresponding to an applied moment of 534 kip-ft, 116% of the calculated available moment capacity. The top pi gauge debonded during testing. The moment-deflection response recorded during testing is shown in Figure 4.22. This was the strongest of the 6 Ward Creek slabs.

During testing, this slab reached deflections close to the maximum achievable with the 40 ft test setup. Results for Ward Creek – Span 4 – Slab 6 are shown in Figure 4.21. Initial loading proceeded smoothly until 11.6 in. midspan deflection and 519 kip-ft applied moment, at which point the hydraulic jacks were stroked out. Supplemental loading jacks affixed to the setup were used to continue testing, but binding of threaded rods produced erroneous load readings, circled in Figure 4.21. The decision was made to fully unload the beam and reload with better sheathing of the threaded rods. Reloading proceeded smoothly, with maximum midspan deflection of 14.0 in., and maximum applied moment of 525 kip-ft. It can thus be concluded that the slab was close to its maximum capacity at the end of the initial loading. Permanent deformation was 1.70 in. after unloading and approximately 2.5 hours with no applied load.

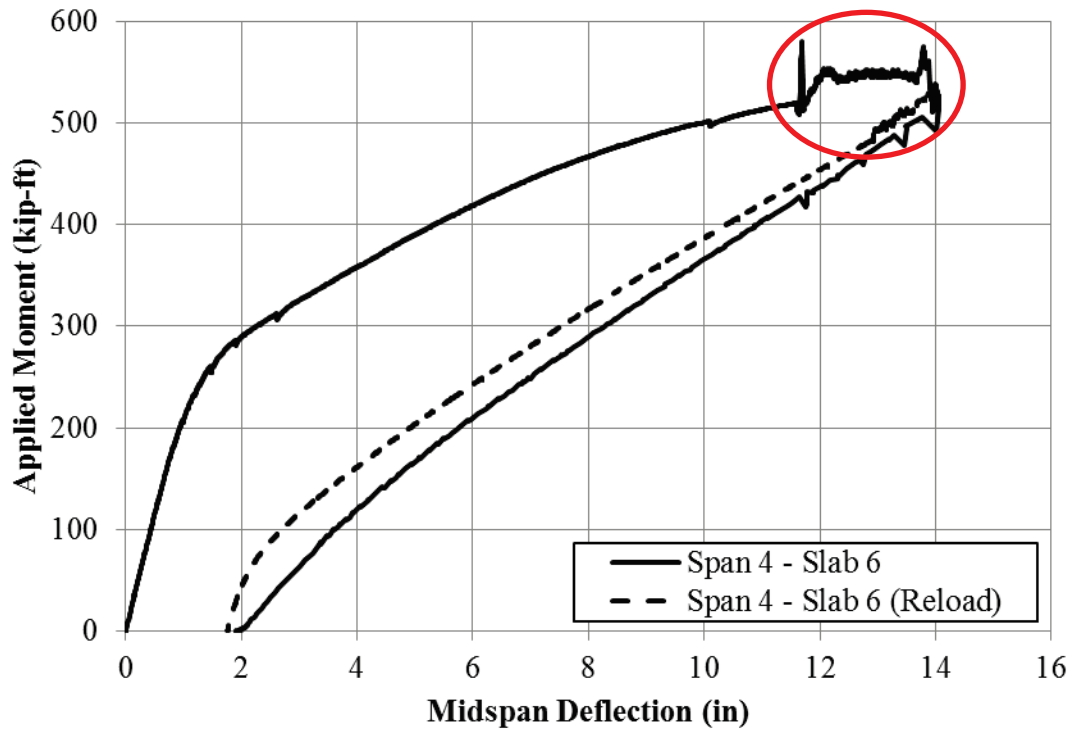


Figure 4.21 - Ward Creek - Span 4 - Slab 6 flexural testing results

Removing erroneous load readings and combining the two tests gives the response shown in Figure 4.22.

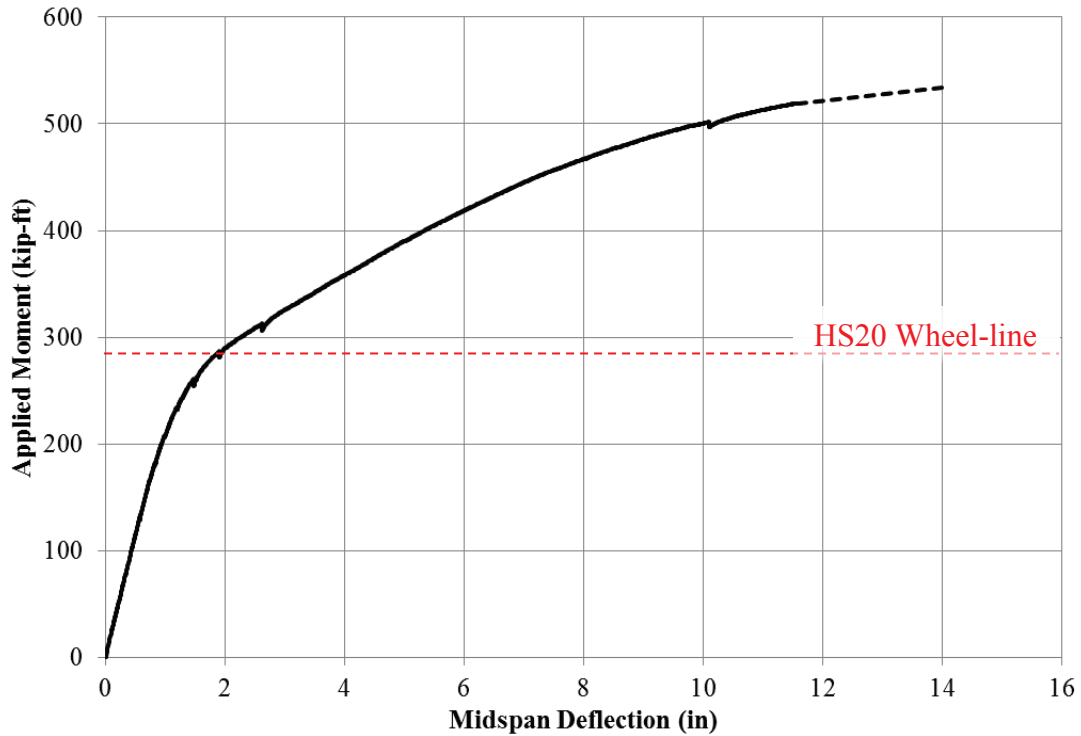


Figure 4.22 - Ward Creek - Span 4 - Slab 6 flexural test results combined

The failure region, 16 to 19 ft, contained no visible deterioration. All strands were in very good condition, with only faint discoloration. Photos of the failure region are shown in Figure 4.23.

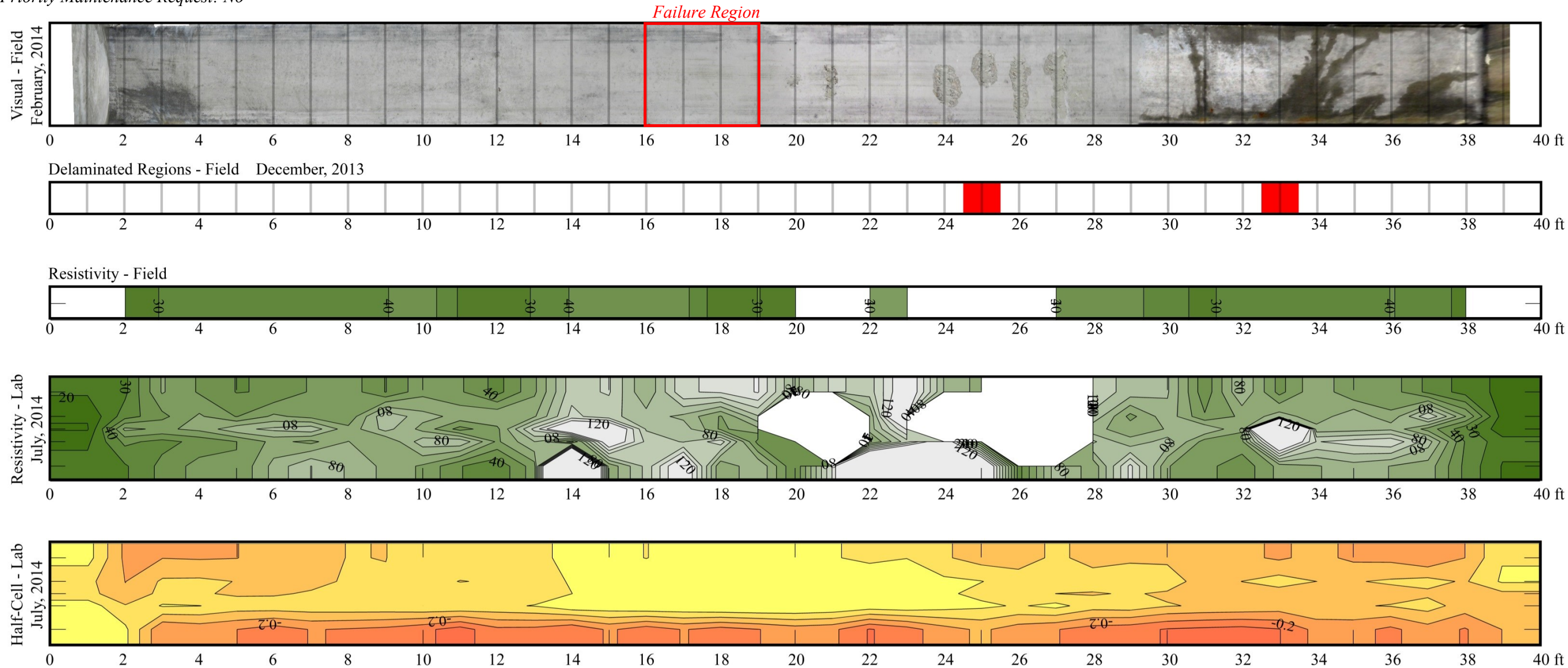


Figure 4.23 - Ward Creek - Span 4 - Slab 6, failed region

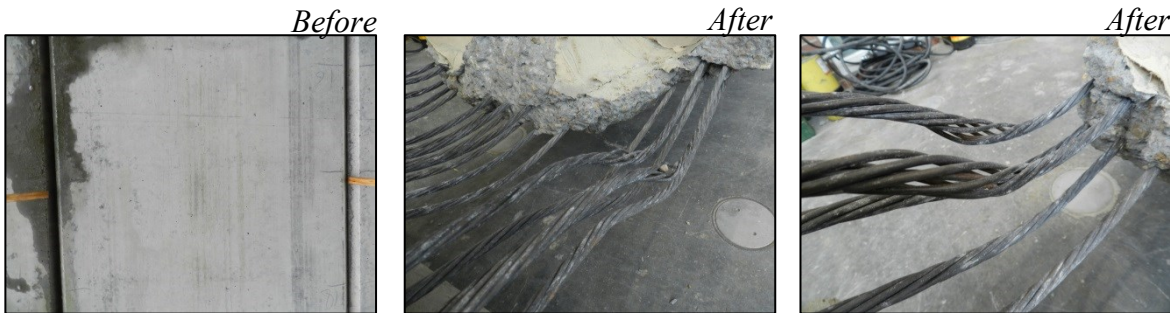
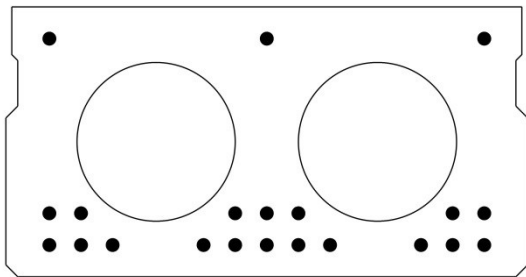
Table 4.11 – Ward Creek – Span 4 – Slab 6

Qualitative Description: Six shallow patched spalls underneath stirrups; two isolated areas of delamination; no widespread deterioration.

Priority Maintenance Request: No



Region of Failure - 16 to 19 ft



Average Resistivity	74.7 kΩ-cm	Applied Moment	
Average Half-Cell	-0.100 V	534 kip-ft	116%
Cylinder Strength	6700 psi		

4.3.5 – Ward Creek – Span 9 – Slab 6

At the conclusion of field inspection, Ward Creek – Span 9 – Slab 6 was described as having “a variety of patches, somewhat deeper spalls with rust stains, and visible/audible delamination under stirrups.”

Flexural testing produced a total maximum moment of 568 kip-ft, corresponding to an applied moment of 484 kip-ft, 105% of the calculated available moment capacity. Measured applied top strain was 2120 $\mu\epsilon$. The moment-deflection response recorded during testing is shown in Figure 4.24.

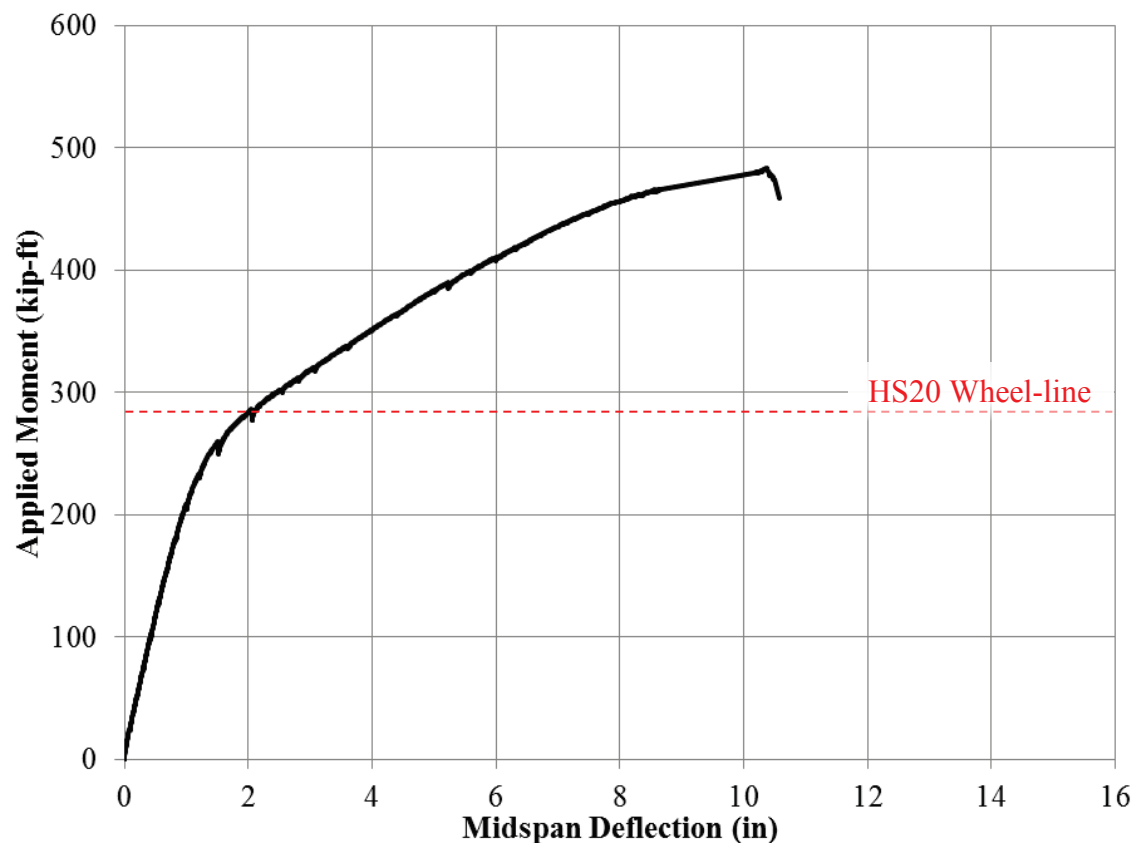


Figure 4.24 - Ward Creek - Span 9 - Slab 6 flexural test results

The failure region, 19 to 21 ft, contained a small spall with a rust stain. Stirrups showed some corrosion, with 5 of 11 bottom strands displaying some pitting near the stirrups, and minor rusting of 4 additional strands. All strands above the bottom layer were in good condition. A photo showing strand conditions in the area surrounding the failure region is shown in Figure 4.25.

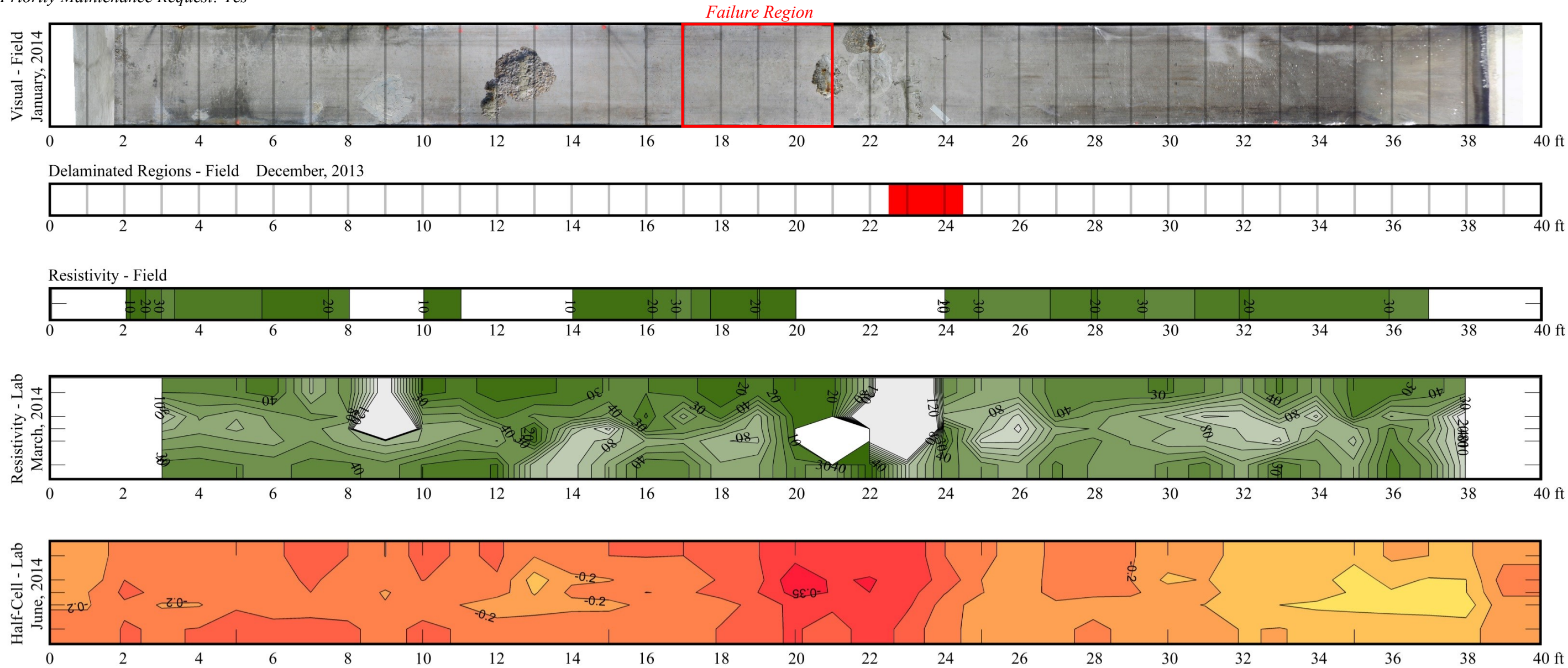


Figure 4.25 - Ward Creek - Span 9 - Slab 6, strands exposed around failure region

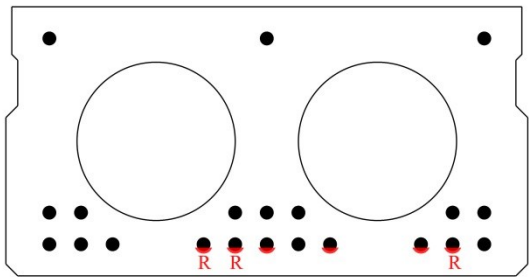
Table 4.12 – Ward Creek – Span 9 – Slab 6

Qualitative Description: Variety of patches, somewhat deeper spalls with rust stains, and visible/audible delamination under stirrups.

Priority Maintenance Request: Yes



Region of Failure - 17 to 21 ft



Average Resistivity	67.9 kΩ-cm	Applied Moment	
Average Half-Cell	-0.212 V	484 kip-ft	105%
Cylinder Strength	10455 psi		

4.3.6 – Ward Creek – Span 9 – Slab 7

At the conclusion of field inspection, Ward Creek – Span 9 – Slab 7 was described as having “deep spalls and patches with extensive longitudinal and transverse rust stains over ~9-ft region.”

Flexural testing produced a total maximum moment of 229 kip-ft, corresponding to an applied moment of 145 kip-ft, 31% of the calculated available moment capacity. This was the weakest of the 6 Ward Creek slabs. Measured applied top strain was 1950 $\mu\epsilon$. The moment-deflection response recorded during testing is shown in Figure 4.26.

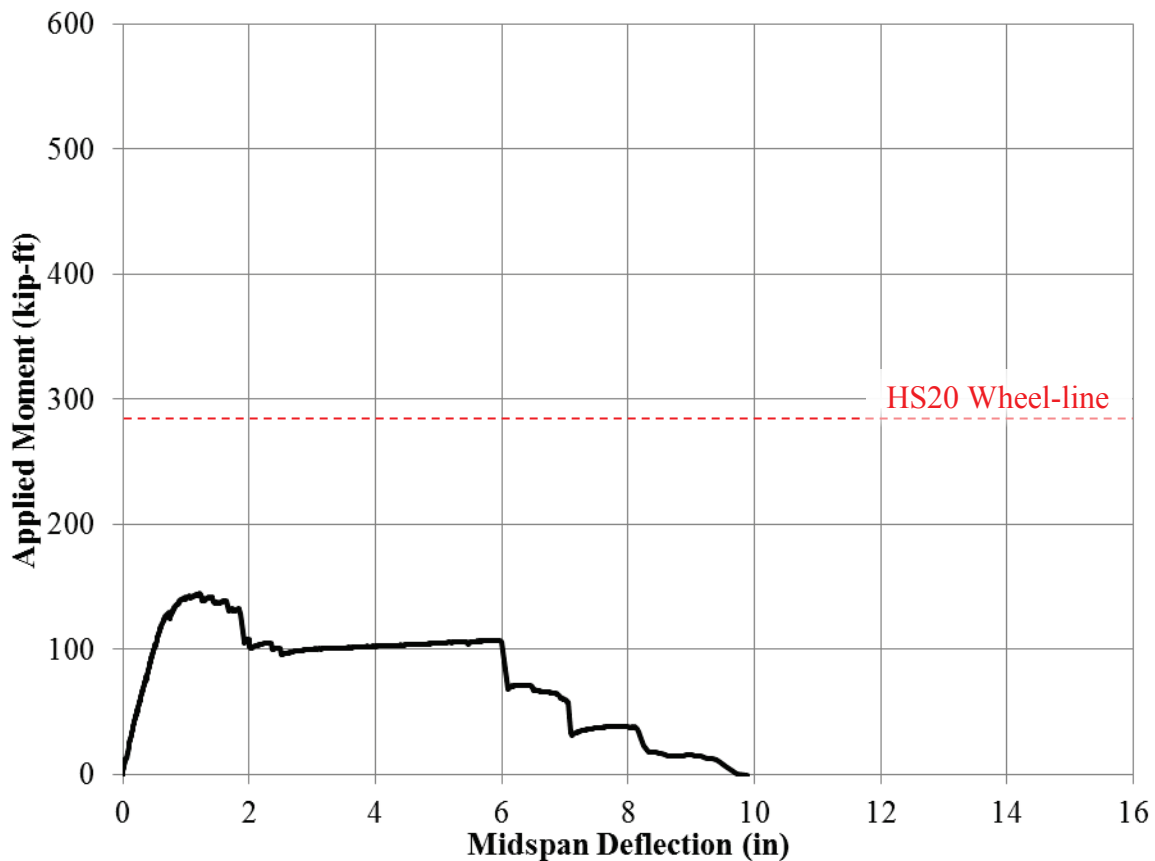


Figure 4.26 - Ward Creek - Span 9 - Slab 7 flexural test results

The failure region, 20 to 23 ft, was in a region with a large patched spall with some prestressing strands visible, and heavy longitudinal and transverse rust stains. The bottom parts of stirrups were completely corroded, and 8 of 11 bottom strands were completely rusted (100% section loss), with 7 additional strands in the bottom and second layer displaying moderate rust. Photos of the failure region are shown in Figure 4.27 to Figure 4.30.



Figure 4.27 - Ward Creek - Span 9 - Slab 7, delamination visible at failed region



Figure 4.28 - Ward Creek - Span 9 - Slab 7, bottom layer of strands at failure plane after testing



Figure 4.29 - Ward Creek - Span 9 - Slab 7, patching material bonded with strands

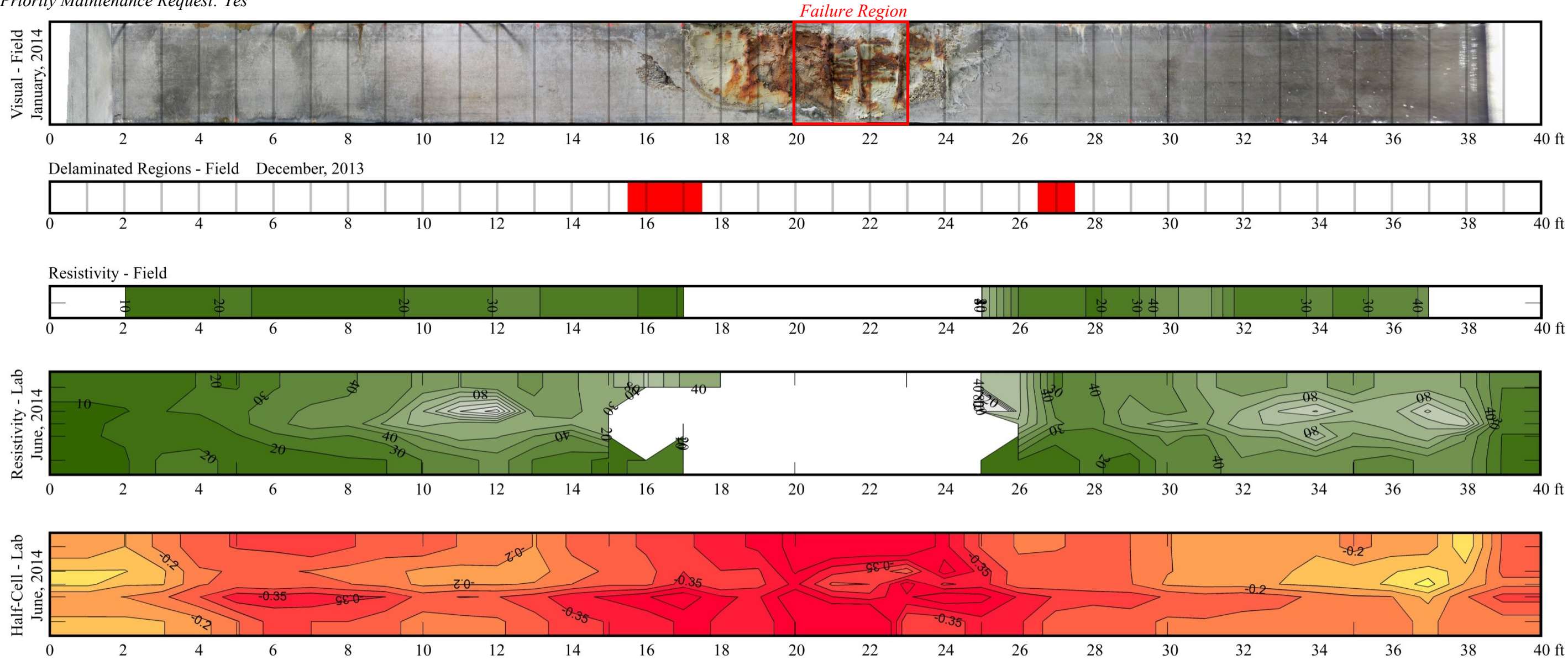


Figure 4.30 - Ward Creek - Span 9 - Slab 7, heavy rust and pitting extends through patched region

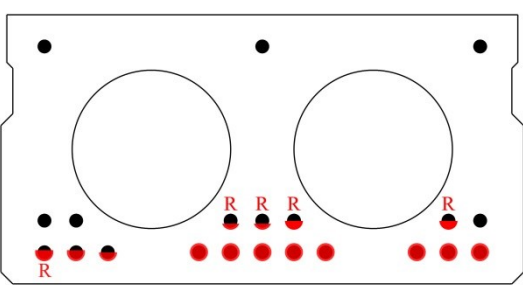
Table 4.13 – Ward Creek – Span 9 – Slab 7

Qualitative Description: Deep spalls and patches with extensive longitudinal and transverse rust stains over ~9-ft region.

Priority Maintenance Request: Yes



Region of Failure - 20 to 23 ft



Average Resistivity	46.8 kΩ-cm	Applied Moment	
Average Half-Cell	-0.275 V	145 kip-ft	31%
Cylinder Strength	6400 psi		

4.3.7 – Oyster Creek – Span 1 – Slab 13

At the conclusion of field inspection, Oyster Creek – Span 1 – Slab 13 was described as having “an ~11 ft heavily spalled and delaminated region with extensive rust stains”

Flexural testing produced a total maximum moment of 483 kip-ft, corresponding to an applied moment of 351 kip-ft, 56% of the calculated available moment capacity. The top pi gauge debonded during testing. The moment-deflection response recorded during testing is shown in Figure 4.31.

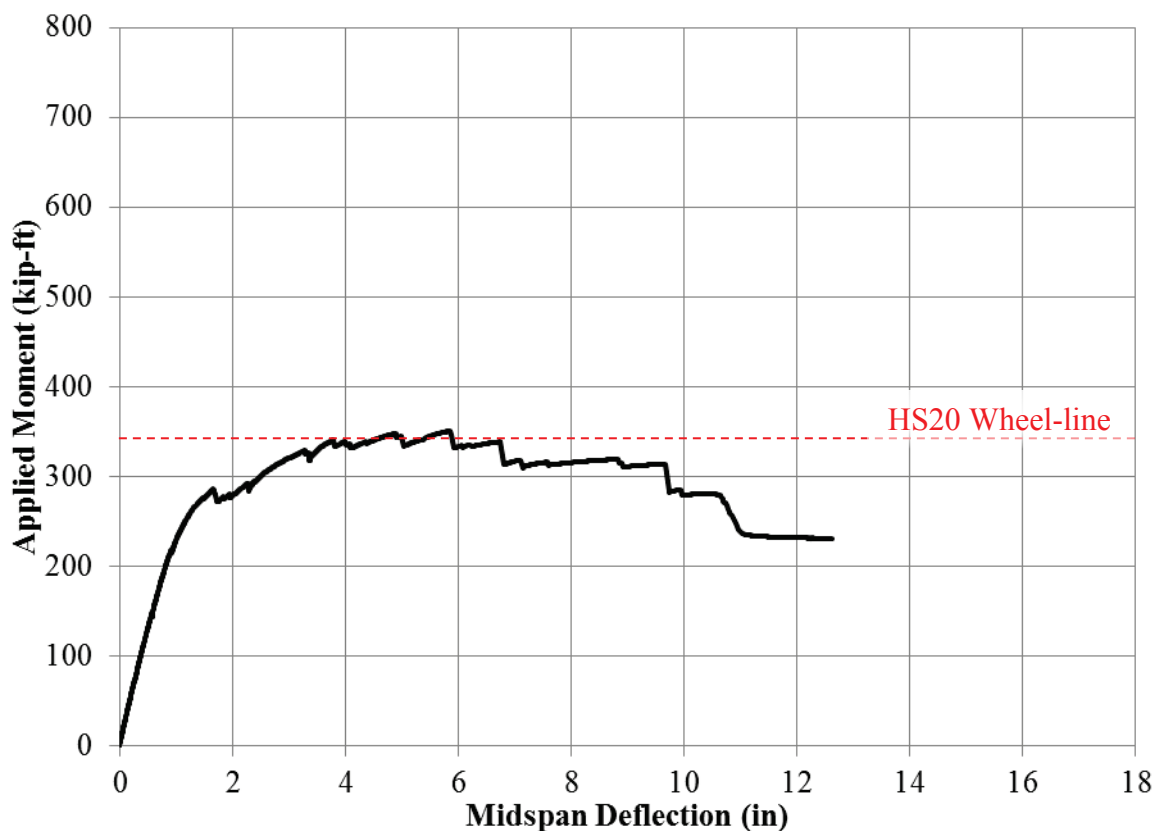


Figure 4.31 - Oyster Creek - Span 1 - Slab 13 flexural test results

The failure region, 20 to 23 ft, contained extensive patching with pronounced longitudinal rust stains, visually similar to Ward Creek – Span 9 – Slab 7 discussed in Section 4.3.6. Nine of eleven bottom strands were either completely corroded or had approximately one wire out of seven left, while the two remaining strands had moderate rusting and pitting. All strands above the bottom layer were in good condition, with only surface rust or light surface rust. A photo of the failure region is shown in Figure 4.32, showing some patching material spalled off during testing while other patching material remained bonded to the concrete above.



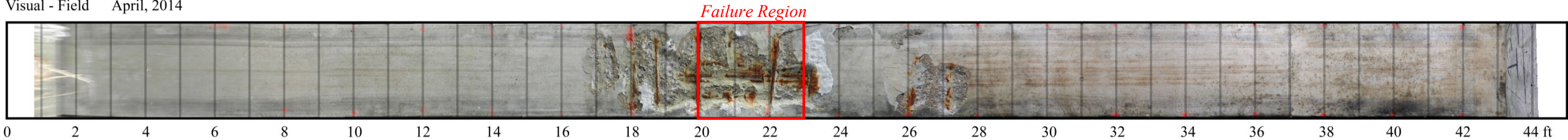
Figure 4.32 - Oyster Creek - Span 1 - Slab 13, slab soffit after failure

Table 4.14 – Oyster Creek – Span 1 – Slab 13

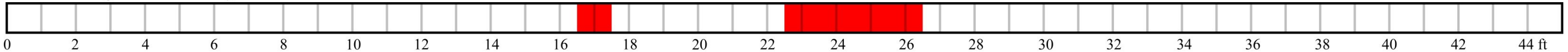
Qualitative Description: ~11-ft heavily spalled and delaminated region with extensive rust stains

Priority Maintenance Request: Yes

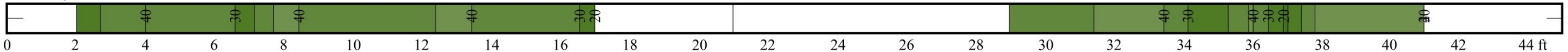
Visual - Field April, 2014



Delaminated Regions - Field May, 2014



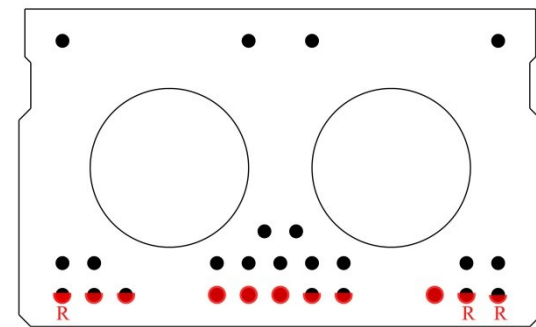
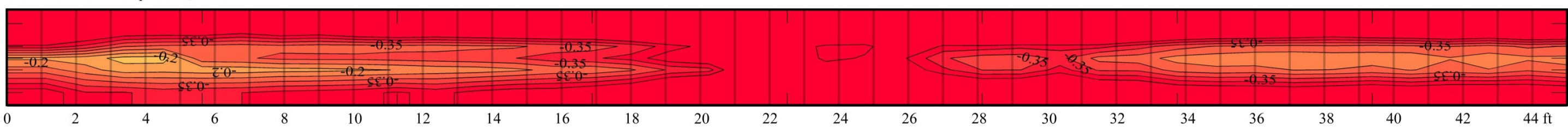
Resistivity - Field



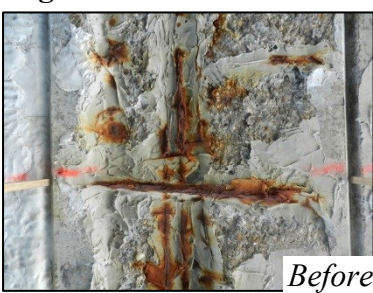
Resistivity - Lab September, 2014



Half-Cell - Lab September, 2014



Region of Failure - 20 to 23 ft



Average Resistivity	76.7 kΩ-cm	Applied Moment	
Average Half-Cell	-0.452 V	351 kip-ft	56%
Cylinder Strength	7620 psi		

4.3.8 – Oyster Creek – Span 1 – Slab 14

At the conclusion of field inspection, Oyster Creek – Span 1 – Slab 14 was described as having a “moderate ~5-ft spalled region with longitudinal rust stains.”

Flexural testing produced a total maximum moment of 628 kip-ft, corresponding to an applied moment of 496 kip-ft, 79% of the calculated available moment capacity. Measured applied top strain was 2870 $\mu\epsilon$. The moment-deflection response recorded during testing is shown in Figure 4.33.

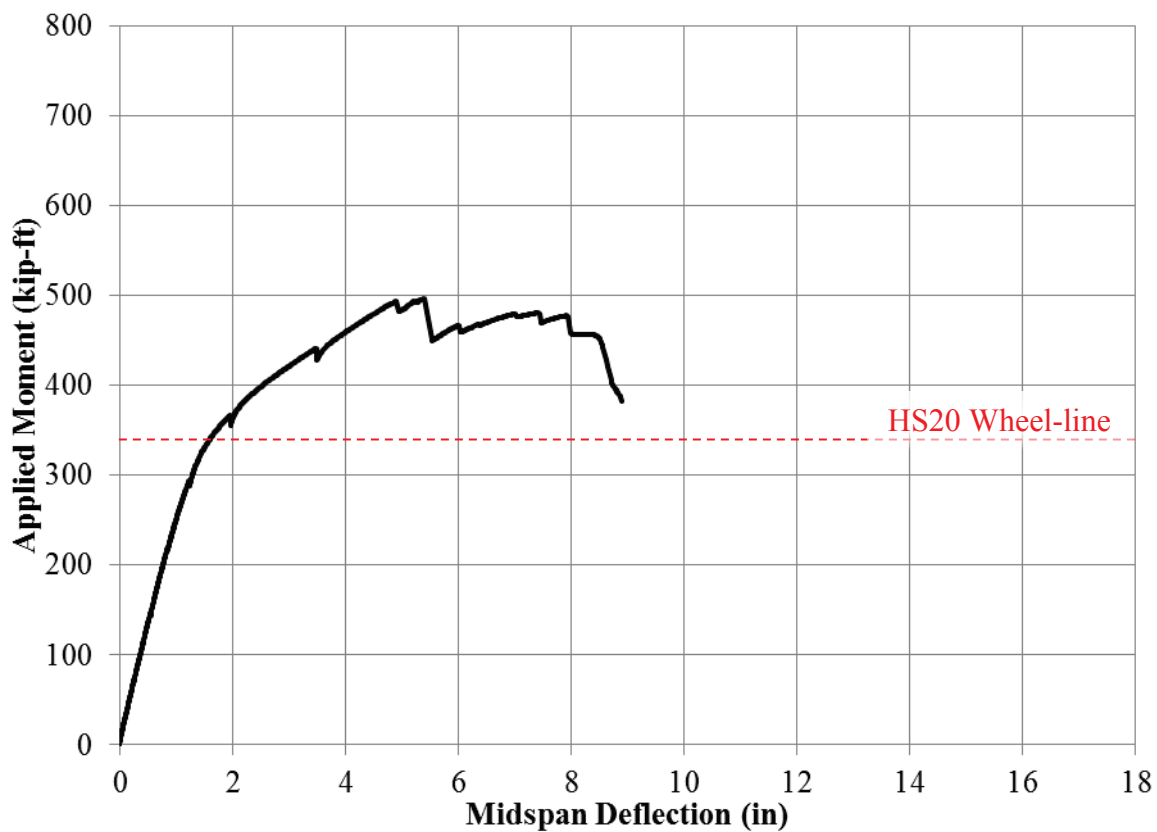


Figure 4.33 - Oyster Creek - Span 1 - Slab 14 flexural test results

The failure region, 18 to 22 ft, contained a patchwork of spalls and patching materials, with transverse and indistinct longitudinal rust stains. Eight of eleven bottom strands ranged from moderate surface rust and pitting to heavy rust and loss of wires, while the three right bottom strands had only light surface rust. All strands above the bottom layer were in good condition. Photos of the failure region are shown in Figure 4.34 and Figure 4.35.



Figure 4.34 - Oyster Creek - Span 1 - Slab 14, slab soffit after failure, showing broken stirrup



Figure 4.35 - Oyster Creek - Span 1 - Slab 14, failed region

Figure 4.36 to Figure 4.38 show steel removed from the failure. The strands are laid out in the same order (left to right) as they are shown in the cross-section in Table 4.15.



Figure 4.36 - Oyster Creek - Span 1 - Slab 14, bottom layer strands from failed region

Figure 4.37 shows pieces of prestressing strands cut from the second layer of strands in this slab. Their condition is typical of almost all strands above the bottom layer.



Figure 4.37 - Oyster Creek - Span 1 - Slab 14, second layer strands from failed region

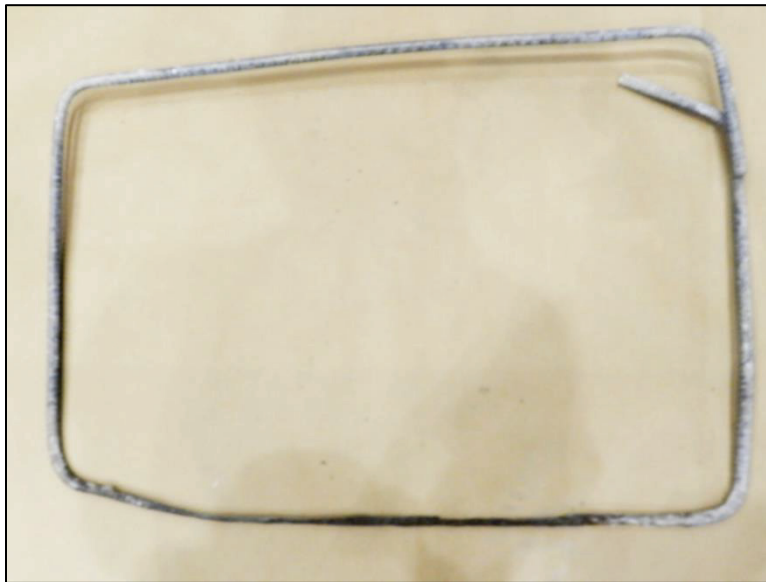
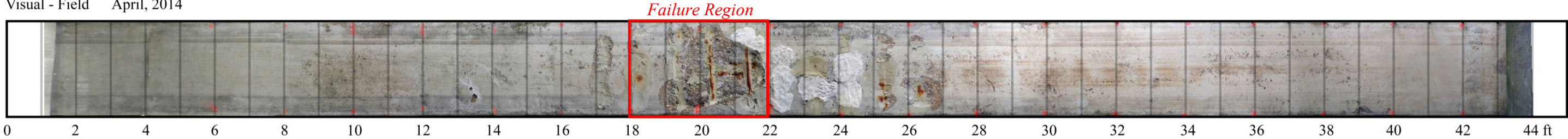


Figure 4.38 - Oyster Creek - Span 1 - Slab 14, corroded stirrup from failed region

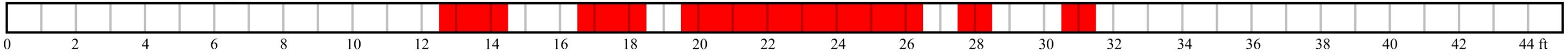
Table 4.15 – Oyster Creek – Span 1 – Slab 14

Qualitative Description: Moderate ~5-ft spalled region with longitudinal rust stains
Priority Maintenance Request: Yes

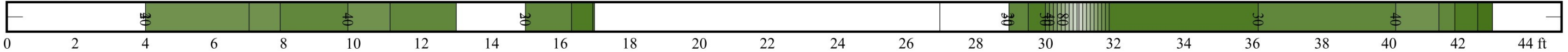
Visual - Field April, 2014



Delaminated Regions - Field May, 2014



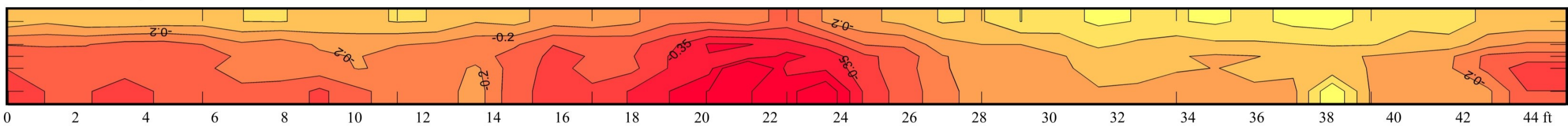
Resistivity - Field



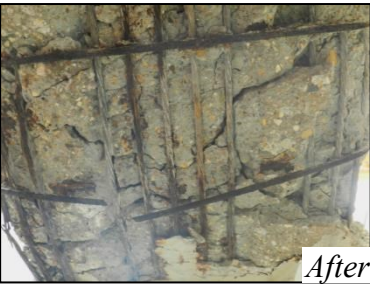
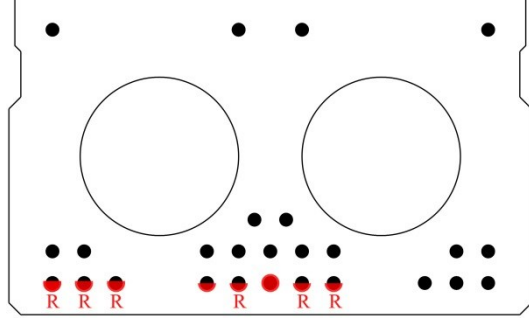
Resistivity - Lab September, 2014



Half-Cell - Lab September, 2014



Region of Failure - 18 to 22 ft



Average Resistivity	45.8 kΩ-cm	Applied Moment	
Average Half-Cell	-0.225 V	496 kip-ft	79%

4.3.9 – Oyster Creek – Span 2 – Slab 4

At the conclusion of field inspection, Oyster Creek – Span 2 – Slab 4 was described as having “shallow spalls with rust stains under stirrups.”

Flexural testing produced a total maximum moment of 900 kip-ft, corresponding to an applied moment of 767 kip-ft, 122% of the calculated available moment capacity. This was the strongest of 6 Oyster Creek slabs. Measured applied top strain was 3100 $\mu\epsilon$. The moment-deflection response recorded during testing is shown in Figure 4.39.

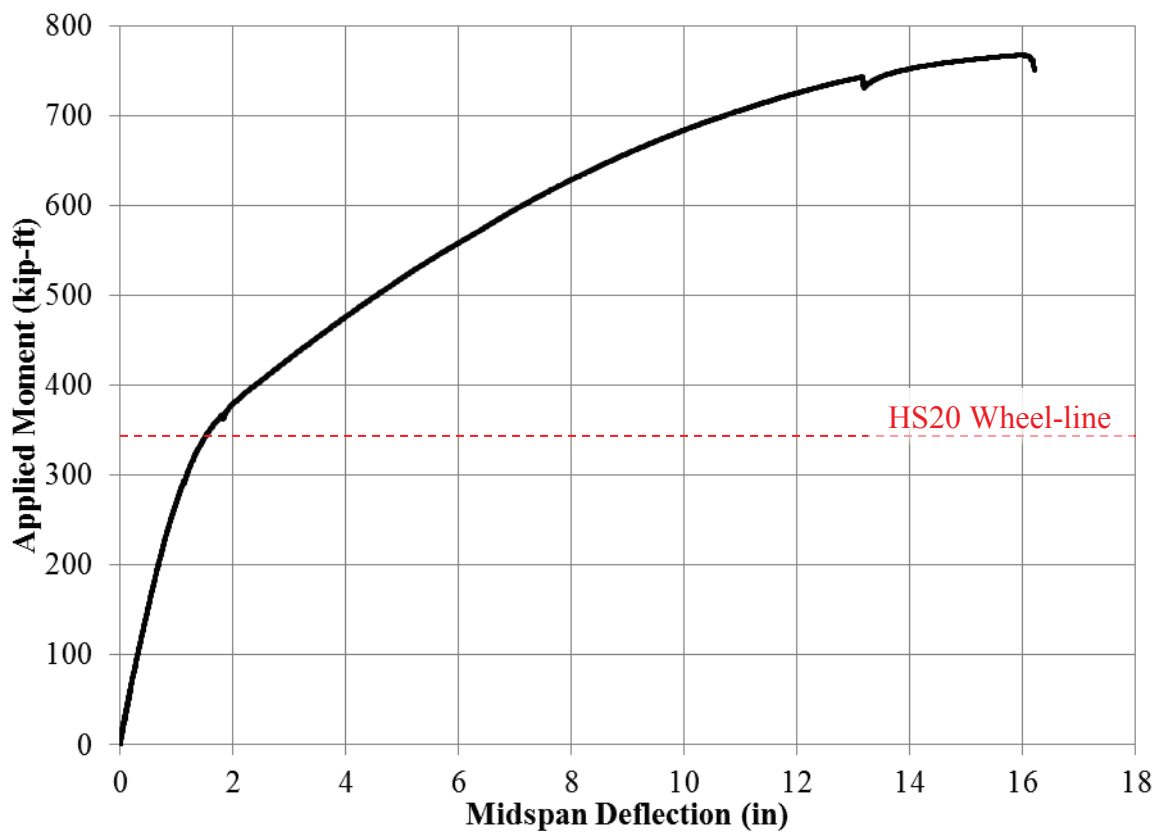


Figure 4.39 - Oyster Creek - Span 2 - Slab 4 flexural test results

The failure region, 16 to 19 ft, contained a couple of shallow, patched spalls. All strands were in generally good condition, with slightly more surface rust near stirrups but no visible section loss.

A photo of the failure region is shown in Figure 4.40.



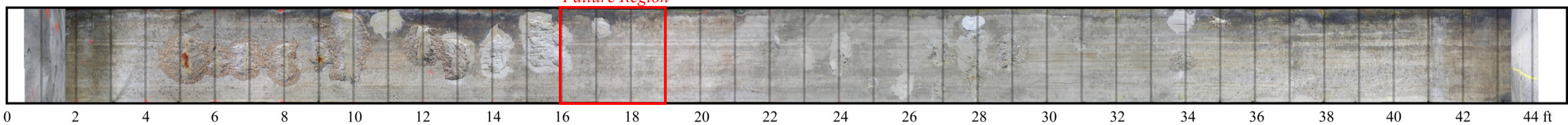
Figure 4.40 - Oyster Creek - Span 2 - Slab 4, central strands at failed region

Table 4.16 – Oyster Creek – Span 2 – Slab 4

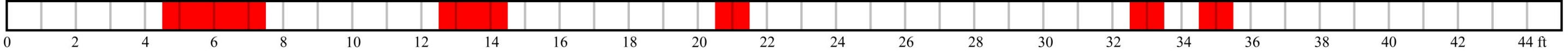
Qualitative Description: Shallow spalls with rust stains under stirrups

Priority Maintenance Request: No

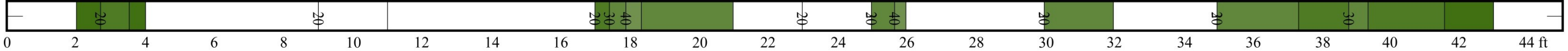
Visual - Field May, 2014



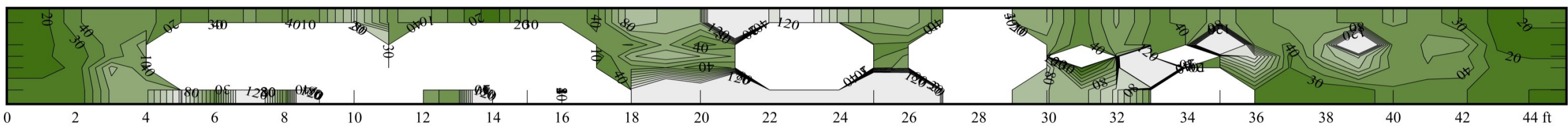
Delaminated Regions - Field May, 2014



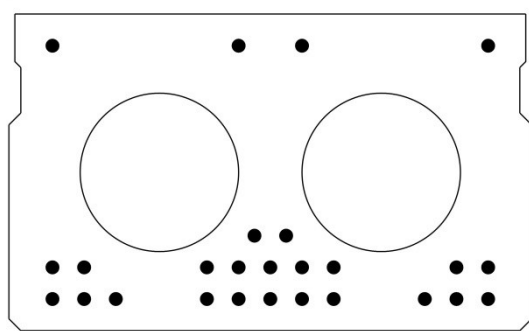
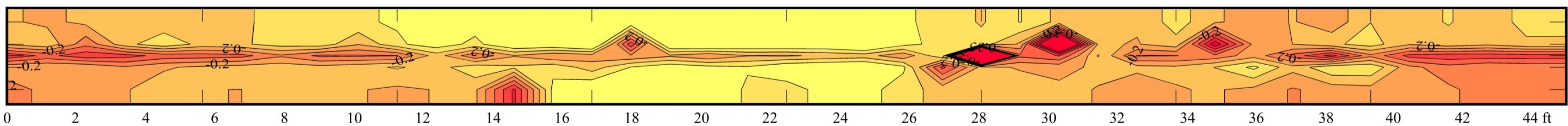
Resistivity - Field



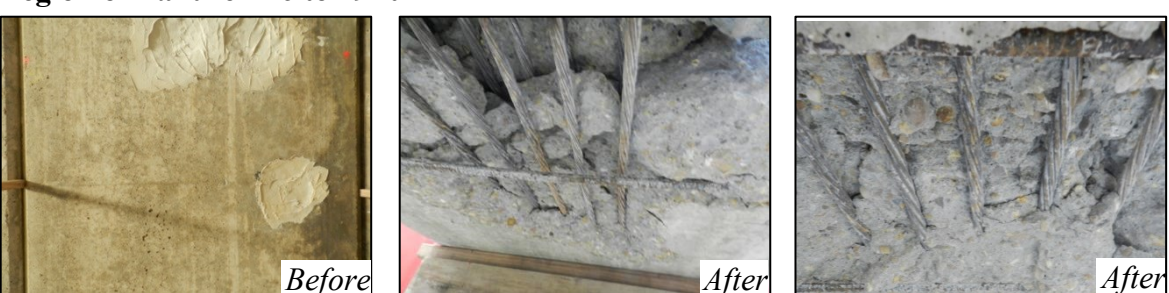
Resistivity - Lab October, 2014



Half-Cell - Lab October, 2014



Region of Failure - 16 to 19 ft



Average Resistivity	78.2 kΩ-cm	Applied Moment	
Average Half-Cell	-0.144 V	767 kip-ft	122%

4.3.10 – Oyster Creek – Span 2 – Slab 5

At the conclusion of field inspection, Oyster Creek – Span 2 – Slab 5 was described as having “no apparent deterioration.”

Flexural testing produced a total maximum moment of 899 kip-ft, corresponding to an applied moment of 766 kip-ft, 121% of the calculated available moment capacity. Measured applied top strain was 3020 $\mu\epsilon$. The moment-deflection response recorded during testing is shown in Figure 4.41.

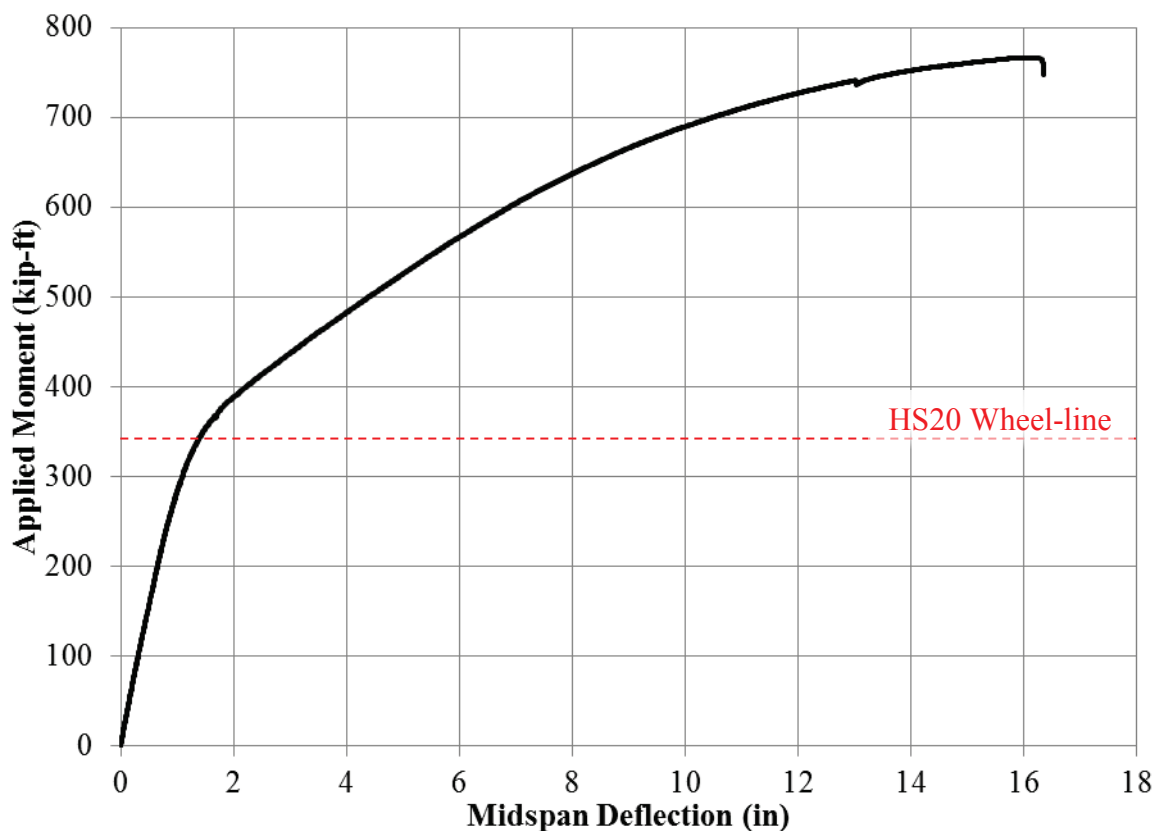


Figure 4.41 - Oyster Creek - Span 2 - Slab 5 flexural test results

The failure region, 17 to 19 ft, had no visible deterioration. All strands were in good condition, displaying only typical light surface rust. A photo of the failure region is shown in Figure 4.42.



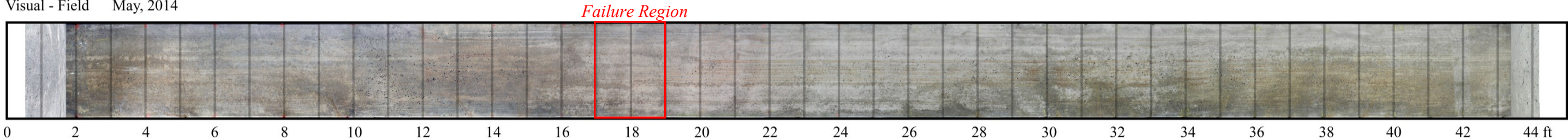
Figure 4.42 - Oyster Creek - Span 2 - Slab 5, strands at failed region

Table 4.17 – Oyster Creek – Span 2 – Slab 5

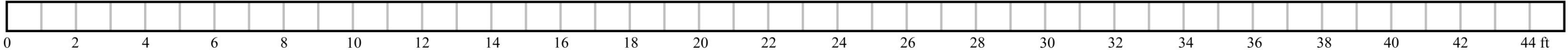
Qualitative Description: No apparent deterioration

Priority Maintenance Request: No

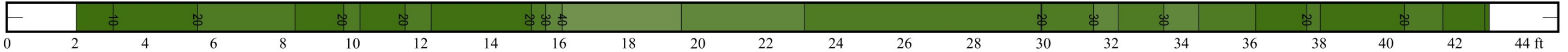
Visual - Field May, 2014



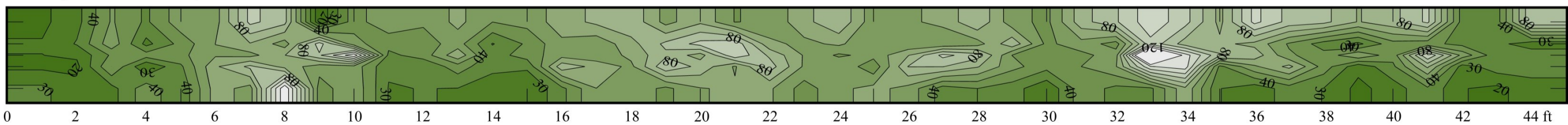
Delaminated Regions - Field May, 2014



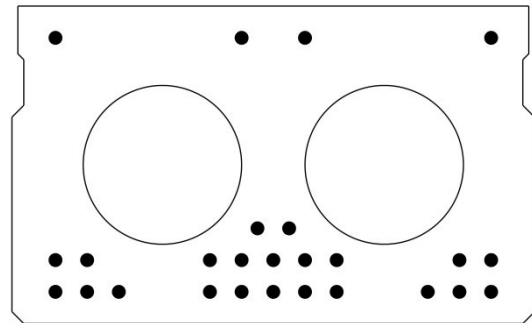
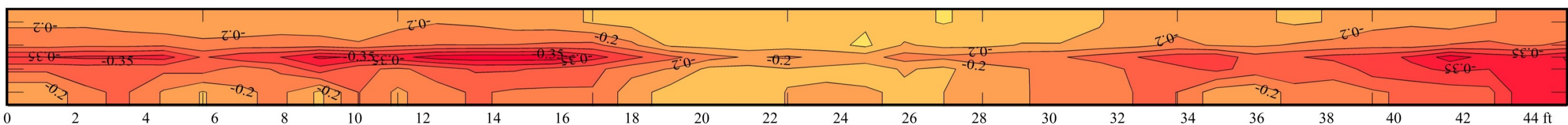
Resistivity - Field



Resistivity - Lab November, 2014



Half-Cell - Lab November, 2014



Region of Failure - 17 to 19 ft



Average Resistivity	55.5 kΩ-cm	Applied Moment	
Average Half-Cell	-0.234 V	766 kip-ft	121%

4.3.11 – Oyster Creek – Span 8 – Slab 12

At the conclusion of field inspection, Oyster Creek – Span 8 – Slab 12 was described as having an “~11-ft icolastic patch, now delaminated.”

Half-cell potentials were not reliably measurable on the large icolastic patch on this slab, and therefore no recordings were taken in that region.

Flexural testing produced a total maximum moment of 465 kip-ft, corresponding to an applied moment of 332 kip-ft, 53% of the calculated available moment capacity. Measured applied top strain was 2440 $\mu\epsilon$. The moment-deflection response recorded during testing is shown in Figure 4.43.

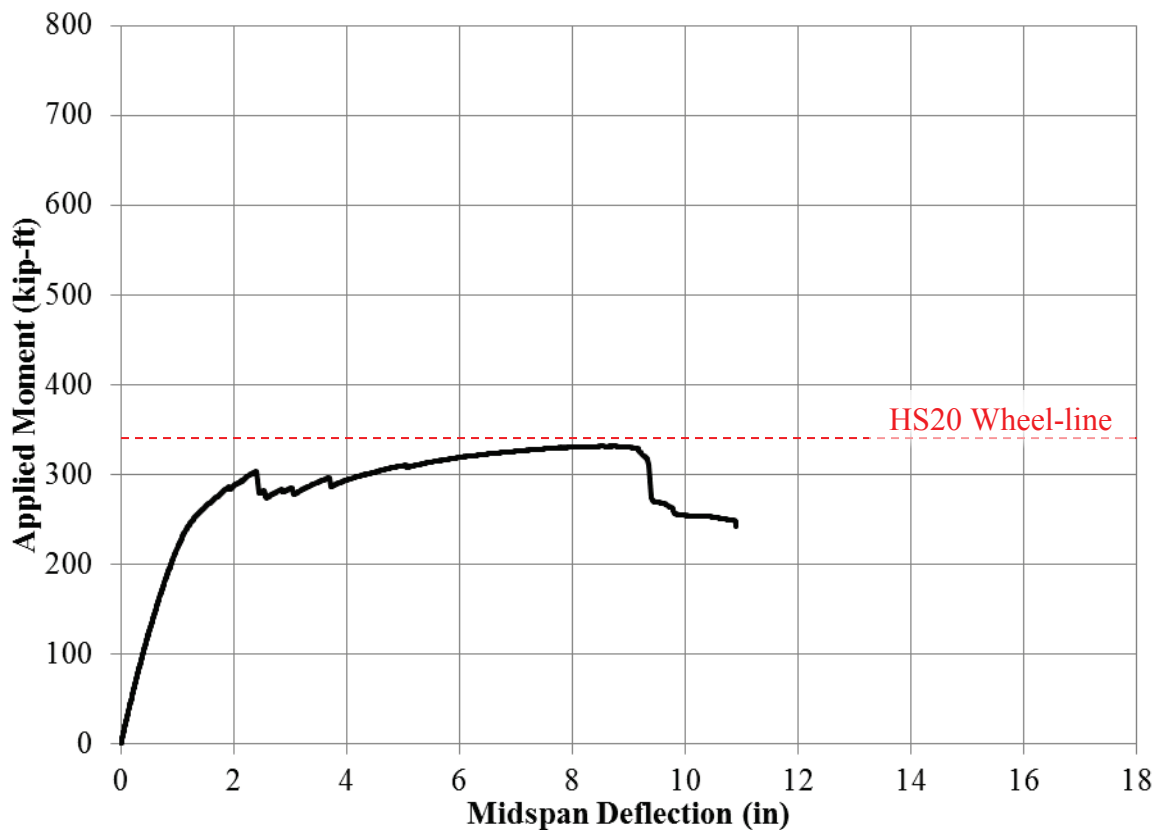


Figure 4.43 - Oyster Creek - Span 8 - Slab 12 flexural test results

The failure region, 19 to 22 ft, was visually a single large, clearly delaminated icolastic patch, with no visible deterioration. Five of eleven bottom strands were fully corroded, with remaining bottom strands heavily corroded and ruptured during testing. One strand in the second layer was heavily rusted and pitted, and effectively completely lost, while one other strand in the second layer displayed significant pitting on all 7 wires. All other strands above the first layer were in very good condition. Photos of the failure region are shown in Figure 4.44 and Figure 4.45.



Figure 4.44 - Oyster Creek - Span 8 - Slab 12, soffit after testing, formerly covered by icolastic patch



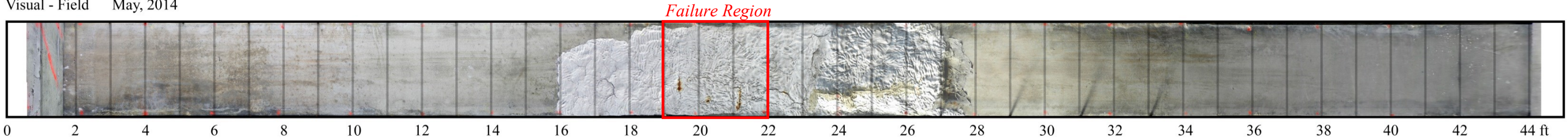
Figure 4.45 - Oyster Creek - Span 8 - Slab 12, strand section loss extends full length of icolastic patch

Table 4.18 – Oyster Creek – Span 8 – Slab 12

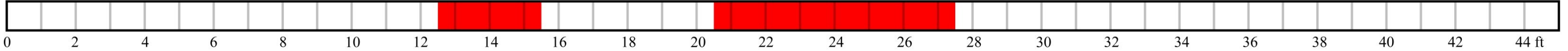
Qualitative Description: ~11-ft icolastic patch, now delaminated

Priority Maintenance Request: Yes

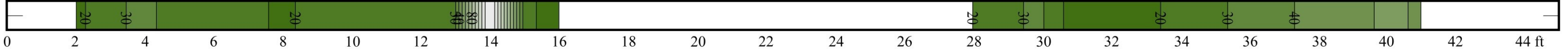
Visual - Field May, 2014



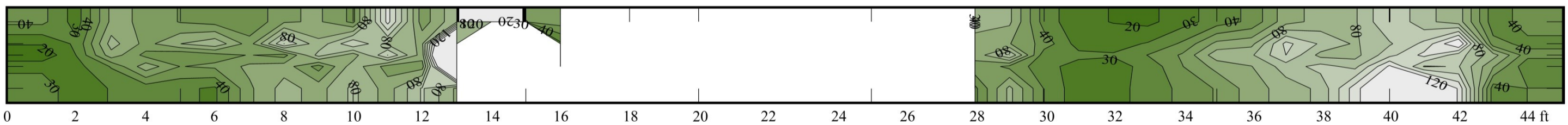
Delaminated Regions - Field April, 2014



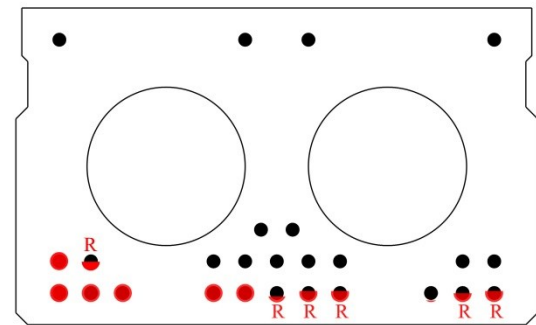
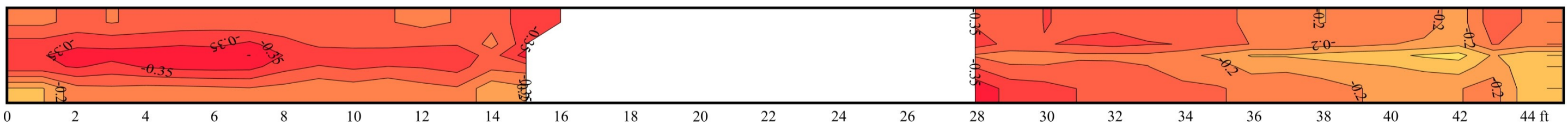
Resistivity - Field



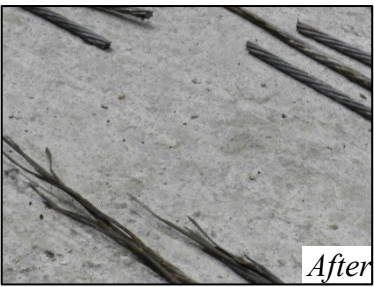
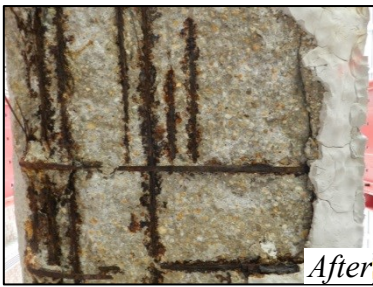
Resistivity - Lab November, 2014



Half-Cell - Lab November, 2014



Region of Failure - 19 to 22 ft



Average Resistivity	67.1 kΩ-cm	Applied Moment	
Average Half-Cell	-0.259 V	332 kip-ft	53%

4.3.12 – Oyster Creek – Span 8 – Slab 13

At the conclusion of field inspection, Oyster Creek – Span 8 – Slab 13 was described as having a “moderate spalled region with rust stains.”

Flexural testing produced a total maximum moment of 746 kip-ft, corresponding to an applied moment of 613 kip-ft, 97% of the calculated available moment capacity. Measured applied top strain was 3320 $\mu\epsilon$. The moment-deflection response recorded during testing is shown in Figure 4.46.

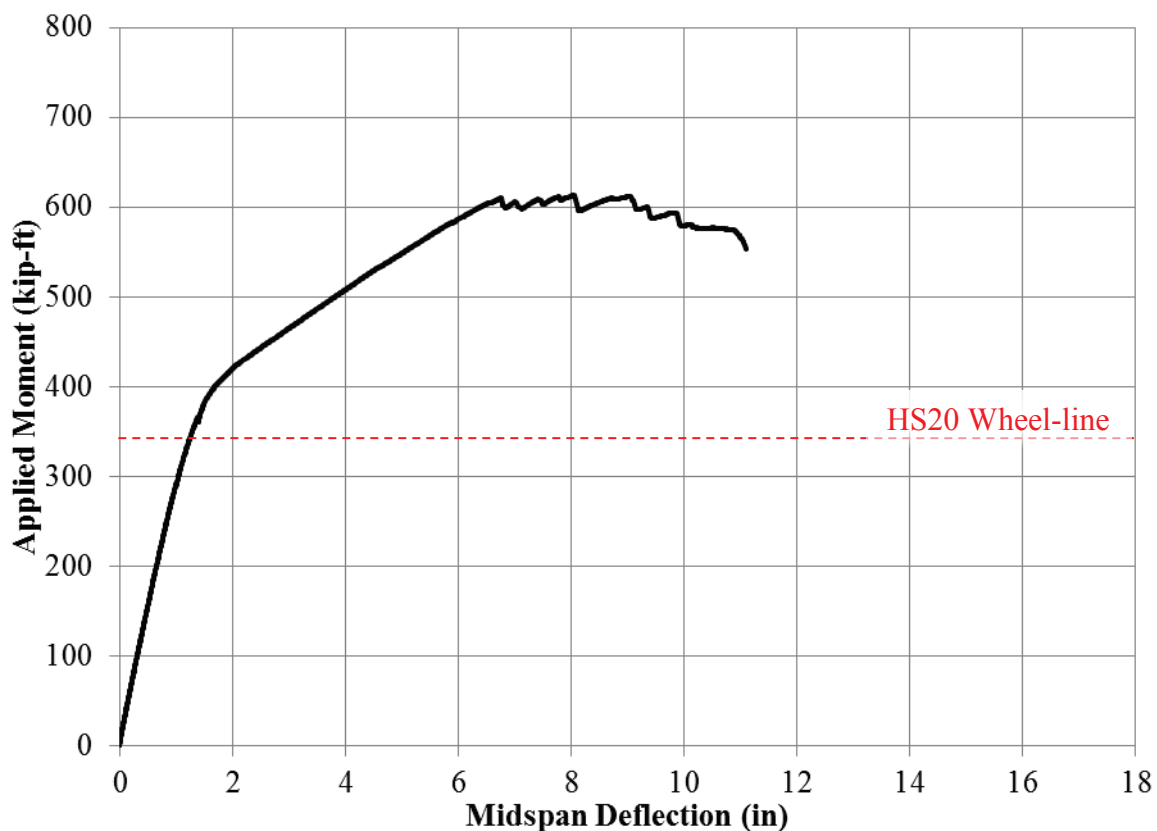


Figure 4.46 - Oyster Creek - Span 8 - Slab 13 flexural test results

The failure region, 22 to 25 ft, contained a large, asymmetrical, patched spall which appeared deeper close to the edge of the slab and contained rust stains of indistinct orientation. Five of eleven bottom strands displayed minor to moderate rust and pitting, with the equivalent of 2 strands worth of wires fully corroded. Other strands in the bottom layer displayed only minor rust. All strands above the bottom layer were in good condition. Photos of the failure region and bottom layer strands removed from it are shown in Figure 4.47 to Figure 4.49.



Figure 4.47 - Oyster Creek - Span 8 - Slab 13, moderate rust and pitting of ruptured corner strand



Figure 4.48 - Oyster Creek - Span 8 - Slab 13, rust and pitting of strands above (removed) stirrup location

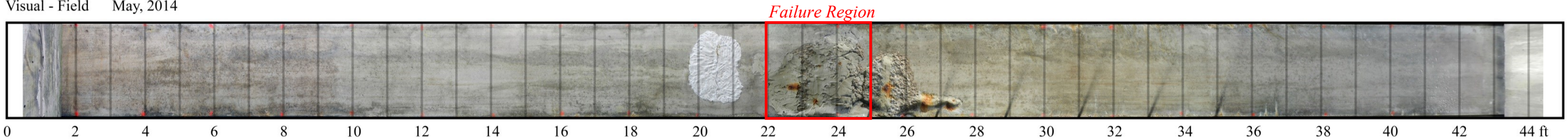


Figure 4.49 - Oyster Creek - Span 8 - Slab 13, bottom layer strands removed from failed region

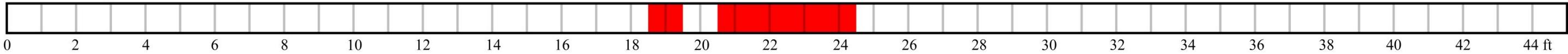
Table 4.19 – Oyster Creek – Span 8 – Slab 13

Qualitative Description: Moderate spalled region with rust stains
Priority Maintenance Request: Yes

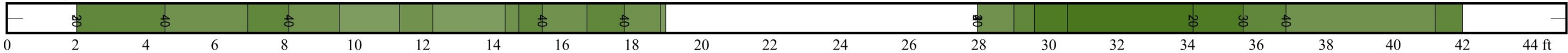
Visual - Field May, 2014



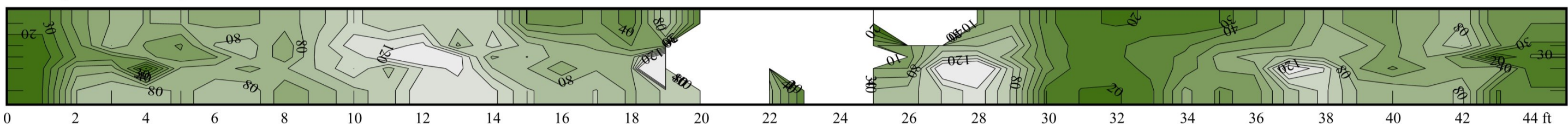
Delaminated Regions - Field April, 2014



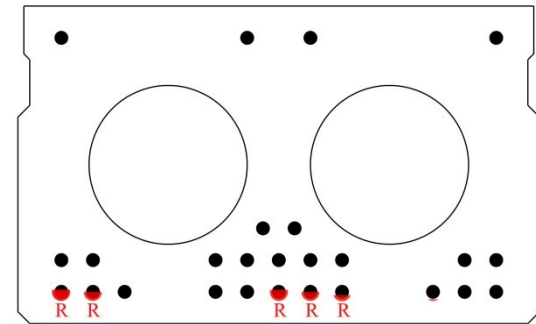
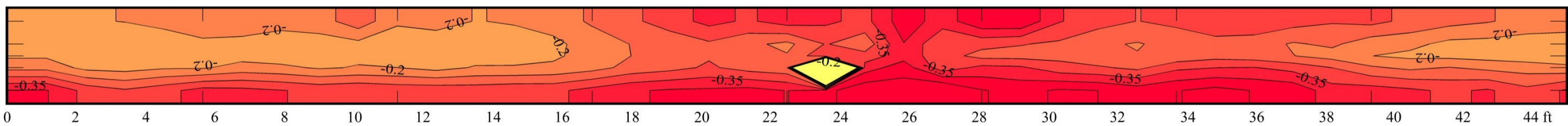
Resistivity - Field



Resistivity - Lab October, 2014



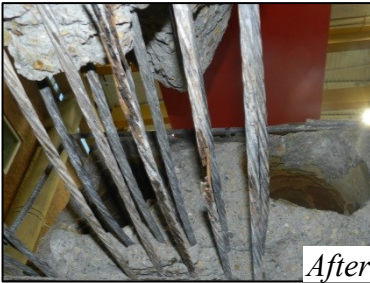
Half-Cell - Lab October, 2014



Region of Failure - 22 to 25 ft



Before



After



After

Average Resistivity	68.6 kΩ-cm	Applied Moment	
Average Half-Cell	-0.269 V	613 kip-ft	97%

CHAPTER 5 – ANALYSIS AND DISCUSSION

This chapter focuses on understanding the relationships between the different data that were presented in the Chapter 4. Information that can be collected in the field by non-destructive means, such as resistivity, half-cell potential, visual inspection, and sounding are compared to the flexural capacity of slabs and extent of corrosion as obtained in the laboratory.

5.1 – General Analysis of Field Observations

Though the focus of this research is on deteriorated cored slabs in general, certain specifics and questions about the Ward Creek and Oyster Creek Bridges are discussed in this section. These bridges have undergone superstructure replacement due to the visible deterioration of the slabs, but their capacity and the extent of deterioration was not fully understood, and their replacement could be viewed as a cautious decision.

As discussed in Chapter 4, there seems to be a significant correlation between the location of the retaining wall support blocks (Figure 5.1) and the location of severely deteriorated regions of the end spans. For Ward Creek Bridge, three support blocks were located underneath the superstructure, with one under the roadway centerline, and two others spaced 17.5 ft on either side. For Oyster Creek Bridge support blocks were not centered and varied in distance from one another. Based on the locations shown in the bridge plans, a distance from the center of each support block to the center of each slab can be calculated for slabs from the end spans. These

distances, along with total moment for each slab from laboratory testing, are shown in Table 5.1 where it can be observed that slabs within the splash zone are more severely deteriorated.



Figure 5.1 - Deterioration of slabs above retaining wall blocks

Table 5.1 - Distance from support blocks, end-span slabs

		Distance from Center of Block <i>ft</i>	Applied Moment <i>kip-ft</i> %	
Ward Creek	Span 1 - Slab 13	3.6	345	75%
	Span 1 - Slab 14	0.9	367	80%
	Span 9 - Slab 6	4.9	484	105%
	Span 9 - Slab 7	2.1	145	31%
Oyster Creek	Span 1 - Slab 13	0.4	351	56%
	Span 1 - Slab 14	3.1	496	79%
	Span 8 - Slab 12	1.6	332	53%
	Span 8 - Slab 13	4.4	613	97%

Deterioration was not limited to the end spans, with spalling or delamination observed on 19 of 32 slabs in the two intermediate spans examined in this research. Slabs chosen for laboratory testing (Slabs 5 and 6 from Ward Creek – Span 4, and Slabs 4 and 5 from Oyster Creek – Span 2) were initially selected to capture a spread of apparent deterioration, with one slab from each bridge chosen with no visible deterioration, and one slab chosen to have more visible deterioration. The region of the slab soffit of Oyster Creek – Span 2 – Slab 4, shown in Figure 5.2, is representative of the typical soffit of an intermediate span slab in “worse” condition.

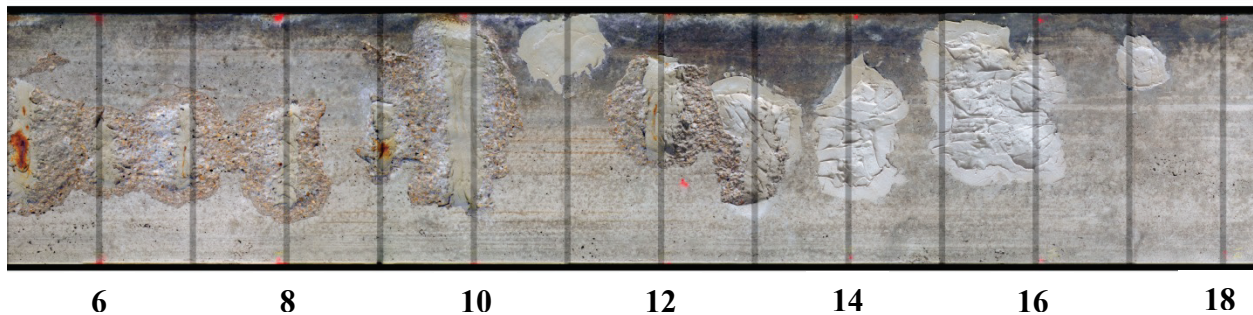


Figure 5.2 - Typical intermediate span spalling, Oyster Creek - Span 2 - Slab 4

In flexural testing, no difference in flexural strength was observed between the slabs in visually excellent condition and their more heavily spalled partners. This suggests that based solely on the condition of slabs prior to replacement, the flexural capacity of intermediate spans was not of significant concern.

Based on the observations provided in the bridge inspection records reviewed in Chapter 2, deterioration was first described in a way that allows comparison with existing slab conditions in 2001. Of those slabs noted as spalled in 2001, some were noted in the 2013 inspection as having

significant deterioration requiring priority maintenance, while others were merely noted as patched. This therefore presents no clear deterioration pattern for slabs on intermediate spans. These results suggest that the flexural capacity of intermediate spans was likely similar to that of an undamaged span at the time of superstructure replacement, though it is not clear based on available records what their current condition would mean for their long-term durability.

5.2 – Resistivity and Half-Cell Potential

Resistivity and half-cell potential are examined more critically than the results for visual inspection and sounding that are discussed later in this chapter. This is because for these tests it is not sufficient to merely have a relationship with deterioration, but that they need to go beyond that, and show a relationship with deterioration *beyond what can be observed by visual inspection alone*. Inevitably in the process of going underneath a slab, its visual condition is observed. This assumes that the decision faced at the inspection level is not whether to replace existing inspections with electrical methods, but whether to add resistivity or half-cell potential testing as an addition to current methods. Therefore, the primary question analyzed here is, “Do these tests add any value to visual inspection?”

5.2.1 - Resistivity

Resistivity is intended fundamentally to characterize the concrete, and in the literature it is taken to not necessarily indicate corrosion, but rather the potential for corrosion to happen. With this

in mind, care must be taken in interpreting results. Two methods are examined here in interpreting resistivity. The first is to use contour plots to examine spatial relationships in the resistivity data, and this is followed by looking at resistivity values.

5.2.1.1 – Spatial relationships in resistivity

One method of interpretation is to look for regions in resistivity contour plots with lower resistivity readings. Then these areas are examined more closely using information about their location in the bridge and the condition of the slabs as determined in the laboratory in order to see if the resistivity contours are indicative of any deterioration or condition that was found to be significant through flexural testing.

This process was carried out by looking for areas of low resistivity on the 12 field and 12 laboratory resistivity contour plots shown in Table 4.8 to Table 4.19 in the Results chapter. In this examination, “low resistivity” generally means less than 30 k Ω -cm, but the difference between an area of interest and the surrounding slab was emphasized more than the resistivity values. For each area of interest, three questions were asked:

- *Was this area found to be significant to the flexural strength of the slab?* This is interpreted here as an area where some corrosion had occurred that was believed to potentially affect the slab’s strength, with some such areas observed directly during flexural testing, and some identified afterward during demolition and exposure of the strands.
- *Was there visible/audible deterioration in the same area?* This identifies areas where resistivity is not providing additional indication of deterioration beyond that already

indicated by the presence of any combination of delamination, spalling, rust stains, cracks, or exposed steel.

- *Does resistivity add value in this location?* Only true if there is no visible/audible deterioration and the area was found to be significant to flexural strength.

As an example, this process was used for Ward Creek – Span 1 – Slab 14 (shown in Figure 5.3) to identify 3 areas in field resistivity and 4 areas in laboratory resistivity to further examine.

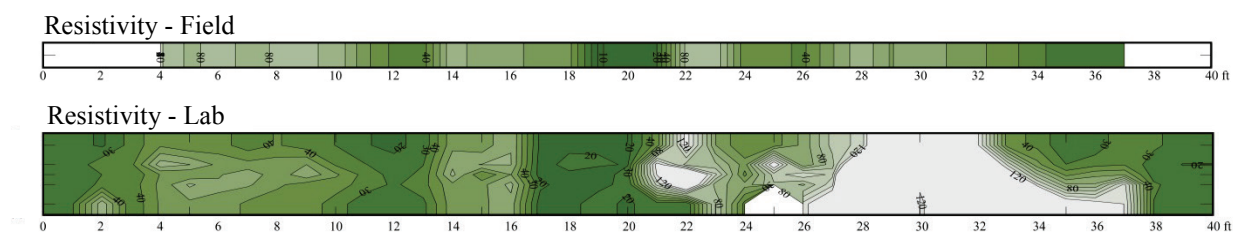


Figure 5.3 - Resistivity Contours, Ward Creek - Span 1 - Slab 14

Areas of interest for field resistivity were 13, 19 – 21, and 36 – 40 ft, while those for laboratory resistivity are 0 – 3, 12, 17 – 20, and 36 – 40 ft. Flexural testing and demolition revealed the area from 16.5 – 21 ft to contain rusting of strands that contributed to a decrease in flexural strength, but this area, shown in Figure 5.4, was also visibly and audibly delaminated. Other areas were not observed to have deterioration contributing to loss of flexural strength, therefore no areas identified through resistivity added value.

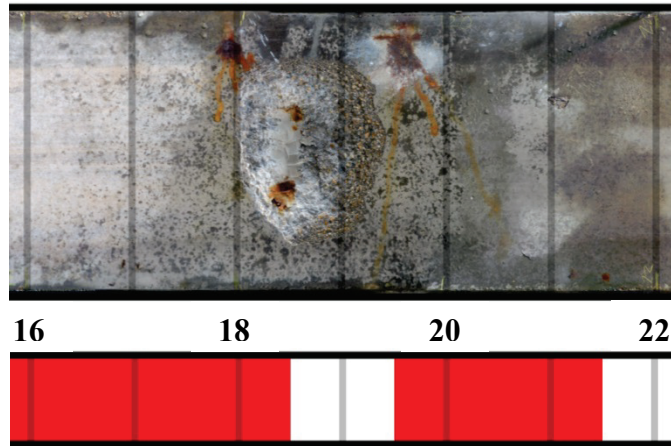


Figure 5.4 - Ward Creek - Span 1 - Slab 14

This process was repeated for all 12 slabs, identifying 37 areas total (including 8 areas that were identified by both field and laboratory resistivity, for 45 total observations), shown in Table 5.2.

Table 5.2 - Areas of interest, resistivity

Slab	Location	Location on Slab (ft)	Significant to flexural strength?	Visible / Audible Deterioration?	Adds Value?
Ward Creek - Span 1 - Slab 13	Field	13	No	No	No
		19 - 21	Yes	Yes	No
		36 - 40	No	No	No
	Laboratory	0 - 3	No	No	No
		12	No	No	No
		17 - 20	Yes	Yes	No
Ward Creek - Span 1 - Slab 14	Field	36 - 40	No	No	No
		18 - 21	Yes	Yes	No
	Laboratory	0 - 2	No	No	No
		18 - 24	Yes	Yes	No
Ward Creek - Span 4 - Slab 5	Laboratory	38 - 40	No	No	No
		0 - 2	No	No	No
		Isolated Locations on one side, 10 - 24	No	No	No
		38 - 40	No	No	No
Ward Creek - Span 4 - Slab 6	Laboratory	0 - 2	No	No	No
		39 - 40	No	No	No
Ward Creek - Span 9 - Slab 6	Field	0 - 40	No	Yes	No
	Laboratory	18 - 22	Yes	Nearby	Possibly
Ward Creek - Span 9 - Slab 7	Field	2 - 28	Yes	Yes	No
	Laboratory	0 - 5	No	Yes	No
		15 - 16	Yes	Yes	No
		25 - 29	Yes	Yes	No
		39 - 40	No	No	No
Oyster Creek - Span 1 - Slab 13	Field	7 - 8	No	No	No
		36 - 37	No	No	No
	Laboratory	0 - 1	No	No	No
Oyster Creek - Span 1 - Slab 14	Laboratory	44 - 45	No	No	No
		0 - 1	No	No	No
		17 - 19	Yes	Yes	No
		30 - 32	No	Yes	No
Oyster Creek - Span 2 - Slab 4	Laboratory	42 - 45	No	No	No
		0 - 2	No	No	No
		43 - 45	No	No	No
Oyster Creek - Span 2 - Slab 5	Field	0 - 3	No	No	No
		9 - 15	No	Yes	No
		37 - 45	No	No	No
	Laboratory	0 - 2	No	No	No
		11 - 15	No	Yes	No
Oyster Creek - Span 8 - Slab 12	Laboratory	One side, 35 - 45	No	No	No
		0 - 2	No	No	No
		30 - 33	No	No	No
Oyster Creek - Span 8 - Slab 13	Field	31 - 35	No	No	No
	Laboratory	0 - 1	No	Yes	No
		30 - 35	No	No	No
Oyster Creek - Span 8 - Slab 13	Laboratory	44 - 45	No	No	No

Resistivity clearly did not add value to the inspection process. Of the 37 areas of interest, one of them possibly yielded additional information useful to assessing the strength of the slab. This was Ward Creek – Span 9 – Slab 6, from 18 – 22 ft, shown in Figure 5.5. This region contained visible deterioration from 21 to 24 ft, and audible delamination at 23 and 24 ft. Resistivity values were below 20 kΩ-cm for a region from 18 to 21 ft that did not appear to be clearly damaged, but demolition suggested that the corrosion of this slab extended into that region.

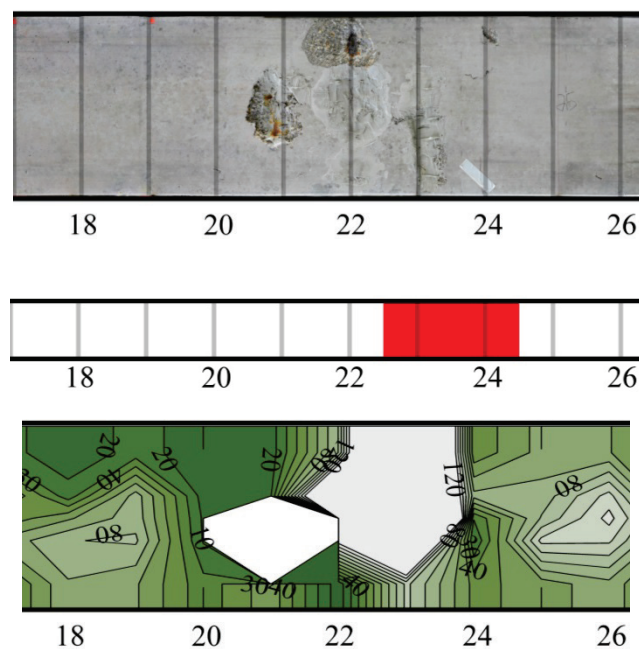


Figure 5.5 - Ward Creek - Span 9 - Slab 6, 17 - 26 ft

No other area of interest provided useful information. Five of twelve slabs did not have any observable areas of interest from field resistivity. Of the 7 slabs for which field resistivity suggested areas, 4 of 12 areas of interest did not display the same trend in laboratory resistivity.

When examined against the lower threshold of whether resistivity data are consistent with expected trends, the data fare somewhat better. Areas of low resistivity coincided with regions

of honeycombing (Figure 5.6) on Oyster Creek – Span 2 – Slab 4 and Oyster Creek – Span 2 – Slab 5, consistent with concrete containing significantly more voids.

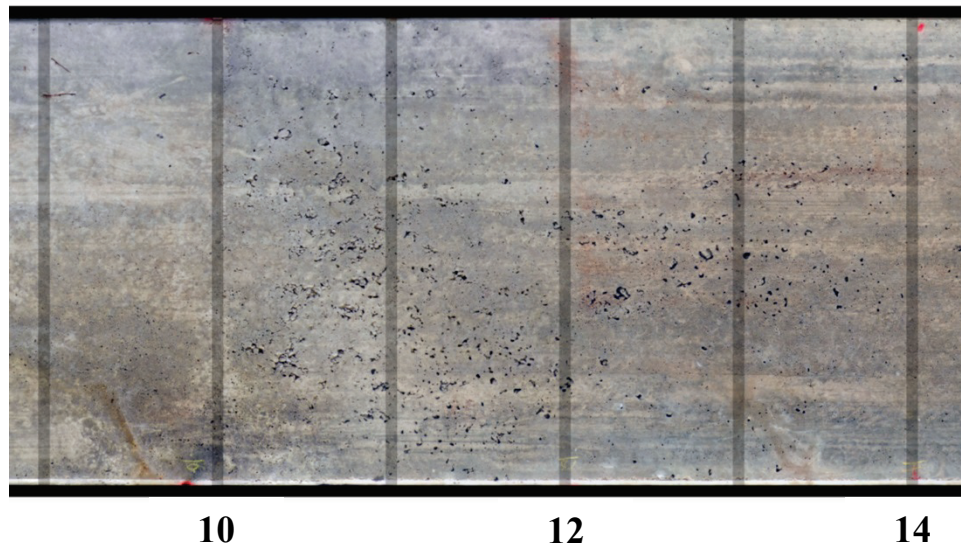


Figure 5.6 – Honeycombing, Oyster Creek - Span 2 - Slab 5, 9 - 14 ft

The ends of slabs were consistently locations of low resistivity, representing 21 of 37 areas of interest (and 21 of 24 slab ends). This is consistent with expectations, as slab ends are frequently subject to additional moisture due to leaking joints and debris buildup around bearing pads. Most slab soffits appeared undamaged in the field, but hairline cracks were visible in the field on a couple, as may be seen in Figure 5.7. Hairline cracks were commonly seen on the sides of slabs near the ends during laboratory testing. The final 1 to 2 in. of strand ends had been encased in grout after casting, and were commonly at least partially rusted, with some pitting and section loss. Despite this deterioration, slab ends exposed during jackhammering after flexural testing were in uniformly good condition. The typical condition of strand ends is shown in Figure 5.8.



Figure 5.7 – Hairline cracks, Ward Creek - Span 9 - Slab 7, 3 ft



Figure 5.8 - Center strands, Ward Creek - Span 1 - Slab 14, 0 - 1 ft

As a means of identifying areas of corrosion, resistivity performs poorly. Of 37 areas of interest, 27 of them (including end regions discussed above) were false positives, with no indication of

corresponding corrosion. In conclusion, spatial analysis of resistivity data, though possibly providing indication of regions of more porous concrete, is not found to be useful in assessing flexural capacity, and does not add value to the inspection process in any way that warrants the care and effort required to obtain the data.

5.2.1.2 – Resistivity values

The other potential method to use resistivity is to examine resistivity values themselves. As discussed in Chapter 4, no scale of permeability ratings was believed to be consistent given the varying moisture conditions found in the field. Here, resistivity values are instead compared to the flexural strength of slabs in order to examine any possible trends. Flexural strength is a product of many different factors, but based on the structural analysis discussed later in this chapter, strength is roughly linearly related to the area of steel in the bottom layer of the slab, and therefore is usable as a measure of potential corrosion for comparison to resistivity. Three values are examined here for each slab: average resistivity values for the entire span, average resistivity values for the middle third of the span, and the percentage of resistivity values below 30 k Ω -cm. Middle third is taken as values recorded from 13 to 27 ft for 40 ft long slabs, and from 15 to 30 ft for 45 ft long slabs. Total moment capacity is taken as a percentage of the maximum for each span length in order to allow all slabs to be compared together.

No relationship was found between any of the three values and total moment capacity. Graphs showing these relationships are presented in Figure 5.9 and Figure 5.10 for field resistivity data and in Figure 5.11 and Figure 5.12 for laboratory resistivity data. Resistivity values as recorded

in the field and the laboratory are not found to be predictive of corrosion or deterioration in any capacity for cored slabs under the conditions examined.

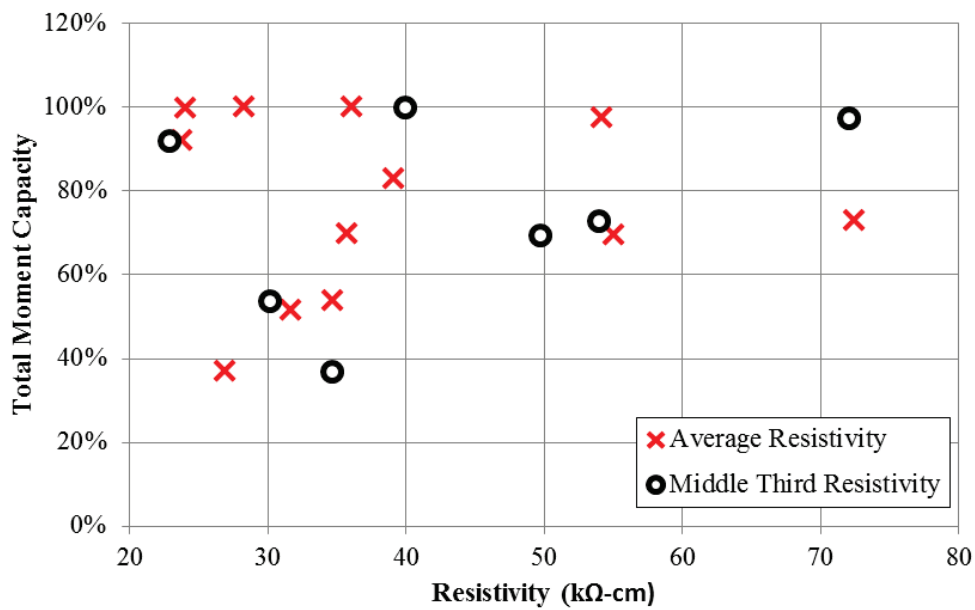


Figure 5.9 – Field data: resistivity vs. total moment capacity

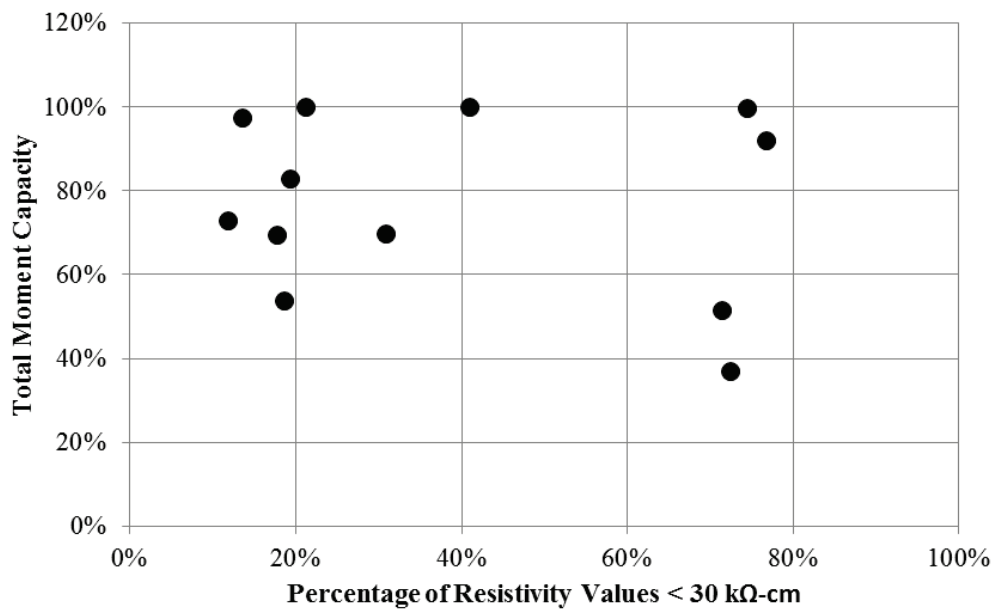


Figure 5.10 - Field data: percentage of resistivity values < 30 kΩ-cm vs. total moment capacity

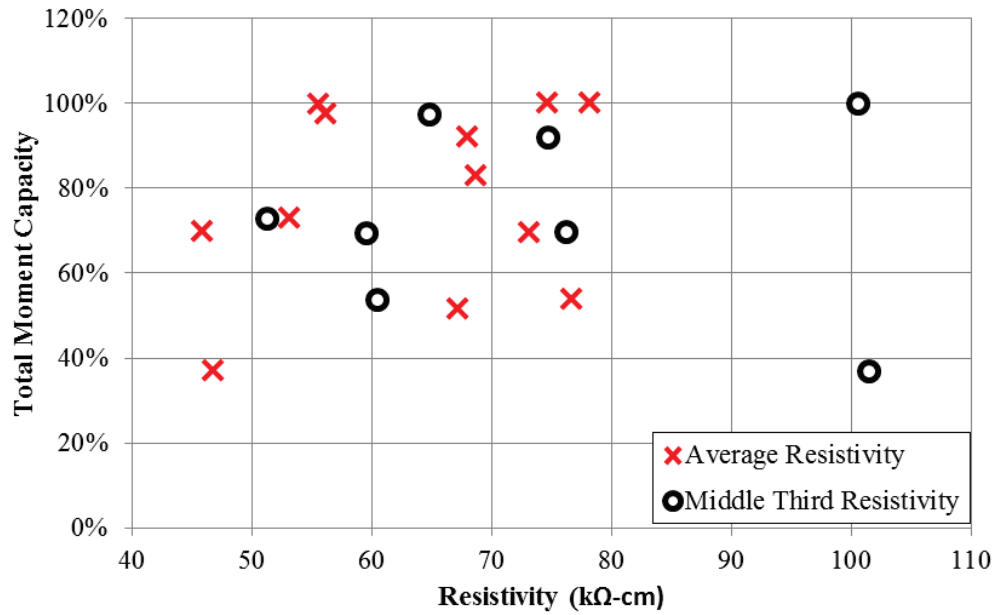


Figure 5.11 – Laboratory data: resistivity vs. total moment capacity

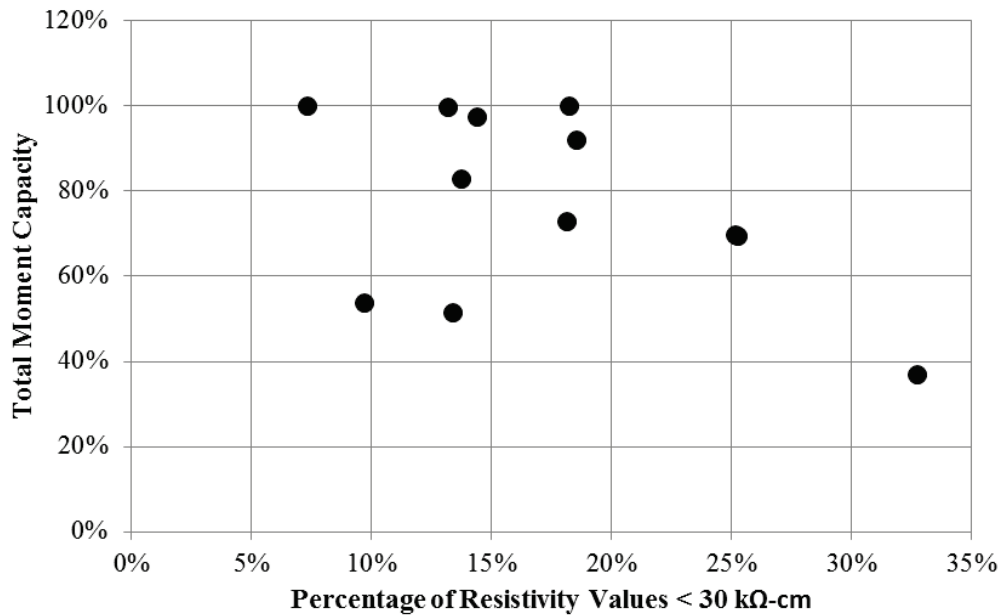


Figure 5.12 - Laboratory data: percentage of resistivity values $< 30 k\Omega\text{-cm}$ vs. total moment capacity

Analysis of resistivity data highlights the need to use it carefully, and suggests that finding useful data from it in the field is difficult. Given the variability observed in the readings and the limited weather conditions in which resistivity readings are consistent across a span, any use of resistivity for field measurement should be approached cautiously.

5.2.2 – Half-Cell Potential

Half-Cell potential was analyzed using the same methods employed in the analysis of resistivity, with both spatial relationships and half-cell potential values used in analysis. Half-cell potentials theoretically give an indication of the likelihood that corrosion is occurring at a given location, and therefore should be assumed as more directly applicable to the analysis of flexural capacity.

5.2.2.1 – Spatial Relationships in Half-Cell Potential

Spatial relationships were examined in half-cell potential using the same three questions as were used in resistivity: “Was the area significant to flexural strength?”, “Was there visible/audible delamination in the area?”, and “Does half-cell potential add value in this location?”. Generally, values more negative than -0.35 V were used as an indication of an area of interest, but half-cell potential data, collected exclusively in the laboratory, generated contour plots which subjectively were felt to present clear regions of high and low values relative to the more scattered readings collected for resistivity. A total of 23 areas of interest were identified across the 12 slabs.

Generally half-cell data allowed for more complete contour plots compared to resistivity, with more data collected in areas of visible deterioration. As a result, 14 of the 23 areas of interest

were regions of visible deterioration. Areas at slab ends represented 3 of 23 areas, with hairline cracks visible in all of them. Results for all areas of interest identified are shown in Table 5.3.

Table 5.3 - Areas of interest, half-cell potential

Slab	Location on Slab (ft)	Significant to flexural strength?	Visible / Audible Deterioration?	Adds Value?
Ward Creek - Span 1 - Slab 13	Middle Strand, 10 - 40	Yes	Yes	No
	17 - 22	Yes	Yes	No
Ward Creek - Span 1 - Slab 14	17 - 24	Yes	Yes	No
Ward Creek - Span 4 - Slab 5	Middle Strand, 0 - 40	No	No	No
Ward Creek - Span 4 - Slab 6	One Side 6 - 38	No	No	No
Ward Creek - Span 9 - Slab 6	4 - 11	No	Yes	No
	19 - 23	Yes	Yes	Possibly
Ward Creek - Span 9 - Slab 7	5 - 9	No	Yes	No
	14 - 27	Yes	Yes	No
Oyster Creek - Span 1 - Slab 13	0 - 45	Yes	Yes	No
Oyster Creek - Span 1 - Slab 14	One Side, 0 - 10	No	No	No
	16 - 25	Yes	Yes	No
	44 - 45	No	Yes	No
Oyster Creek - Span 2 - Slab 4	14	No	Yes	No
	18	No	No	No
	28	No	Yes	No
	30	No	No	No
	35	No	No	No
Oyster Creek - Span 2 - Slab 5	Middle Strand, 0 - 16	No	No	No
	Middle Strand, 34 - 45	No	No	No
Oyster Creek - Span 8 - Slab 12	2 - 7	No	Yes	No
Oyster Creek - Span 8 - Slab 13	One Side, 0 - 40	No	No	No
	19 - 28	Yes	Yes	No

Areas of interest identified through half-cell potential added no more value than those identified through resistivity, with the same area of Ward Creek – Span 9 – Slab 6 indicating additional corrosion not observed through visual/audible observation. Relative to resistivity the half-cell potential data produces fewer apparent false-positives, with most areas identified being either areas of corrosion identified through visual testing, or areas where corrosion could plausibly be occurring (based on location along slab). Four slabs displayed more negative half-cell potentials along the middle strand, but only 1 of the 4 appeared to be related to corrosion. This may be an indication of poor electrical connection with the strand, and ensuing erroneous measurements.

Though areas of low half-cell potential agree well with those of visible deterioration, analysis of contour plots are not found to identify any additional corrosion that is significant to the flexural capacity of the slab, and this use is not recommended. Compared to resistivity, areas of low half-cell potentials more clearly resemble the shapes of visible deterioration found on the slabs, and though it is not recommended for use in evaluating deteriorated cored slabs, half-cell potential may present value in other related applications.

5.2.2.2 – Half-Cell Potential Values

Half-cell potentials were analyzed as an average over the entire span, an average of the middle third of the span, and a percentage of values more negative than -0.35 V. Additionally, in a continuation of the observations made in the previous section, average half-cell potential values were obtained for regions of visible deterioration. This was possible for 9 of 12 slabs, as Ward Creek – Span 4 – Slab 5 and Oyster Creek – Span 2 – Slab 5 had no indication of deterioration,

while Oyster Creek – Span 8 – Slab 12 had no half-cell potentials recorded on the large icolastic patch that covered the entire deteriorated region.

Compared to resistivity, there may be the potential for a trend in the half-cell potential values. This is best seen in Figure 5.13 comparing half-cell potentials for the middle third of each slab with the total moment capacity. However, it is based on only 11 usable data points (excluding Oyster Creek – Span 8 – Slab 12, whose icolastic patch prevented measurement for the middle third of the slab) and limits the certainty with which this can be generalized to other deteriorated prestressed cored slabs.

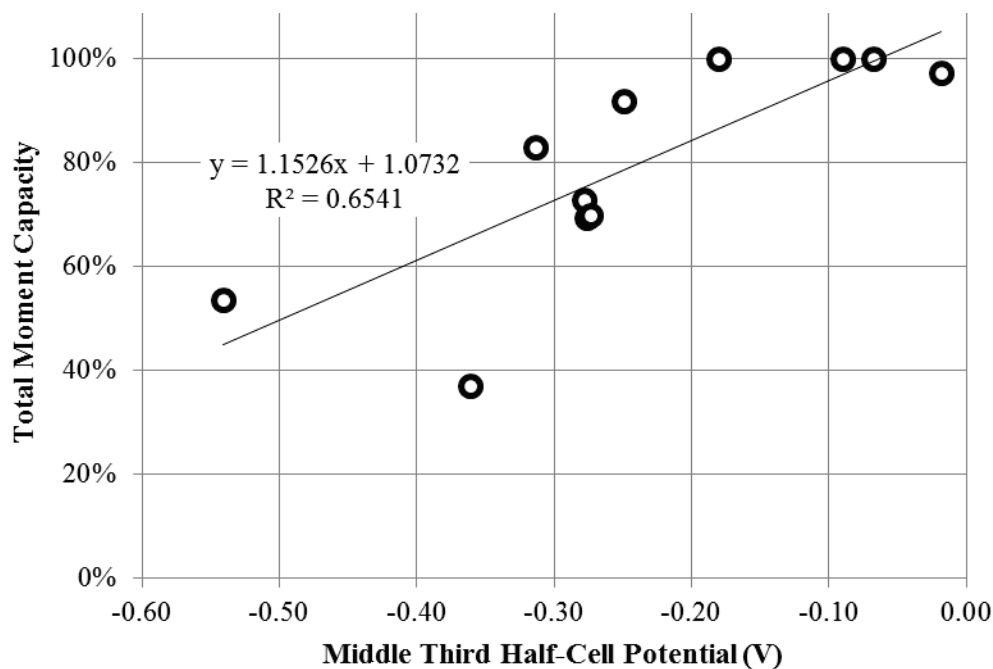


Figure 5.13 – Moment vs. average half-cell potential, middle third of slabs

The relationships between total moment capacity and average half-cell potential, half-cell potential at the location of deterioration, and percentage of half-cell potential below -0.35 V are shown in Figure 5.14 to Figure 5.16, respectively.

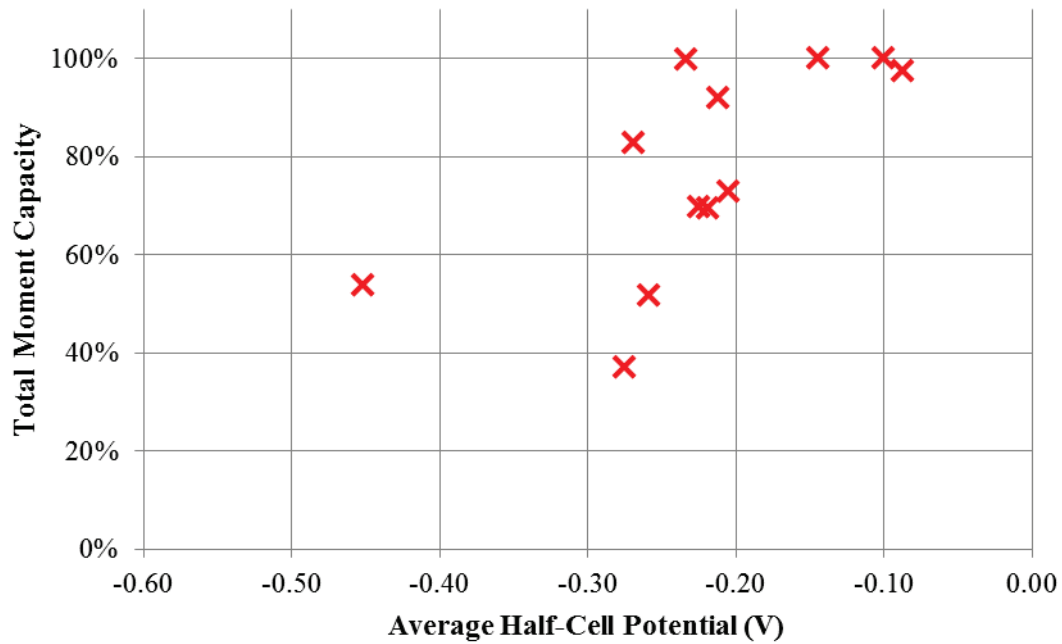


Figure 5.14 – Moment vs. average half-cell potentials, entire slab

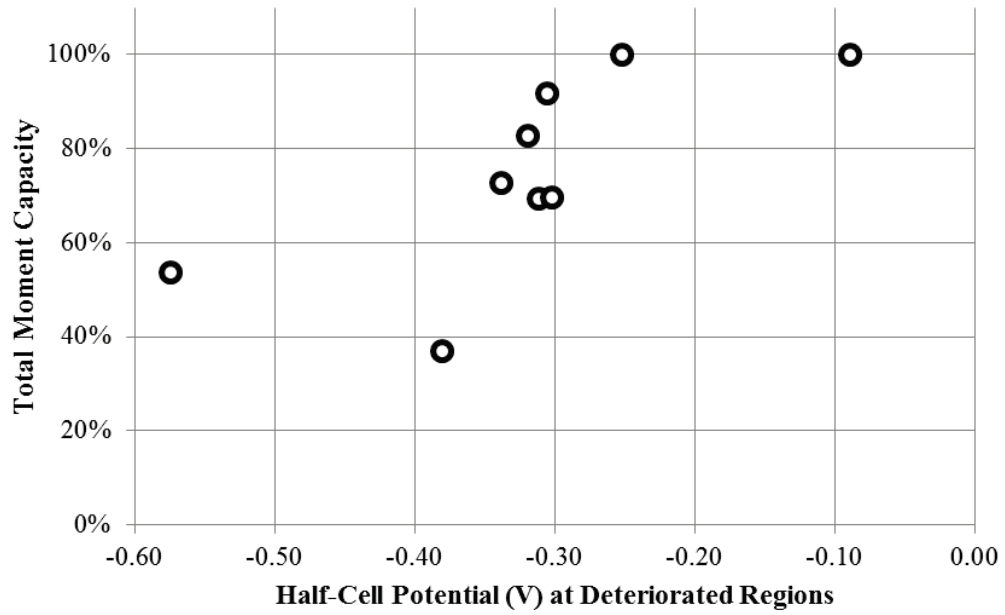


Figure 5.15 Moment vs. average half-cell potentials, locations of visible or audible deterioration

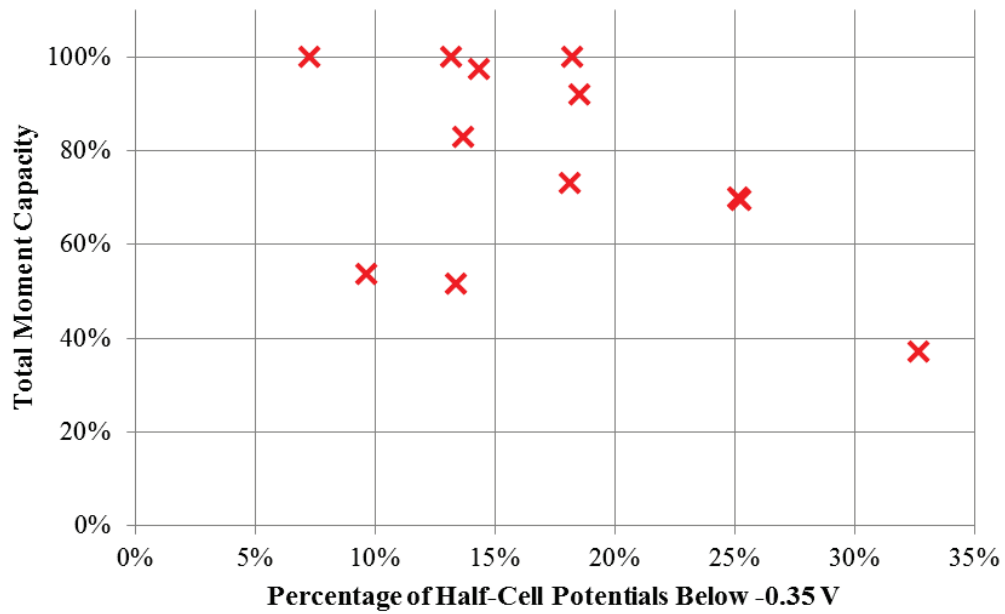


Figure 5.16 - Moment vs. percentage of half-cell potentials below -0.35 V

Based on the results obtained, half-cell potential is not likely to significantly contribute to the ability to analyze the flexural strength of cored slabs at this time. The potential relationship between middle-third half-cell potential may merit further research, but it is not strong enough to warrant recommendation for use in load rating in-service structures. Further challenging the recommendation of using half-cell potential is the time and procedure required to perform the testing. As discussed in Chapter 3, half-cell potential testing requires direct access to strands (drilling through cover concrete) and may require pre-wetting the slab to comply with ASTM C876. The entire process required 2 to 4 hours of work for one operator under laboratory conditions at the CFL, and is conjectured to take double that time in the field.

To conclude the analysis of half-cell potential, contour plots frequently highlight regions of deterioration, but not usefully beyond what can be determined by visual inspection alone. Due to this, half-cell potential contour plots are not recommended for use in the evaluation of cored slabs. Half-cell potential values from the middle third of slabs appear weakly correlated with moment capacity, and are the only result from any half-cell potential or resistivity data that could merit future research, but they do not add significant value beyond what predictions can be made with traditional inspection techniques.

5.3 – Structural Analysis to Predict Flexural Response

Prior to discussing the analysis of the visual condition and sounding data, the methods used to provide context for those results need to be discussed. Unlike resistivity and half-cell potential, which were only analyzed after the fact, visual information was used to make predictions prior to

testing for the 6 slabs from Oyster Creek Bridge based on observations made from the earlier testing of Ward Creek Bridge slabs (along with engineering judgment). The first six slabs tested in the laboratory, those from Ward Creek Bridge, were observed during testing, and informal relationships were examined between strand loss and visual deterioration, sounding, resistivity, and half-cell potential. Based on this, more formal attempts were made to predict the flexural response and capacity of each slab in Oyster Creek Bridge, primarily using the slabs' visual conditions.

Results of structural analysis were previously used in Chapter 4 to display applied moment as a percentage of the calculated maximum available moment. In those results, recall that the maximum applied moment obtained experimentally was 116% of the calculated available moment for Ward Creek slabs, and 122% of the calculated available moment for Oyster Creek slabs. This difference between calculated and observed slab strength presents a challenge for accurately assessing the quality of predictions, and because of this challenge, structural analysis was more extensive than what would typically be warranted in the load rating of a slab. This section discusses two methods of structural analysis: a stress block analysis as described in the PCI design handbook, and a more detailed layered sectional analysis.

5.3.1 – Stress Block Analysis

Initial structural analysis of slabs was carried out using the “unified method” where concrete compressive stress is assumed to be applied over an equivalent rectangular stress block (Whitney Stress Block), as shown in Figure 5.17. This is the procedure for determining ultimate strength

commonly taught in prestressed concrete classes, and the one shown in the PCI Design Handbook (Prestressed Concrete Institute, 2010), and in ACI 318 (2014). This procedure relies on the assumption of a linear strain profile, with a top strain in compression concrete of 0.003, and all prestressing steel treated as a lumped quantity, A_{ps} , at distance e from the top of the slab.

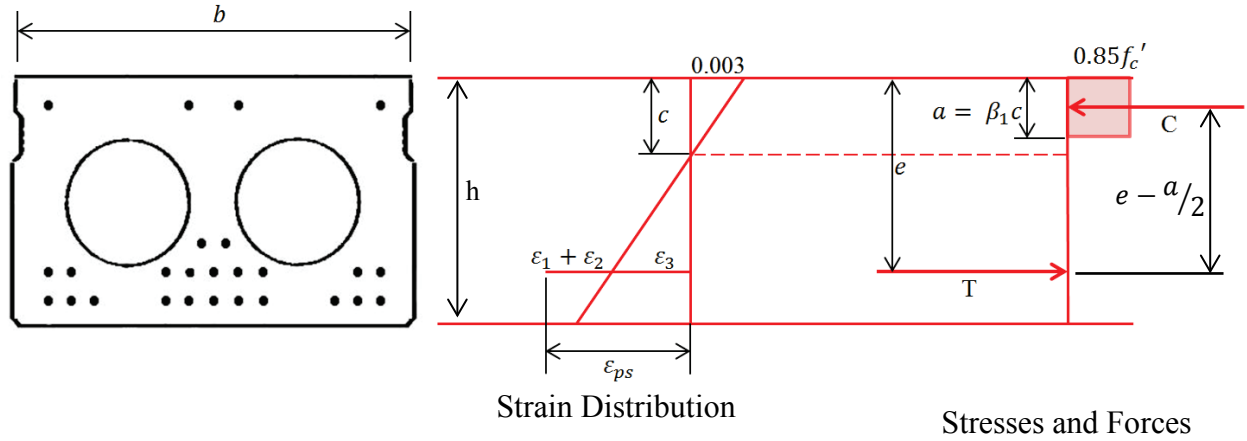


Figure 5.17 - Stress Block Analysis

Strain in prestressing steel, ϵ_{ps} , is taken as the sum of initial prestressing strain ϵ_1 , strain to straighten section ϵ_2 , and compatibility strain ϵ_3 , as shown in Equation 3 to Equation 6.

$$\epsilon_{ps} = \epsilon_1 + \epsilon_2 + \epsilon_3 \quad \text{Equation 3}$$

$$\epsilon_1 = \frac{\sigma_{res}}{E_{steel}} \quad \text{Equation 4}$$

$$\epsilon_2 = \frac{\sigma_{res} * A_{ps}}{A_{conc}} + \frac{\sigma_{res} * A_{ps} * (e - h/2)^2}{I_{conc}} \quad \text{Equation 5}$$

$$\epsilon_3 = \frac{0.003}{c} * (e - c) \quad \text{Equation 6}$$

The stress in the strand from initial prestressing, σ_{res} , is taken as 80% (assumed losses) of the initial stress. Steel modulus of elasticity, E_{steel} , is taken as 28800 ksi (Prestressed Concrete Institute, 2010). Steel area A_{ps} , is 2.415 in.² for Ward Creek (40 ft) slabs, and 2.990 in.² for

Oyster Creek (45 ft) slabs, with corresponding values of eccentricity e of 12.48 in. and 14.54 in., respectively. Per bridge plans, initial jacking force in strands was 21,700 lbs.

Steel stress, f_{ps} , is calculated using the typical design stress-strain curve for 7-wire low-relaxation prestressing strands as given in the PCI Design Handbook (2010), shown in Equation 7.

$$\begin{aligned} \varepsilon_{ps} \leq 0.0085 & \quad f_{ps} = 28800 * \varepsilon_{ps} \quad (\text{ksi}) \\ \varepsilon_{ps} > 0.0085 & \quad f_{ps} = 270 - \frac{0.04}{\varepsilon_{ps} - 0.007} \quad (\text{ksi}) \end{aligned} \quad \text{Equation 7}$$

The tension force in the steel, T , is calculated as shown in Equation 8.

$$T = f_{ps} A_{ps} \quad \text{Equation 8}$$

The compressive force in concrete, C , is relatively simple to calculate. Concrete is treated as having a constant stress of $0.85f'_c$ acting over a depth, a , equal to $\beta_1 c$, with c the distance to the neutral axis. Concrete strength f'_c was taken as 5000 psi, the same assumed value used in NCDOT load rating. For this concrete strength, β_1 is equal to 0.8. The compressive force C is then calculated as shown in Equation 9.

$$C = 0.85f'_c * A_{conc} \quad \text{Equation 9}$$

The area of concrete, A_{conc} , is simply $b*a$ for the case where stress block depth, a , is less than the depth of the top of the cores in the cored slabs, otherwise the two segments of the circular voids must be subtracted from the area, in which case A_{conc} is calculated as shown in Equation 10 (Wikipedia, 2015), with value d_{sb} equal to the distance the stress block extends into the voided region.

$$A_{conc} = b * a - 2 * \left[(r_{void})^2 * \arccos\left(\frac{r_{void} - d_{sb}}{r_{void}}\right) - (r_{void} - d_{sb})\sqrt{2r_{void}d_{sb} - (d_{sb})^2} \right] \quad \text{Equation 10}$$

By force equilibrium of the section, $T = C$, which can be satisfied by varying the neutral axis depth, c . Moments can then be summed about any point to find the strength of the section in flexure.

This stress block analysis procedure was implemented in Microsoft Excel, producing moment capacities of 513 kip-ft and 738 kip-ft for Ward Creek (40 ft) and Oyster Creek (45 ft) slabs, respectively. These under-predict the available moment capacity of the slabs by approximately 20%, as shown in Table 5.4.

Table 5.4 – Calculated moment capacities, Stress Block Analysis

	Ward Creek	Oyster Creek
M_n (kip-ft)	513	738
Available Moment (kip-ft)	429	605
Maximum Applied (kip-ft)	534	767
Error	20%	21%

Stress block analysis with assumed material properties clearly provides conservative results.

This conservatism is detrimental to the desired use of comparing predictions based on visual and sounding data. This is due to the manner in which errors in predicting the flexural strength of the cored slabs arise from two sets of assumptions. First are assumptions used in the overall structural analysis (concrete strength, analysis procedure, steel stress-strain response). Second are assumptions about how to evaluate the condition of the slab, which change the estimates of how many prestressing strands have corroded. In order to compare predictions to experimental

results, it is desirable to focus solely on the error arising from assumptions about strand corrosion. In order to isolate this effect, more accurate structural analysis is needed. Layered Sectional Analysis was chosen as a method that would allow for greater flexibility in varying assumptions, and this method is discussed in the next section.

5.3.2 – Layered Sectional Analysis

5.3.2.1 – Method of Calculation

The concept of a layered sectional analysis is to take a given slab cross-section and discretize it into layers of concrete and steel, as illustrated in Figure 5.18. The area of each layer of concrete and steel can then be calculated based on known properties of the cored slab cross-section and assumptions about deterioration. As shown in Figure 5.19, an arbitrary top strain (ϵ_{top}) is chosen to analyze the section, and a neutral axis depth (c) assumed, from which the strain at the centroid of each layer of concrete and steel can be obtained (considering strain difference for prestressing strands). Appropriate stress-strain relationships for each material are then used to find a stress at each layer, which can then be multiplied by the area of that layer to determine the resultant force component (compressive or tensile) acting through the centroid of the layer. The forces are summed to determine net axial force on the cross-section corresponding to the assumed strain distribution.

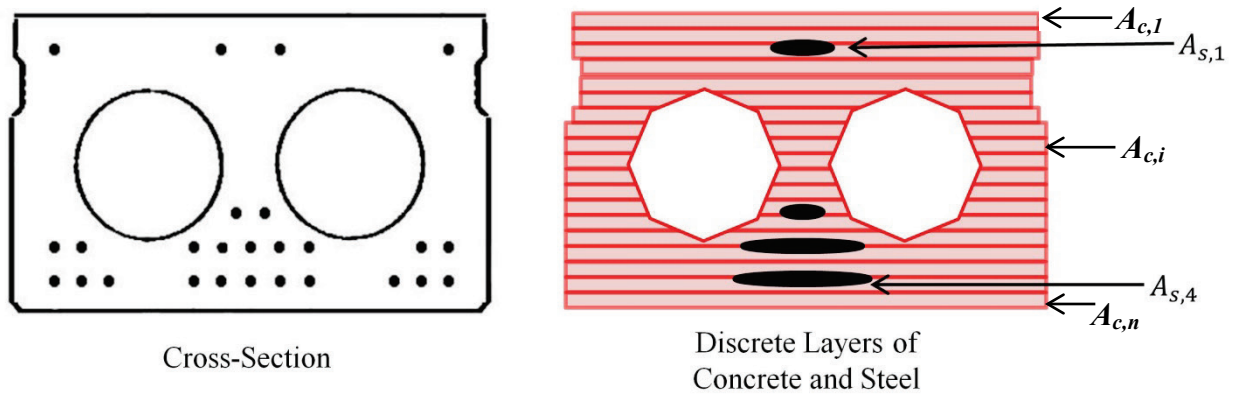


Figure 5.18 - Layered Sectional Analysis, discretizing into layers

The correct strain distribution corresponding to a given ϵ_{top} is found when the sum of axial forces equals the applied axial load, which is equal to zero for the slabs in question. This neutral axis depth, c , is varied until equilibrium is obtained, at which point the moment can be calculated, along with the corresponding curvature ϕ (ϵ_{top} / c).

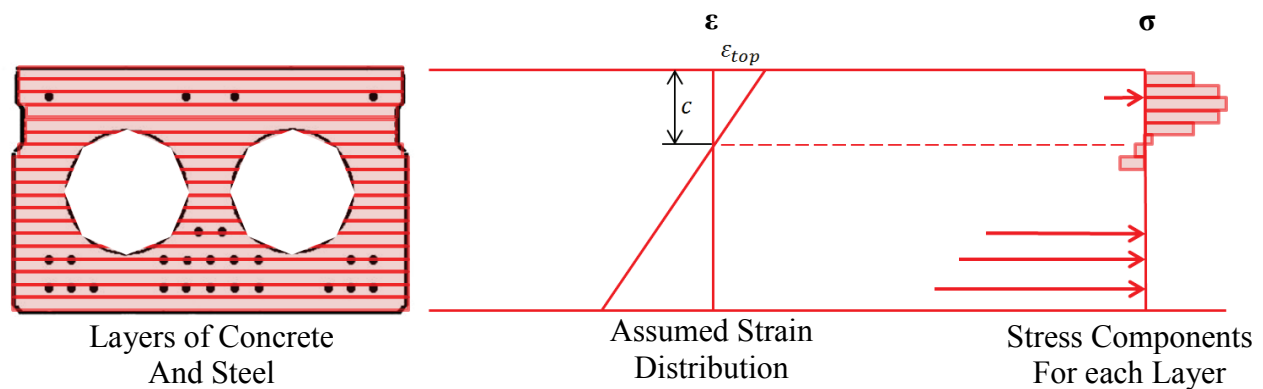


Figure 5.19 - Layered Sectional Analysis, determining force components

By repeating this process for different top strains (ϵ_{top}), the full relationship between moment and curvature can be found, including the prediction of moment capacity of the section. A typical

moment-curvature plot (not corresponding to any particular slab), in this case for an undamaged 45 ft cored slab in positive bending, is shown in Figure 5.20.

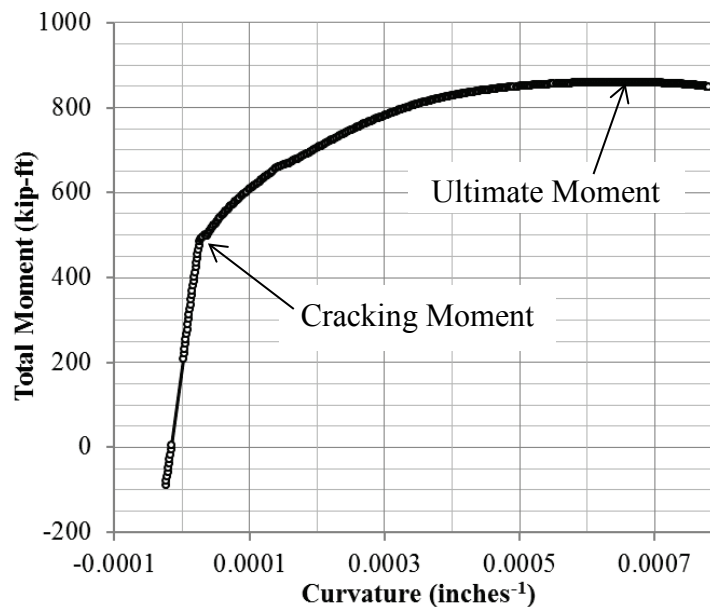


Figure 5.20 - Calculated moment-curvature plot

The moment-curvature response obtained from layered sectional analysis can then be used to predict the deflection at midspan for a given applied load. This is accomplished by calculating, for a given applied load, the total moment (dead load and live load) at set intervals between the supports and midspan along the slab, from which the curvature corresponding to each total moment may be determined using the moment-curvature response (as in Figure 5.20). Assuming a linear variation in curvature between each interval, the curvature is then integrated numerically to obtain a midspan deflection for that loading condition. This is repeated for each applied load (up to the applied load calculated to produce total moment equal to moment capacity) until a complete load-deflection relationship has been generated. A graph generated using this method is shown in Figure 5.21.

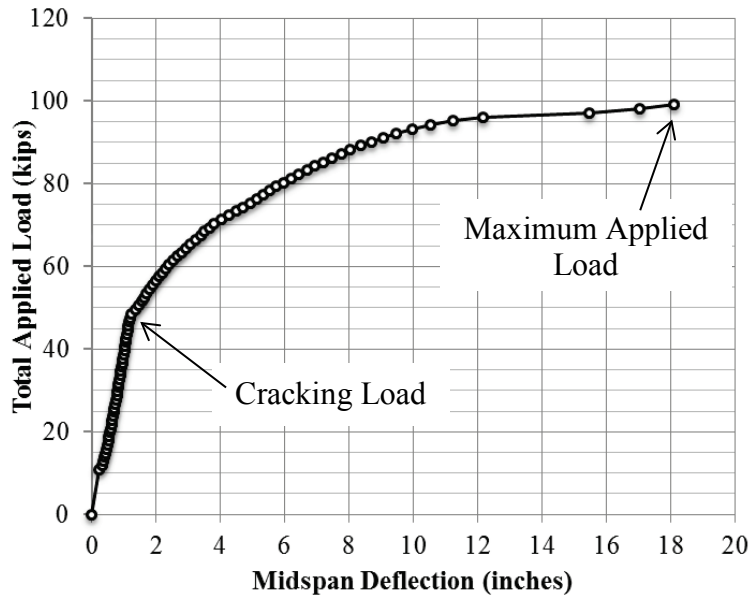


Figure 5.21 - Calculated load-deflection plot

This process of calculating the full load-deflection plots is not typically useful in analyzing beam capacity because generally only a few points, such as ultimate moment and cracking moment, are desired. In the context of this research, however, this process is valuable because it allows different assumptions about slab behavior to be easily varied individually and examined against results during experimentation. The ultimate capacity of the slab can vary with concrete strength and stiffness, strand area and location, strand strength and stiffness, and variations in slab cross-section. In order to understand the combinations of deterioration and material strength that are present in the actual tested slabs, it was important to try and differentiate between variations in capacity for each of those reasons. Relative to a prediction that only yields a single value for maximum moment capacity, such as that produced by the stress block analysis in the previous section, layered sectional analysis allows for the possibility of obtaining agreement between the full shape of a theoretical load-deflection response and an experimental response. This provides

a greater degree of certainty in the validity of modeling. A secondary benefit of this process is the avoidance of black-box software, by using basic fundamentals of structural analysis and flexural behavior.

5.3.2.2 – Material Models

Concrete in compression was modeled using the modified parabolic-linear relationship shown in Equation 11, Equation 12, and Figure 5.22, equivalent in shape to that given by Hognestad (1951). The strain at peak stress, ϵ_0 was assumed as 0.002, while ϵ_{cu} was chosen as 0.0034, the maximum measured applied top strain during testing.

$$f_c = f'_c \left[\frac{2\epsilon_c}{\epsilon_0} - \left(\frac{\epsilon_c}{\epsilon_0} \right)^2 \right] \quad 0 \leq \epsilon_c \leq \epsilon_0 \quad \text{Equation 11}$$

$$f_c = f'_c \left[1 - 0.15 \left(\frac{\epsilon_c - \epsilon_0}{\epsilon_{cu} - \epsilon_0} \right)^2 \right] \quad \epsilon_0 \leq \epsilon_c \leq \epsilon_{cu} \quad \text{Equation 12}$$

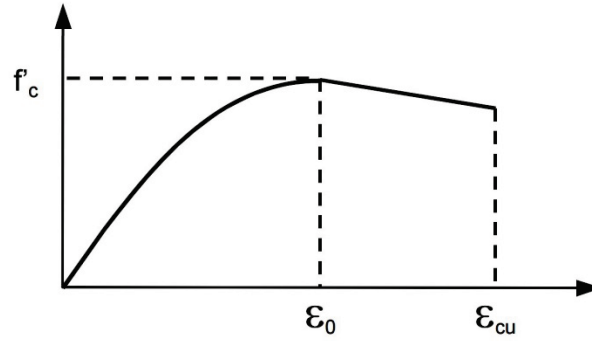


Figure 5.22 - Theoretical stress-strain for concrete in compression (Bramblett, 2000)

Concrete in tension was assumed linearly elastic up to cracking, f_{cr} , with modulus of elasticity, E_{ct} , as given in ACI 318 (2014). Cracking stress was assumed to be the modulus of rupture as presented in ACI 318. These values are shown in Equation 13 and Equation 14.

$$E_{ct} = 57000\sqrt{f'_c} \quad \text{Equation 13}$$

$$f_{cr} = 7.5\sqrt{f'_c} \quad \text{Equation 14}$$

Concrete after cracking was modeled using a tension stiffening model to consider tension in uncracked concrete between flexural cracks. This is desirable when used to predict deflection behavior. This is modeled as shown in Equation 15, which was based on empirical observations (Collins, 1991), where constant α is 0.7 for prestressing strands under short-term loading.

Concrete tension stiffening as an effect is limited to concrete layers located less than $7.5*d_{strand}$ from prestressing strands.

$$f_c = \alpha * \frac{f_{cr}}{1 + \sqrt{500\varepsilon_c}} \quad \varepsilon_{cr} < \varepsilon_c \leq 10\varepsilon_{cr} \quad \text{Equation 15}$$

Steel prestressing strands in tension are modeled using a modified Ramberg-Osgood relationship (1943), which considers the response to be effectively bilinear with a smoothed transition.

$$f_s = E_s \varepsilon_s \left[A + \frac{1 - A}{(1 + [B * \varepsilon_s]^c)^{1/c}} \right] \quad \text{Equation 16}$$

Where E_s is the modulus of elasticity taken as 29000 ksi, per ACI 318 (2014), and A, B, and C are coefficients that are fit to a given prestressing curve. Bridge construction plans provided an initial jacking force on prestressing strands of 21700 lbs (189 ksi). This was modified by assuming 20% lump-sum losses for a remaining prestress of 150 ksi.

The strength of a layered sectional analysis is its root in these basic relationships from individual material components, and how they interact.

5.3.2.3 – Slab Load-Deflection Response Obtained from Layered Sectional Analysis

Predicted slab strengths and responses are shown in this section for varying assumed concrete strengths and steel stress-strain responses.

Initial predicted response used assumed material properties similar to those used in the stress block analysis. These are:

- Concrete strength f'_c was taken as 5000 psi.
- Modified Ramberg-Osgood parameters A, B, and C were assumed as 0.003, 109, and 8 respectively, which produces a response similar to that recommended by the PCI equation.

These material properties produced moment capacities of 568 kip-ft and 784 kip-ft for Ward Creek (40 ft) and Oyster Creek (45 ft) slabs, respectively. These under-predict the available moment capacity of the slabs by 9% and 15%, as shown in Table 5.5.

Table 5.5 – Calculated moment capacities, assumed material properties

	Ward Creek	Oyster Creek
M_n (kip-ft)	568	784
Available Moment (kip-ft)	484	651
Maximum Applied (kip-ft)	534	767
Error	9%	15%

In this case, the layered sectional analysis predicts available moments 11% and 6% closer to experimental results than the stress block approach. Calculated load-deflection responses are shown in Figure 5.23, compared to results from the two strongest slabs from each bridge.

Predicted responses for both bridges display similar shapes to those found experimentally, but neither reaches deflection or load values seen in testing. The prediction for Oyster Creek slab is

noticeably lower than that observed in testing. Predicted failure was by rupturing of the bottom layer of strands, while failures observed in testing were by crushing of concrete for all slabs in good condition.

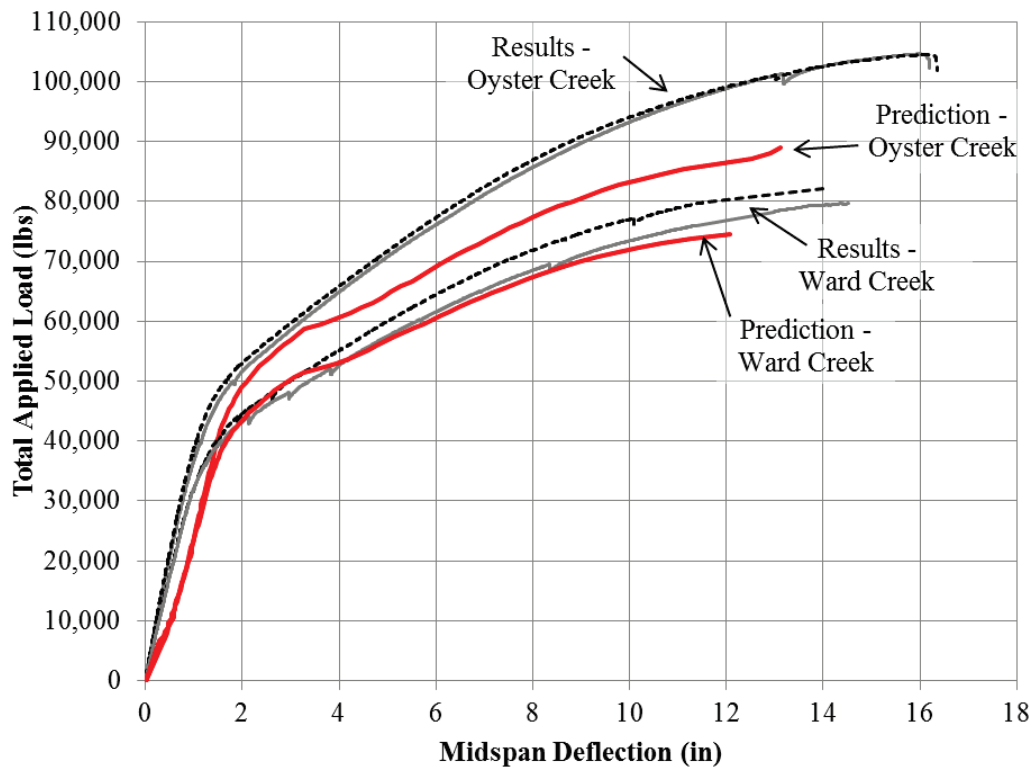


Figure 5.23 – Predicted load-deflection responses, 5000 psi concrete

Predictions were calculated again with concrete strength as obtained from cores. Maximum concrete compressive stress, f'_c , is taken as 7 ksi, rounded from the average measured concrete strength of 7130 psi based on the concrete cores discussed in Chapter 4. These material properties produced moment capacities of 596 kip-ft and 820 kip-ft for Ward Creek (40 ft) and Oyster Creek (45 ft) slabs, respectively. These under-predict the available moment capacity of

the slabs by 4 and 10%, as shown in Table 5.6. This is a uniform 5% improvement relative to assumed 5000 psi concrete.

Table 5.6 – Calculated moment capacities, 7000 psi concrete

	Ward Creek	Oyster Creek
M_n (kip-ft)	596	820
Available Moment (kip-ft)	511	688
Maximum Applied (kip-ft)	534	767
Error	4%	10%

Calculated load-deflection responses are shown in Figure 5.24. Predicted responses align more closely with the experimental results compared to those using 5000 psi concrete. Predicted failure was again by rupturing of the bottom layer of strands.

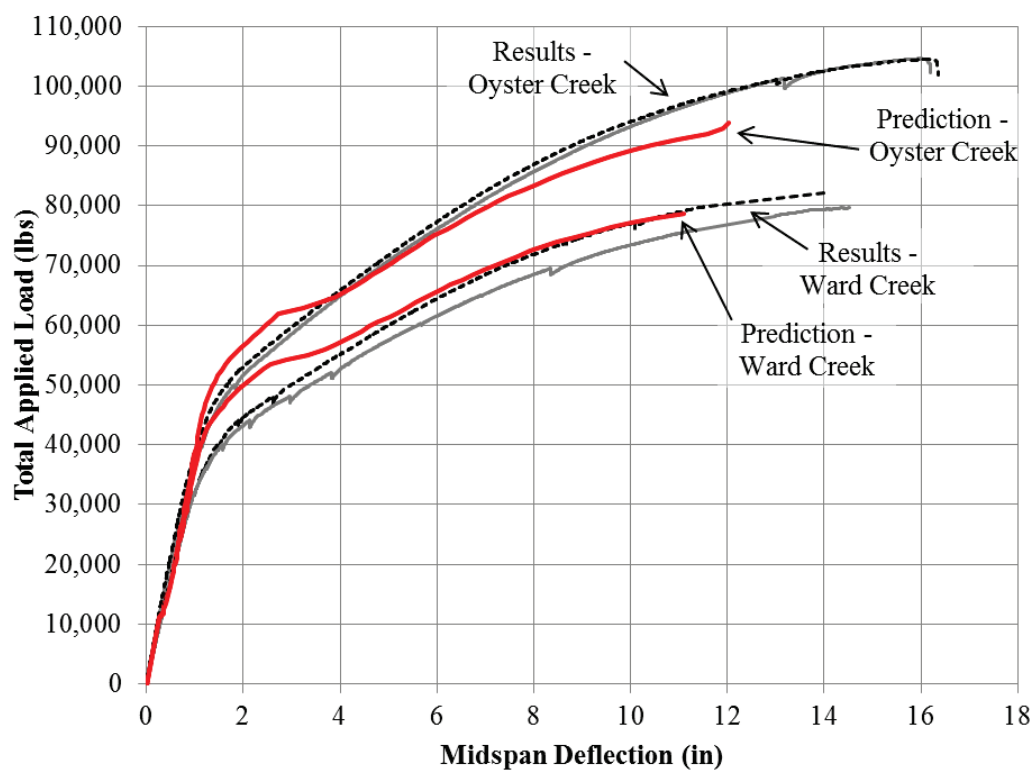


Figure 5.24 – Predicted load-deflection responses, 7000 psi concrete

Predictions were then calculated using steel stress-strain curve parameters fit to experimental responses found from material testing. This produced values of A, B, and C of 0.018, 108, and 8 respectively, to match the values observed in strand testing as shown in Figure 5.25.

Additionally, the ultimate stress of strands was increased to 285 ksi, the lower of the two strengths measured during testing.

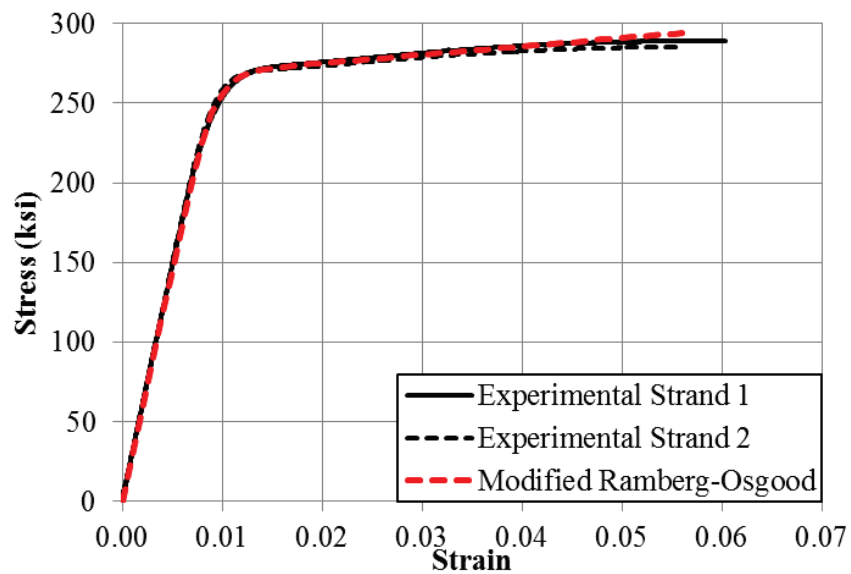


Figure 5.25 – Modified Ramberg-Osgood stress-strain relationship fit to Ward Creek strand tests

These material properties produced moment capacities of 617 kip-ft and 853 kip-ft for Ward Creek (40 ft) and Oyster Creek (45 ft) slabs, respectively. This accurately calculates the available moment for Ward Creek slabs, and under-predicts the available moment for Oyster Creek slabs by 6%, as shown in Table 5.7. This is a uniform 4% improvement compared to using the assumed steel stress-strain response.

Table 5.7 – Calculated moment capacities, calibrated steel stress-strain response

	Ward Creek	Oyster Creek
M_n (kip-ft)	617	853
Available Moment (kip-ft)	533	720
Maximum Applied (kip-ft)	534	767
Error	0%	6%

Calculated load-deflection responses are shown in Figure 5.26. With the given ultimate strength of strands increased, strands were not calculated to rupture, and analysis was stopped at a top strain of 0.0031, at which point moment values were observed to have plateaued.

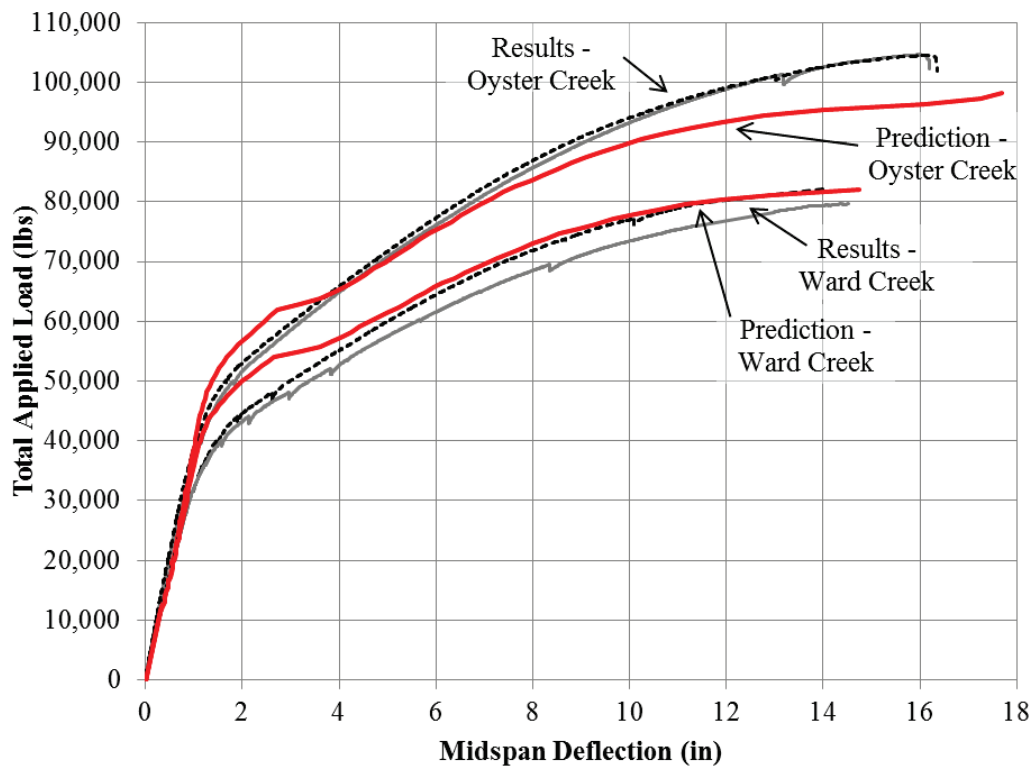


Figure 5.26 – Predicted load-deflection responses, calibrated steel stress-strain response

The calculated load-deflection response for Ward Creek slabs follows very closely with experimental results, with the noticeable exception of the region near initial cracking (1 to 3

inches of deflection), where analysis predicts substantially more strength than is displayed in testing. Calculated response for Oyster Creek slabs also aligns well with experimental results initially and after cracking, but the calculated load-deflection response over-predicts the slab strength during cracking, and plateaus at higher deflections.

This layered sectional analysis using concrete strength f'_c of 7000 psi and modified Ramberg-Osgood constants A, B, and C of 0.018, 108, and 8 presents a substantial improvement over the initial calculation using assumed material properties and a stress block analysis. The changes in prediction error based on different analysis procedures and assumptions are summarized in Table 5.8.

Table 5.8 – Error as a percentage of experimental applied load

	Ward Creek	Oyster Creek	<i>Reduction in Error</i>
Stress Block	20%	21%	
Layered Sectional Analysis	9%	15%	6 to 11%
$f'_c = 7000$ psi	4%	9%	5%
Fit steel σ - ϵ response	0%	5%	4%

Based on this, it can be concluded that the details of analysis procedure have an appreciable effect on the calculated strength of a slab. Additionally, the assumed concrete strength of 5000 psi was exceeded in all cores tested, and if a higher value of f'_c can be justified by concrete coring, field tests, or construction data, it noticeably improves the strength of the slab.

5.3.2.4 – Fitting Load-Deflection Response to Experimental Results

The material properties discussed in the previous section 5.3.2.3 are the extent of modifications to the analysis that can be made with a strong basis in prior data. However, in Section 5.4 this structural analysis procedure is used to test a variety of assumptions about the relationship between visual and sounding data and steel section loss. So that the error in these assumptions can be looked at independently, further modifications were made to the material models used in layered sectional analysis in order to fit the calculated load-deflection response to that obtained experimentally. These modifications are as follows:

- Concrete cracking stress f_{cr} was taken as $5\sqrt{f'_c}$ instead of the initially assumed $7.5\sqrt{f'_c}$.
- Steel stress-strain relationship was modified for Oyster Creek Bridge (45 ft) slabs to values of A, B, and C of 0.01, 105, and 8.
- Concrete tension stiffening used $\alpha = 0.4$, with no upper strain limit.

These modifications are not recommended for consideration in typical analysis, and are only used here for the reasons described above. They result in the calculated load-deflection responses shown in Figure 5.29, and available moments within 3% of experimental results for slabs from both bridges.

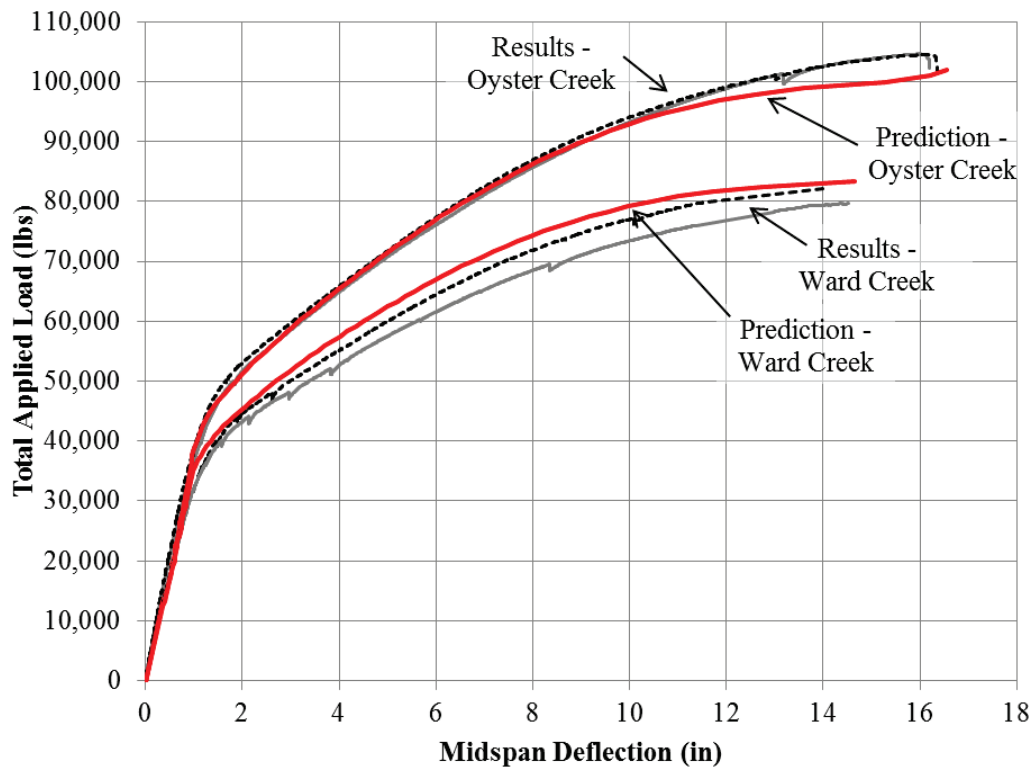


Figure 5.27 - Calculated load-deflection response fit to experimental results

This model was used to obtain estimates of cored slab strengths and behaviors for different numbers of strands in the bottom layer, since that is observed to be the primary location of deterioration significant to flexural strength. Estimates of total applied load versus midspan deflection are shown for Ward Creek Bridge in Figure 5.28 and for Oyster Creek Bridge in Figure 5.29.

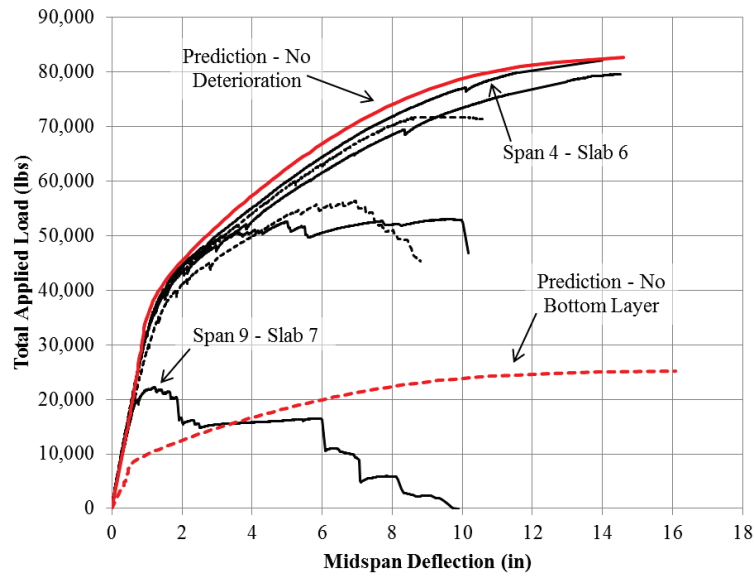


Figure 5.28 - Ward Creek Bridge predicted load-deflection response

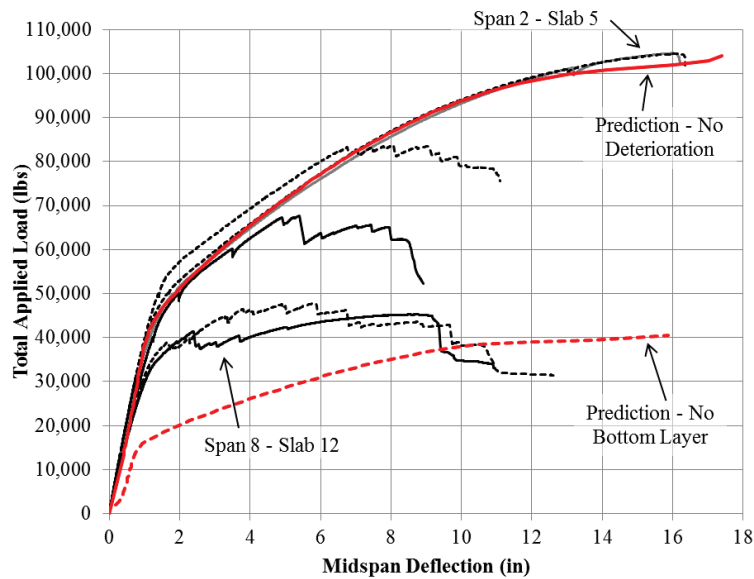


Figure 5.29 - Oyster Creek Bridge predicted load-deflection response

Slabs with significant corrosion of strands, however, do not display a flexural response in line with that predicted for a slab with less prestressing present, but rather initially respond to loading

with stiffness indicative of less deterioration, followed by progressive rupture of deteriorated strands. This implies that deterioration works as much to increase the brittleness of strands as it does to reduce their cross-sectional area, possibly due to high stress concentrations in pitted sections of strands. This can be observed visually in the section of strand from Oyster Creek – Span 8 – Slab 13 shown in Figure 5.30, where some wires (left) ruptured earlier in testing (greater distance between failure surfaces) than others (right).



Figure 5.30 – Ruptured wires in strand, Oyster Creek - Span 8 - Slab 13

This effect is not reflected in the model, hence the deviation between estimated and observed response for weaker slabs despite good agreement in slab flexural strength.

Estimations of total moment capacity of slabs based on this model are shown in Figure 5.31 for Ward Creek Bridge and Figure 5.32 for Oyster Creek Bridge. Relationships are not truly linear, but can be effectively treated as such with only 11 strands, with each strand in the bottom layer adding approximately 34 kip-ft to the total strength for Ward Creek (17 in. deep, 40 ft span) slabs, and adding approximately 42 kip-ft to the total strength for Oyster Creek (20 in. deep, 45 ft span) slabs.

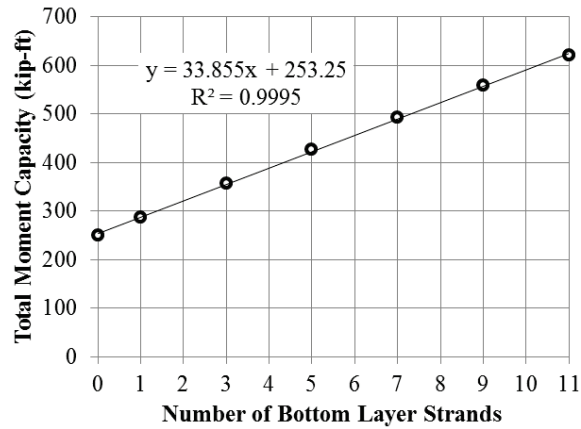


Figure 5.31 - Ward Creek Bridge - Predicted moment capacity vs. number of bottom strands

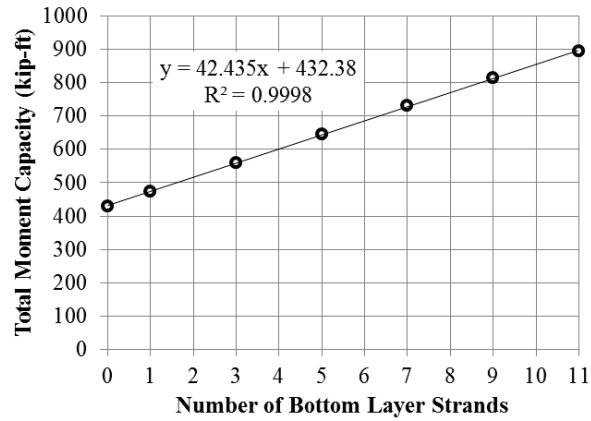


Figure 5.32 - Oyster Creek Bridge - Predicted moment capacity vs. number of bottom strands

Based on observations made in deterioration, the assumption that only the bottom layer of strands had appreciable deteriorated was appropriate for all but two slabs. These were the two slabs with the lowest strengths: Ward Creek – Span 9 – Slab 7; and Oyster Creek – Span 8 – Slab 12.

5.4 – Visual Inspection and Sounding

Unlike resistivity and half-cell potential, which are evaluated on their ability to add value to the inspection process, visual inspection and sounding are evaluated on how best to interpret the data. It is assumed that visual observation of the bridge will always be the primary component of an inspection, with sounding as a common and readily applicable option for interpreting areas of delaminated concrete. Existing bridge inspection records contain images and descriptions of delaminated regions of concrete of the type shown in Figure 5.33. Based on discussion with NCDOT personnel, current analysis is based on guesswork and frequently limited by the ability to discern corrosion in inspection photos. Specific issues discussed in this section are the condition of slabs in delaminated regions, the condition of slabs in previously patched regions, and varying strategies for analyzing visual/sounding data.



Figure 5.33 – Delamination, 2007 Inspection, Oyster Creek Bridge

5.4.1 – Delaminations

Of the 12 slabs tested at the CFL, 10 had some region of delamination, indicating that the presence of delamination is not something that can be interpreted in one way uniformly.

Delamination is best understood, instead, in the context of the surrounding deterioration of the slab. Laboratory demolition suggests delaminations can be interpreted as falling into four different categories:

- **Small delaminations**, generally sounding higher-pitched, generally less than 1 ft long are frequently located under stirrups that are corroding. Typically these will be accompanied by several locations on the same (or adjacent) slabs where delaminated concrete has already spalled off. Demolition did not find any significant deterioration of strands under these locations, and they are generally an indication of the early stages of deterioration. A typical location of this type of delamination is visible at 25 ft on Ward Creek – Span 4 – Slab 6 (Figure 5.34), where a small delamination indicates the continuation of the same stirrup corrosion that has caused shallow spalling in the surrounding area. No strands were corroded in this section.

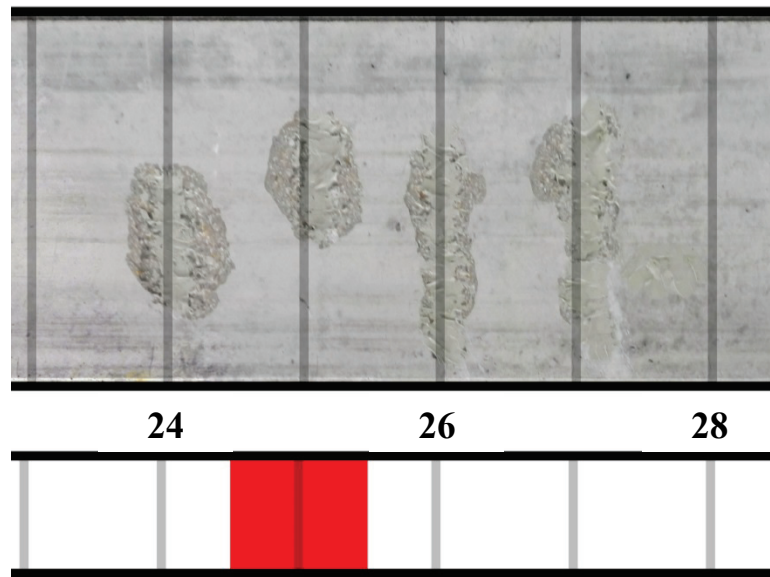


Figure 5.34 - Delaminated region, Ward Creek - Span 4 - Slab 6

- **Large delaminated regions** stretching across multiple stirrups and covering more than half the width of a slab indicate substantial underlying corrosion. These are sometimes accompanied by multiple longitudinal cracks and visible sagging of the soffit concrete. In the case of visibly sagging concrete it appears the delaminated concrete layer is being held to the slab by its existing bond to stirrups. This necessarily means the bottoms of stirrups have debonded from the concrete above them and are sagging to some extent as well, leading to greater strand exposure. One slab was chosen for laboratory testing displaying this type of corrosion, Ward Creek, Span 1 – Slab 13 (Figure 5.35, visible cracks circled). This region spalled off during flexural testing (Figure 5.36), with 6 of the 11 bottom strands estimated to be lost.

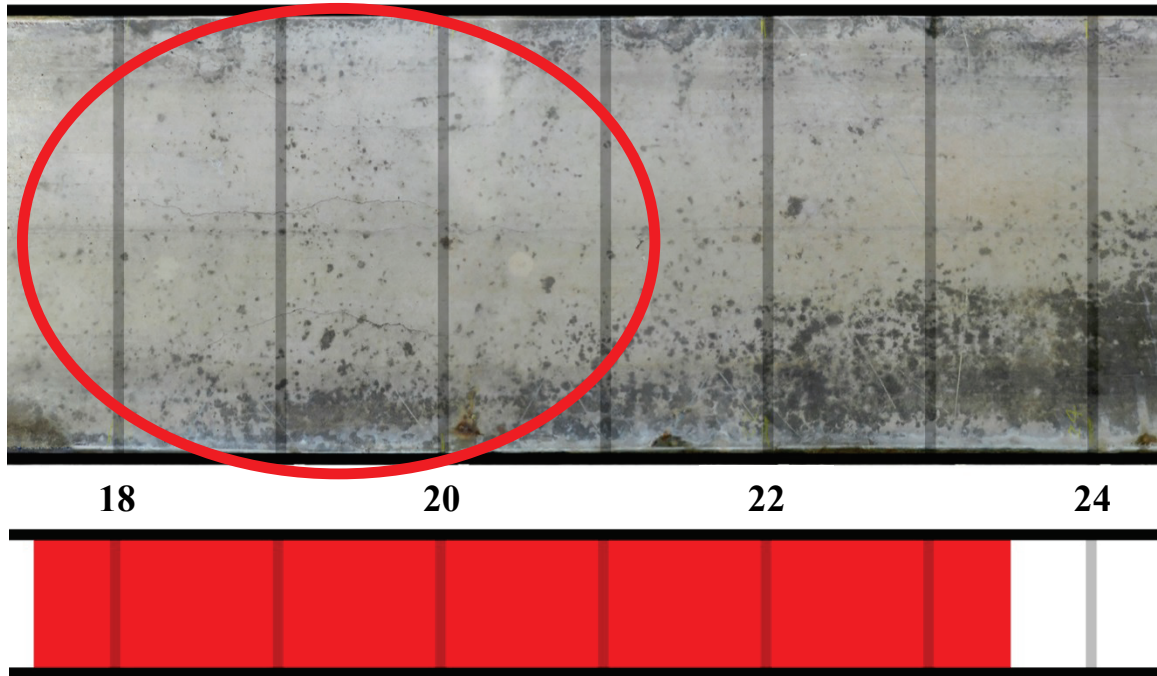


Figure 5.35 - Delaminated region, Ward Creek - Span 1 - Slab 13



Figure 5.36 - Delaminated region after testing, Ward Creek - Span 1 - Slab 13

- **Delamination next to visibly spalled regions** generally indicates the continuation of whatever depth and extent of spalling is visible in the spalled region to which they are adjacent. Frequently the depth of delamination is visible to the inspector, though delaminated regions seem to often be deepest at an adjacent spall, and become shallower as they move away from existing visible deterioration.
- **Further delamination of existing spalls and patches** generally can be taken as a deepening of whatever spall was there before. The condition of strands underneath these delaminated areas varies depending on the extent of spalling that had existed before. If existing spalls and rust stains indicate corroding of strands, further delamination indicates total loss of those strands. The worst deterioration observed of this type in laboratory testing was on Oyster Creek – Span 8 – Slab 12 (Figure 5.37), where the entire icolastic patch had delaminated and was hanging from what remained of heavily corroded stirrups. This patch continued to the adjacent slab and was separated by several inches from the concrete above when the slab arrived at the CFL. All bottom strands displayed corrosion, and this was 1 of only 2 locations where strands above the bottom layer showed deterioration. An estimated equivalent 10 of 11 bottom strands were lost.

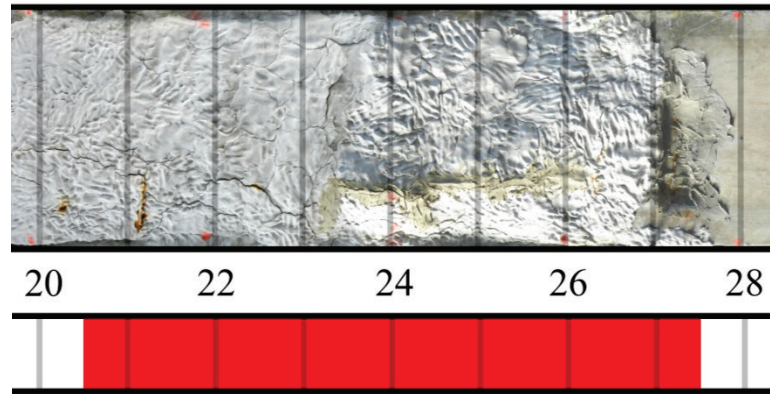


Figure 5.37 – Delaminated patched region, Oyster Creek - Span 8 - Slab 12

5.4.2 – Patched Regions

Little about patched regions is consistent enough to group analysis into broad statements.

Patching of slabs on the two bridges varied in type and extent, with some patches performing effectively, while others deteriorated. Of the 32 slabs examined in intermediate spans (Ward Creek – Span 4 and Oyster Creek – Span 2), 15 slabs contained some spalling. This spalling was almost always shallow spalls directly underneath a stirrup, and the patches placed on these varied in their effectiveness, sometimes in the same location, as is visible on Oyster Creek – Span 2 – Slab 4 at 10 ft (Figure 5.38). Based on the review of bridge inspection records from Chapter 2, icolastic patching material (as seen in Figure 5.37) was no more effective than other materials at limiting corrosion, with patches applied between 2001 and 2003 on Oyster Creek – Span 8 surrounded by delamination by 2007, seemingly comparable to the progression of deterioration in other end spans.



Figure 5.38 - Small patches, Oyster Creek - Span 2 - Slab 4 at 10 ft

For the purposes of load rating, patches need to be interpreted on a case-by-case basis. At a minimum, however, patching should not be taken as an improvement in the condition of an already-deteriorated section. Attention should be drawn to the process of reevaluating the load rating for a bridge after every inspection cycle, which can potentially cause erroneous increase in the bridge condition if the deterioration prior to patching was not documented and said deterioration is no longer visible.

5.4.3 – Analysis Strategies

Experience predicting moment capacity for slabs from Oyster Creek Bridge prior to testing reinforced the general understanding that good predictions could be made purely through examining visible and audible deterioration on slabs. No approach will work perfectly for all

slabs, but a consistent, reliable strategy for accurately interpreting this data is necessary in order for it to be useful to load rating engineers. Three strategies for interpreting this data to make predictions are discussed here.

5.4.3.1 – Prediction Strategy: Only Visible Corrosion

One method of interpreting the condition of slabs is to assume that there is only corrosion of a strand if longitudinal rust stains are clearly visible. This is the “optimistic” assumption, and assumes that any significant corrosion of primary reinforcement *must* be accompanied by significant spalling of concrete in that region, and that no corrosion extends past the bottom layer of strands unless clearly visible. On the other hand, it assumes that any longitudinal rust stain is associated with total loss of the strand above it, an assumption more conservative than that currently used in load rating. The implementation of this strategy is as follows:

1. Identify all areas of visible corrosion in the middle ~75% of the slab (in order to only consider deterioration in regions with substantial applied moments).
2. For each location, identify any *longitudinal* rust stains.
3. Consider each longitudinal rust stain as the loss of the strand above it. If the orientation of a rust stain is not clear and seems ambiguous in the photo, assume loss of half a strand.
4. Based on this, count how many of the bottom strands are lost. Do not assume any deterioration of higher layers of strands unless spalls have made them visibly corroded.

Detailed pictures of regions of deterioration for 4 slabs are shown in Figure 5.39 to Figure 5.42.

These 4 slabs are used to illustrate this process.

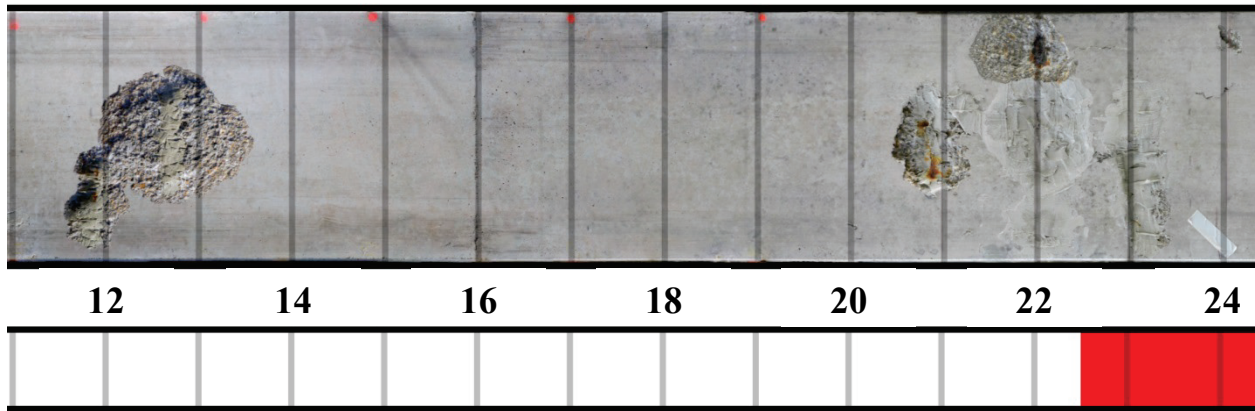


Figure 5.39 – Ward Creek - Span 9 - Slab 6

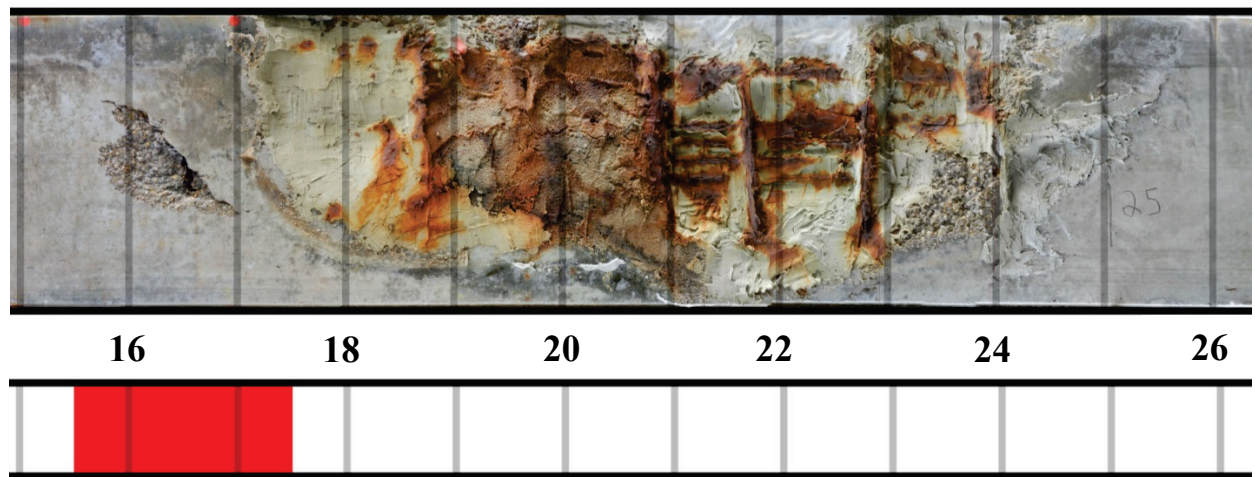


Figure 5.40 - Ward Creek - Span 9 - Slab 7

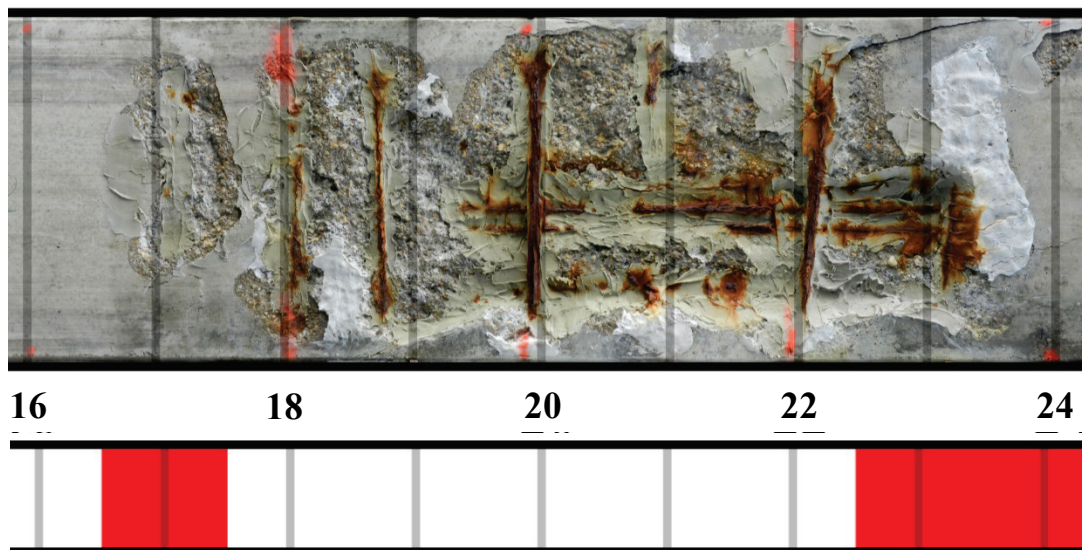


Figure 5.41 - Oyster Creek - Span 1 - Slab 13

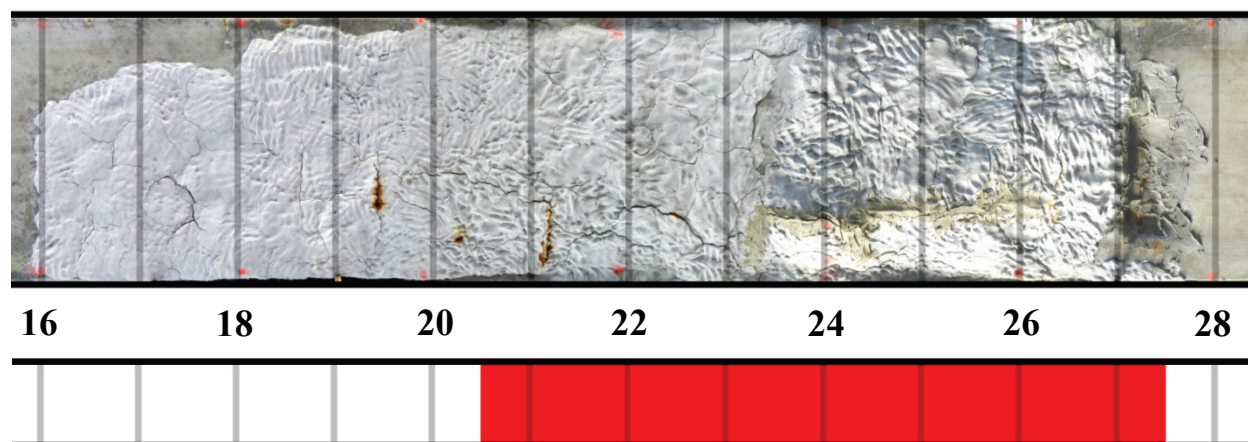


Figure 5.42 - Oyster Creek - Span 8 - Slab 12

- *Ward Creek – Span 9 – Slab 6*: Two regions of deterioration, at 13 ft and 21-24 ft. Neither show longitudinal rust stains. Assume 0 strands lost. Structural analysis predicts $M_n = 622$ kip-ft. Tested strength = 568 kip-ft; analysis over-predicting by 10%.

- *Ward Creek – Span 9 – Slab 7*: One region of deterioration, 16 to 26 ft. Not entirely clear, 4 to 5 longitudinal rust stains. Assume 4.5 strands lost. Structural analysis predicts $M_n = 476$ kip-ft. Tested strength = 229 kip-ft; analysis over-predicting by 46%.
- *Oyster Creek – Span 1 – Slab 13*: One region of deterioration, 17 to 25 ft. Not entirely clear, 2 to 4 longitudinal rust stains. Assume 2 strands lost. Structural analysis predicts $M_n = 815$ kip-ft. Tested strength = 483 kip-ft; analysis over-predicting by 43%
- *Oyster Creek – Span 8 – Slab 12*: One region of deterioration, 16 to 28 ft. No visible longitudinal rust stains. Assume 0 strands lost. Structural analysis predicts $M_n = 896$ kip-ft. Tested strength = 465 kip-ft; analysis over-predicting by 56%.

Predicted flexural strengths for all slabs are shown in Table 5.9. This strategy consistently over-predicts slab strength, but is easily implementable without further requirements from inspectors, does not rely on delamination data and likely will not lead to any unnecessary load posting of bridges. No strategy less conservative than this should be considered.

The error term given in Table 5.9 and in the examples above is the difference between predicted and experimental strength as a percentage of the observed maximum applied moment for that slab length. This value was 534 kip-ft for Ward Creek (40 ft) slabs, and 767 kip-ft for Oyster Creek (45 ft) slabs. This error term was chosen to best reflect the intended use of the data of determining decrease in live-load capacity for any given slab.

Table 5.9 - Predicted strength using "Only Visible Corrosion" strategy

	Experimental		Only Visible Corrosion		
	<i>kip-ft</i>	<i>Strands Lost</i>	<i>Strands Lost</i>	<i>kip-ft</i>	<i>% error</i>
Ward Creek - Span 1 - Slab 13	429	6	0	622	36%
Ward Creek - Span 1 - Slab 14	451	5	0.5	606	29%
Ward Creek - Span 4 - Slab 5	602	0.5	0	622	4%
Ward Creek - Span 4 - Slab 6	618	0	0	622	1%
Ward Creek - Span 9 - Slab 6	568	1.5	0	622	10%
Ward Creek - Span 9 - Slab 7	229	12	4.5	476	46%
Oyster Creek - Span 1 - Slab 13	483	10	2	815	43%
Oyster Creek - Span 1 - Slab 14	628	6.5	2	815	24%
Oyster Creek - Span 2 - Slab 4	900	0	0	896	-1%
Oyster Creek - Span 2 - Slab 5	899	0	0	896	0%
Oyster Creek - Span 8 - Slab 12	465	10	0	896	56%
Oyster Creek - Span 8 - Slab 13	746	3.5	0	896	20%

Average: 23%

5.4.3.2 – Prediction Strategy: Depth of Spall

This method incorporates most observations made throughout testing into a strategy that requires information on *depth of spalling*, along with delamination. Accurate measurement of depth of spalling is frequently difficult in the field due to lack of an established reference point in regions of heavy deterioration, but this information is essential to understanding the extent of corrosion, and is frequently not discernable in photographs. For ease of inspection, depth of spalling is determined not as a measured value, but as one of four descriptions, with spalling characterized as “*without steel exposed*”, “*to bottom of stirrups*”, “*to bottom layer of strands*”, or “*beyond bottom layer of strands*”. This “depth of spall” prediction strategy rests on a number of assumptions and observations about how slabs deteriorate and what information is available to

an inspector. Some of these have been discussed earlier in this report. These assumptions and observations are summarized here:

- Information is available from inspection about depth of deterioration (using descriptions described previously) and locations and appearance of delaminations.
- Spalling is not structurally significant until it extends to the bottom layer of prestressing strands (“*to bottom layer of strands*”). Therefore, spalls “*to bottom of stirrups*” are not significant.
- Strands above the bottom layer are undamaged unless concrete above the bottom layer (“*beyond bottom layer of strands*”) is delaminated **or** spalled.
- Strands within the slabs (for all cored slab standards) are in three distinct groups, as visible in Figure 5.43. If spalling extends clearly to the depth of strands in any one of the groups, assume *all strands* for that group in the bottom layer (3 strands for sides, 5 for center) are lost. In the 12 tested slabs there are 36 such groups, and demolition revealed that in 25 of the groups, if any strand in the group was corroded the entire group was corroded, and if any strand was not corroded no strand in the group was. In the remaining 7 groups corrosion of one strand meant at least one other strand in the group was corroded. No strands were observed to corrode in isolation.

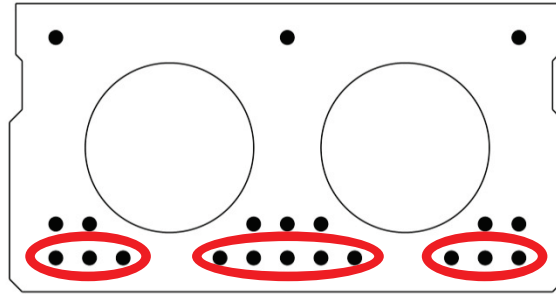


Figure 5.43 - Cored slab cross-section, grouping of strands

- Longitudinal rust stains indicate loss of the group of strands in the bottom layer above them (3 or 5 strands). Transverse rust stains (stirrups) do not seem to indicate corrosion that significantly affects the strength of the slab.
- For patches that have become delaminated, if there is indication that the patching initially was to bottom layer of strands then assume strands are lost. (Discretion must be used, but depth of patch may be able to be determined from older bridge inspection records if available, or consider any continuous patch extending across more than 2 stirrups.)
- Ideally, remove delaminated concrete and photograph and document corrosion prior to repair work. If that is not possible, only show concern for delaminated regions that are sagging from slab or accompanied by parallel longitudinal cracks.

The implementation of this strategy is as follows:

1. Identify all areas of spalling or delamination in the middle ~75% of the slab
2. For each location, identify depth of spalling and any longitudinal rust stains.
3. Count any region with spalling *to bottom layer of strands* or showing longitudinal rust stains as the loss of that group of bottom-layer strands. If ambiguous, assume half of group is lost.

4. **If slab is patched**, determine depth of deterioration prior to patching.
 - a. If patch depth cannot be determined, assume *to bottom of stirrups* if less than 1 ft long, assume *to bottom layer of strands* if more than 2 ft long. (This is based on observations of the 12 slabs tested, which had stirrup spacing of approximately 1 ft).
 - b. If patch was *to bottom layer of strands* and is now delaminated, assume group of bottom layer strands above it is lost.
5. **If slab is delaminated**, and no pictures can be obtained with delaminated area removed, determine whether delamination is sagging or has parallel longitudinal cracking. Assume any group of bottom strands above either sagging or parallel longitudinal cracking is lost.
6. Based on the above, count how many of the bottom strands are lost. Do not assume any deterioration of higher layers of strands unless spalling or delamination of concrete *beyond bottom layer of strands*.

This strategy is implemented on the 4 slabs that were discussed in Section 5.4.3.1 as follows:

- *Ward Creek – Span 9 – Slab 6*: Two regions of deterioration, at 13 ft and 21-24 ft. Neither show longitudinal rust stains. No spalls appear to be to level of strands. Assume 0 strands lost. Structural analysis predicts $M_n = 622$ kip-ft. Tested strength = 568 kip-ft; analysis over-predicting by 10%.
- *Ward Creek – Span 9 – Slab 7*: One region of deterioration, 16 to 26 ft. Longitudinal rust stains and clearly spalled to depth of strands in middle group and right group (top in picture), possibly to depth of strands in left group. Assume 9.5 strands lost. Structural

analysis predicts $M_n = 304$ kip-ft. Tested strength = 229 kip-ft; analysis over-predicting by 14%.

- *Oyster Creek – Span 1 – Slab 13*: One region of deterioration, 17 to 25 ft. Longitudinal rust stains in middle group. Clearly to depth of strands on middle group and left group (bottom in picture). Assume 8 strands lost. Structural analysis predicts $M_n = 561$ kip-ft. Tested strength = 483 kip-ft; analysis over-predicting by 10%.
- *Oyster Creek – Span 8 – Slab 12*: One region of deterioration, 16 to 28 ft. No visible longitudinal rust stains. Patch is visibly to bottom layer of strands, and is completely delaminated. Assume 11 strands lost. Structural analysis predicts $M_n = 430$ kip-ft. Tested strength = 465 kip-ft; analysis under-predicting by 5%.

Predicted flexural strengths for all slabs are shown in Table 5.10. This strategy gives predictions within ~10% for 8 of 12 slabs, with an average error of 9%. It is more closely rooted in the observations made in this research project compared to the “Only Visible Corrosion” strategy. It does require additional information about the depth of spalling to be recorded during inspection, or photographs to be taken from an angle or lighting condition that makes such depth apparent.

Table 5.10 - Predicted strength using "Depth of Spall" strategy

	Experimental		Depth of Spall		
	<i>kip-ft</i>	<i>Strands Lost</i>	<i>Strands Lost</i>	<i>kip-ft</i>	<i>% error</i>
Ward Creek - Span 1 - Slab 13	429	6	8	357	-13%
Ward Creek - Span 1 - Slab 14	451	5	0	622	32%
Ward Creek - Span 4 - Slab 5	602	0.5	0	622	4%
Ward Creek - Span 4 - Slab 6	618	0	0	622	1%
Ward Creek - Span 9 - Slab 6	568	1.5	0	622	10%
Ward Creek - Span 9 - Slab 7	229	12	9.5	304	14%
Oyster Creek - Span 1 - Slab 13	483	10	3	561	10%
Oyster Creek - Span 1 - Slab 14	628	6.5	5	692	8%
Oyster Creek - Span 2 - Slab 4	900	0	0	896	-1%
Oyster Creek - Span 2 - Slab 5	899	0	0	896	0%
Oyster Creek - Span 8 - Slab 12	465	10	11	430	-5%
Oyster Creek - Span 8 - Slab 13	746	3.5	5.5	671	-10%
<i>Average:</i>					9%

5.4.3.3 – Prediction Strategy: Two-Stirrup Spall

The final strategy considered is one that, like the minimal “Only Visible Corrosion” strategy, does not require any additional effort on the part of bridge inspectors. It uses the same concept of groups of strands as the “Depth of Spall” strategy and attempts to rely on the same assumptions, but without requiring consistent data about delamination and spall depth. Instead, it uses the length and location of spalls as a predictor of strand deterioration, using the assumption that any continuous spall that extends across more than 2 stirrups and contains a rust stain has total loss of the group of bottom strands above it. Shallow spalls of the type present in Figure 5.38 can be ignored, but only if they have been described and photographed in a way that makes this readily apparent, otherwise they are interpreted as any other spall. Patches are assumed to be unrelated to strength unless rust stains bleed through.

The implementation of this strategy is as follows:

1. Identify all spalls or patches in the middle ~75% of the slab
2. Count any spall that extends more than 2 ft and contain rust stains as loss of the group of bottom layer strands underneath the spalled area.
3. *If slab is patched*, treat as if it was not patched, with the same requirements for length and rust stains. If the patch extends across the full width of the slab (such that the slab edges have spalled off) or if a single patching surface extends across multiple slabs, assume all bottom strands are lost.
4. *If delamination has been noted*, consider any group of bottom strands under noted delamination as lost.
5. Using above, count to determine how many of the bottom strands are lost. Do not assume any deterioration of higher layers of strands unless there is visible spalling or delamination beyond the bottom layer of strands.

This strategy is implemented on the 4 slabs that were discussed in Section 5.4.3.1 as follows:

- *Ward Creek – Span 9 – Slab 6*: Two regions of deterioration, at 13 ft and 21-24 ft. Spall at 13 ft stretches across two stirrups with faint rust stain, and covers the middle and left group of bottom strands. Assume 8 strands lost. Structural analysis predicts $M_n = 357$ kip-ft. Tested strength = 568 kip-ft; analysis under-predicting by 40%.
- *Ward Creek – Span 9 – Slab 7*: One region of deterioration, 16 to 26 ft. Spall with rust stains and patching across almost entire width of slab, extending across multiple stirrups.

Assume 11 strands lost. Structural analysis predicts $M_n = 250$ kip-ft. Tested strength = 229 kip-ft; analysis over-predicting by 4%.

- *Oyster Creek – Span 1 – Slab 13*: One region of deterioration, 17 to 25 ft. Spall extends across multiple stirrups, near full width of slab. Assume 11 strands lost. Structural analysis predicts $M_n = 430$ kip-ft. Tested strength = 483 kip-ft; analysis under-predicting by 7%.
- *Oyster Creek – Span 8 – Slab 12*: One region of deterioration, 16 to 28 ft. Icolastic patch across full width of slab, with faintly visible rust stains. Assume 11 strands lost. Structural analysis predicts $M_n = 430$ kip-ft. Tested strength = 465 kip-ft; analysis under-predicting by 5%.

Predicted flexural strengths for all slabs are shown in Table 5.11. Six of 12 predictions fall within 10%, but error is significantly higher in other cases, with deterioration being missed for Ward Creek – Span 1 – Slab 13 due to difficulty in identifying delamination using only photographs, and the assumption of full strand loss yielding conservative estimates for other slabs.

Table 5.11 - Predicted strength using “Two-Stirrup Spall” strategy

	Experimental		Two-Stirrup Spall		
	<i>kip-ft</i>	<i>Strands Lost</i>	<i>Strands Lost</i>	<i>kip-ft</i>	<i>% error</i>
Ward Creek - Span 1 - Slab 13	429	6	0	622	36%
Ward Creek - Span 1 - Slab 14	451	5	0	622	32%
Ward Creek - Span 4 - Slab 5	602	0.5	0	622	4%
Ward Creek - Span 4 - Slab 6	618	0	0	622	1%
Ward Creek - Span 9 - Slab 6	568	1.5	8	357	-40%
Ward Creek - Span 9 - Slab 7	229	12	11	250	4%
Oyster Creek - Span 1 - Slab 13	483	10	11	430	-7%
Oyster Creek - Span 1 - Slab 14	628	6.5	11	430	-26%
Oyster Creek - Span 2 - Slab 4	900	0	8	561	-44%
Oyster Creek - Span 2 - Slab 5	899	0	0	896	0%
Oyster Creek - Span 8 - Slab 12	465	10	11	430	-5%
Oyster Creek - Span 8 - Slab 13	746	3.5	8	561	-24%

Average: 19%

5.4.4 – Discussion of Analysis Strategies

Analysis strategies were compared using average error, but over-prediction of slab capacity is taken as unconservative and undesirable for load rating. The “Only Visible Corrosion” strategy over-predicts available moment capacity by 15% (of maximum applied moment) or more for 7 of 12 slabs, while the “Depth of Spall” strategy does this once, and “Two-Stirrup Spall” does it twice. Significant under-prediction of the type seen in 4 of 12 slabs for the “Two-Stirrup Spall” strategy should also be avoided. Though there are many ways to interpret the visual condition of slabs and therefore many analysis strategies that could be considered, the “Only Visible Corrosion” and “Two-Stirrup Spall” strategies are felt to be reasonable bounds for the type of assumptions that should be made.

All three strategies predicted Ward Creek – Span 1 – Slab 14 (Figure 5.44) poorly, with over-predictions of 29% to 32%. This slab presented a more subtle hybrid of deterioration types, with pronounced, dark rust stains under what appeared to be shallow spalls, surrounded by 7 ft of audible delamination that was observed in the field to stretch across more than 50% of the width of the slab, but did not appear particularly deep or visibly significant from casual observation.

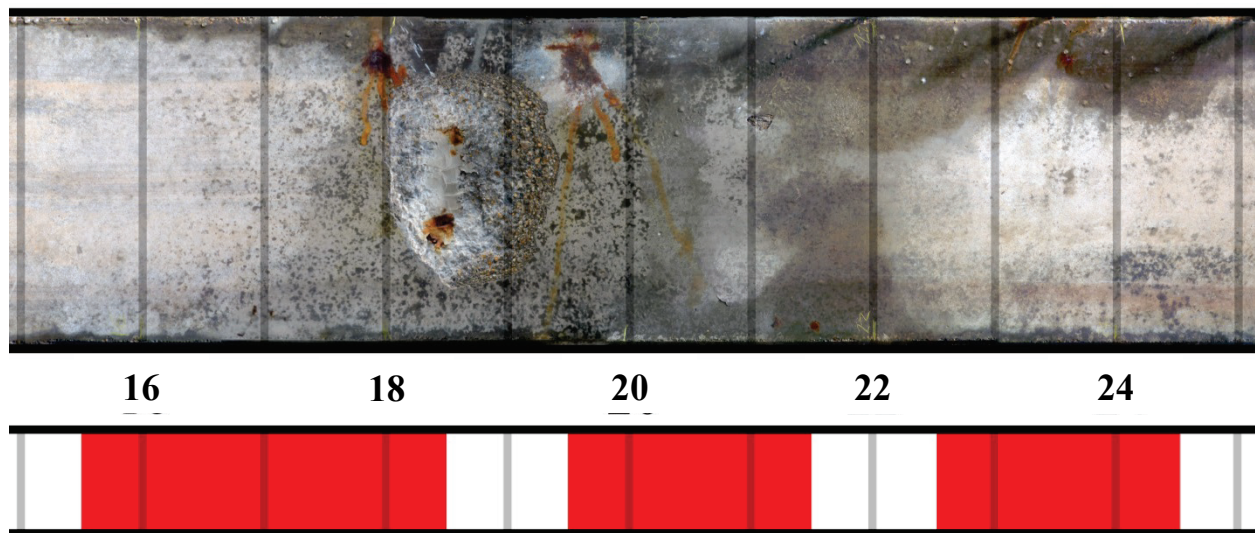


Figure 5.44 - Deteriorated region, Ward Creek - Span 1 - Slab 14

The critical region at failure appeared to be near 18 ft, in the vicinity of the patched spall. More accurate analysis of slabs with conditions such as this is likely only possible with concerted efforts to remove delaminated concrete and document corrosion in the field.

An added benefit of the “Depth of Spall” method is its relationship to typical considerations of a load-rating engineer. A substantial challenge inherent in the NCDOT bridge inspection process is the mostly one-way communication between bridge inspectors and load rating personnel, with little time available for engineers to look at individual slabs in the field. The “Depth of Spall”

method, by asking for consideration of the exposure of strands, works to bring the consideration of deterioration made in the field closer to that made by load-rating engineers in the office.

All strategies discussed included a limited focus on deterioration occurring in approximately the middle 75% of the span. This research was inherently focused on flexural capacity, and limited to the types of deterioration observed on Ward Creek and Oyster Creek Bridge, where the primary splash zones were near midspan. If other bridges display substantially different patterns of deterioration, they should be analyzed for the moment capacity that can be developed in the slab at each location.

As discussed in Section 5.3, strength predictions made using assumed material properties may give estimates of available moment capacity 5 to 20% lower than those discussed in this section, depending on the analysis procedure and assumptions used.

5.5 – Observations Not Found to Affect Strength

A number of indications of possible deterioration were found not to have any significant observed effect in the laboratory. Resistivity and Half-Cell Potential have been extensively discussed earlier in this chapter. Other observations are discussed here.

5.5.1 – Red marks on slab soffit

Light reddish longitudinal stains of the type visible in Figure 5.45 were observed on a number of slabs, and were considered as a possible indication of rust. No such relationship was observed, and the marks are potentially staining of concrete from the formwork during casting.

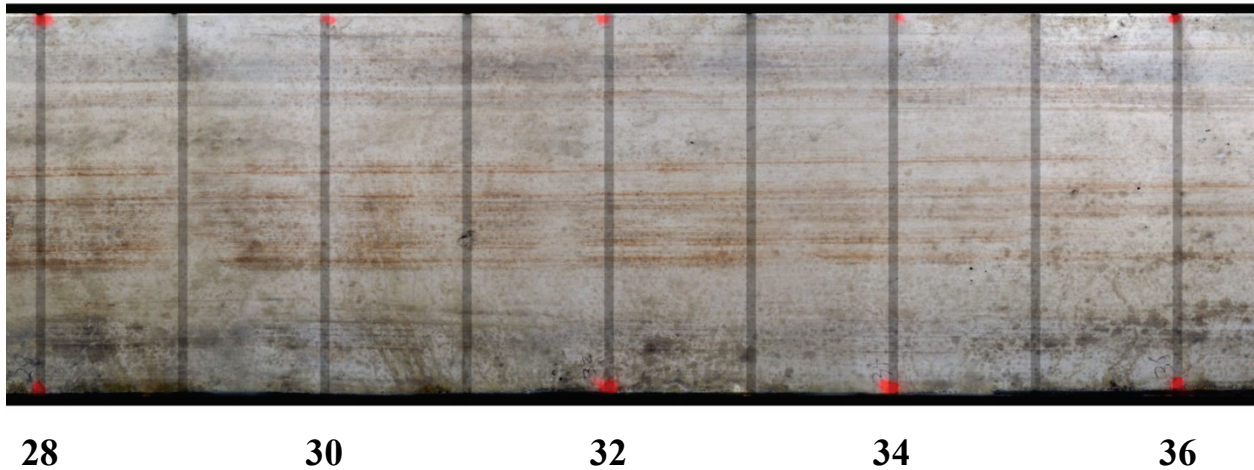


Figure 5.45 - Parallel red marks, Oyster Creek - Span 1 - Slab 13

5.5.2 – Cracking of Slab Ends

Map-pattern cracking was observed on a number of slab ends similar to that visible in Figure 5.46. Some of these slab ends were damaged in the process of slab removal and transportation to the CFL, with some small reduction in bearing area. Despite apparent deterioration and reduction of the concrete bearing area, end regions did not control in any laboratory testing.



Figure 5.46 - Map-pattern cracking and minor spall at slab end, Oyster Creek - Span 1 - Slab 14

5.5.3 – Shear Capacity

The scope of the testing and analysis done within this research did not include examination of shear capacity. However in the course of field and laboratory testing, two types of deterioration were observed that could be construed as affecting shear strength of the beams. These are map-pattern cracking observed near beam ends, as seen in Figure 5.46 in Section 5.5.2, and heavy rusting and total section loss of the bottom of hoop stirrups in the beams, as seen in Figure 5.47. These are mentioned here to note that no damage was observed in testing or transportation that appeared related to shear.



Figure 5.47 – Total section loss of bottom of stirrup, Oyster Creek – Span 8 – Slab 14

5.5.4 – Relationships from Literature Review

Hartle's report on AASHTO Box Beams for the Pennsylvania DOT (2008) found that longitudinal cracks on box beam soffits were generally directly underneath strands and propagated into the void sections. Longitudinal cracking in cored slabs did not display this behavior, with cracking more often indicating either the initiation or advancement of delamination. No cracks or spalling of concrete were observed to propagate into the cores.

Loss of camber is frequently considered as a potential indication of corrosion of steel (Aktan, 2009) and (Hartle, 2008). Due to the grouted shear keys and transverse post-tensioning, this is not observable in the field. As discussed in Section 5.3, slabs tested in the laboratory generally

displayed results directly counter to this concept, with initial slab camber and stiffness not as affected by corrosion as ultimate moment capacity.

Conclusions and comprehensive recommendations derived from the analysis contained in this chapter and all components of the research project are contained in the following chapters.

CHAPTER 6 – FINDINGS AND CONCLUSIONS

Two clear conclusions can be drawn from the data and analysis undertaken: First, visual inspection and sounding may be used to estimate the number of strands lost due to corrosion, which may then be implemented in an appropriate sectional analysis of the cored slab to predict the remaining flexural capacity. Second, concrete resistivity and half-cell potential testing, though at times presenting interesting agreement with visual observations, do not appear to add significant value over visual inspection alone and are not recommended at this time for the evaluation of cored slabs. A summary of other conclusions and results from this research follows.

6.1 – Flexural Capacity of Slabs

Twelve prestressed cored slabs from Ward Creek and Oyster Creek Bridge were delivered to the CFL for flexural testing to failure. Ward Creek Bridge used 40 ft long slabs that were 17 in. deep. Predicted flexural capacity for an undamaged slab was 617 kip-ft, and in experimental testing slabs ranged in strength from 618 kip-ft (full strength) to 229 kip-ft. Oyster Creek Bridge used 45 ft long slabs that were 20 in. deep, with a predicted flexural capacity of 853 kip-ft. In experimental testing strengths varied from 900 kip-ft (full strength) to 465 kip-ft.

The typical deterioration observed in intermediate (not end-span) slabs was a series of spalls and delaminations extending to the bottom of stirrups as well as surface rust staining indicative of stirrups rusting. A large number of such spalls are visible in the photograph in Figure 6.1. In the absence of other information, this type of damage did not correlate to structural performance.

That is, strands in such slabs were structurally in a good condition. A total of two slabs with this type of deterioration were tested and their flexural capacities were within 3% of slabs that did not show any visible deterioration and were located adjacent to these deteriorated slabs.

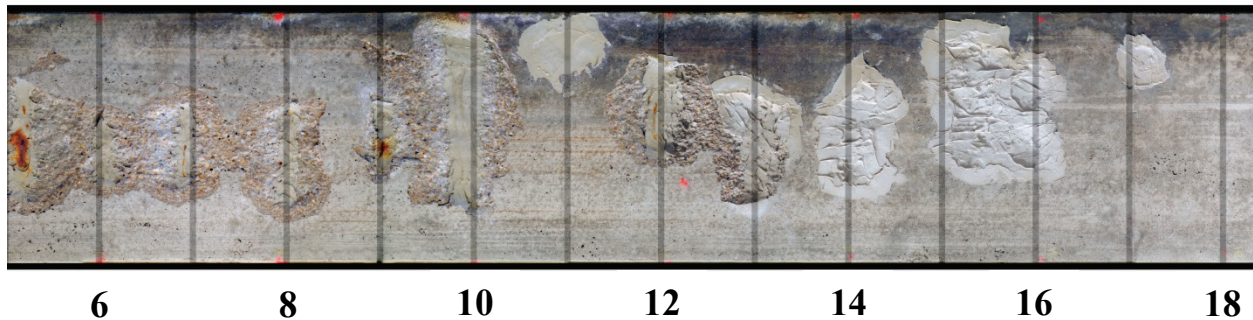


Figure 6.1 - Typical intermediate span spalling, Oyster Creek - Span 2 - Slab 4

It should be noted that extensive corrosion does not necessarily result in spalling. In this research, the only reliable method to determine the extent of corrosion was to remove the delaminated concrete cover. Delaminated regions are detectable by hammer tapping.

In all slabs, corrosion of prestressing strands was only observed in regions with visible spalling or audible delamination. The corrosion of prestressing strands was also generally accompanied by visible longitudinal rust stains. A method to interpret the visual condition of the slabs based on incorporating information from the depth of spalling was developed. This method provides an estimate of slab strengths within 15% of experimental results for 11 of 12 slabs. This method is discussed in the following “Recommendations” chapter.

6.2 – Shear Capacity of Slabs

Shear capacity of cored slabs was not within the scope of this research. However, during flexural testing no slabs failed in shear. Further, there was no indication based on test results that shear would control the capacity of the cored slabs despite several instances of total loss of the bottom of the closed hoop stirrups.

6.3 – Load Rating of Slabs

Structural analysis using layered sectional analysis accurately predicts the flexural strength of slabs. A more typical flexural analysis using a stress block for the concrete compression zone, when combined with assumed values of 5000 psi compressive strength of concrete and 270 ksi ultimate strength of prestressing strands, will yield conservative estimates of strength.

Generally, calculated moment capacities will benefit from a higher assumed compressive strength of concrete if such an assumption can be justified. Seven concrete cores were taken from seven slabs after laboratory testing and tested in compression, with strengths for 6 of the cylinders ranging from 6400 psi to 7620 psi, and one cylinder with the outlier value of 10460 psi.

CHAPTER 7 – RECOMMENDATIONS

Recommendations in this chapter are divided into two groups: recommendations for load rating, and recommendations for field inspection.

7.1 – Recommendations for Load Rating Procedures

7.1.1 – “Depth of Spall” Strategy

In the process of analyzing slabs, 3 strategies were examined for evaluating the condition of slabs in order to estimate loss of prestressing strands. Among them, the “Depth of Spall” strategy provided a good agreement with experimental results. This strategy is discussed in detail in Section 5.4.3.2 of this report. The Depth of Spall strategy is summarized here as the recommended evaluation procedure for deteriorated cored slabs. This strategy was developed with an appreciation for the limitations inherent in load rating a structural member based on limited pictures and access to information, and it identifies the depth of spalling as a key measurement that would aid in load rating procedures. In this strategy the depth of spall is categorized as “*spall without steel exposed*”, “*spall to bottom of stirrups*”, “*spall to bottom layer of strands*”, or “*spall beyond bottom layer of strands*”. It incorporates various observations made about delaminations, patching materials, and varying rust stains.

During the experimental program and testing, it was observed that strands that were grouped close together tended to deteriorate with a similar rate. In the Depth of Spall method, strands in cored slabs are grouped as seen in Figure 7.1.

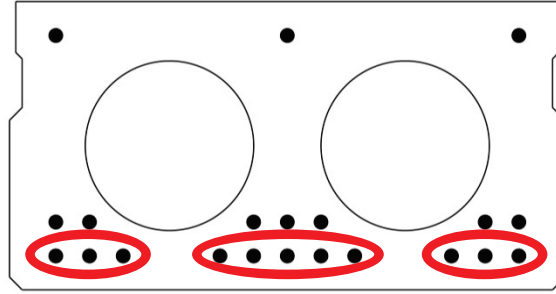


Figure 7.1 - Cored slab cross-section

The “Depth of Spall” evaluation strategy is as follows:

For a given cored slab:

1. Identify all areas of spalling and/or delamination in the central ~75% length of the slab.
2. For each spall location, identify the depth of spalling and any longitudinal rust stains.
3. Count any region with spalling *to bottom layer of strands* and any region with longitudinal rust stains as the loss of that group (see Figure 7.1) of bottom-layer strands.
If ambiguous, assume half of group is lost.
4. **If slab is patched**, determine the depth of deterioration that existed prior to patching.
 - a. If patch depth cannot be determined, assume *to bottom of stirrups* if the patch is less than 1 ft long and assume *to bottom layer of strands* if the patch is more than 2 ft long (this measurement is based on observations of the 12 slabs tested, which had stirrup spacing of approximately 1 ft).
 - b. In the case of a delaminated patch that was *to bottom layer of strands*, assume the group of bottom layer strands above the patch is lost.

5. **If slab is delaminated**, and no pictures can be obtained with delaminated area removed, determine whether delamination is sagging or has parallel longitudinal cracking. Assume any group of bottom strands above either sagging or parallel longitudinal cracking is lost.
6. Based on the above, count how many of the bottom strands are lost. Do not assume any deterioration of higher layers of strands unless there exists spalling or delamination of concrete *beyond bottom layer of strands*.

The “depth of spall” strategy was used to estimate the strength of the 12 tested slabs. Error between estimated strengths and measured strengths ranged from 4 kip-ft to 171 kip-ft. For 11 of 12 slabs, this meant that the estimated reduction in available moment capacity (total moment capacity minus the moment due to slab self-weight, as a percentage of what this value was calculated to be for an undamaged slab) was within 15%. One slab was poorly predicted, with an estimated reduction in available moment capacity over-predicted by 32%. This slab contained a delaminated region that was not removed and examined prior to testing, underlining the importance of removing delaminated concrete if a slab is felt to be critical for load rating.

7.1.2 – Additional Load Rating Recommendations

Analysis: Structural analysis performed in this research using a stress block approach, with assumed concrete strength of 5000 psi under-predicted the applied moment for undamaged slabs by 20%. For slabs with marginal load ratings using default procedures, more careful examination of analysis can lead to substantial increases in estimated capacity. If coring concrete can be accomplished in a way that does not damage the slab, it should be considered if

it can be used to justify higher slab strength. Due to the variability of field data collected it is not believed that use of a rebound hammer would result in more accurate results.

Patching: Patching materials cover up deterioration, and therefore, deterioration is not clearly visible during the bridge inspection. This means that structurally significant corrosion that was evident prior to patching may no longer be visible. The only reliable method to accurately assess the extent of deterioration is to study the older inspection reports. Patching does not contribute to increase in the capacity of a bridge, unless it is accompanied by strengthening efforts.

Additional Considerations: While this research focuses on estimating the flexural capacity of the individual beams, other factors are equally important in the load rating of bridges such as the distribution of wheel-loads among slabs in a span. An extensive discussion of these factors is outside of the scope of this research, however, two recommendations that might be considered concerning load-rating procedures are as follows:

- Asphaltic wearing surface thickness is not necessarily less than 6 inches. The 6 in. limit is initially called for in the 1970s plan sheets for the construction of the bridge, and asphalt measurements at drain-holes should not be substituted for estimates of the thickness of the asphalt under the relevant critical beam. Observed asphalt thickness on the bridges examined was up to 8.5 in. at midspan (twice the 4 in. estimate that would be used if following the inspection report).

- The distribution of load between slabs in a span is a significant factor that may increase the capacity of a bridge above the estimated capacity from the weakest slab in the span. However slabs adjacent to one another on the two bridges tested often had similar deterioration. Overall, the worst deterioration on the two inspected bridges was observed to be caused by splashing water in the end spans. The areas deteriorated by splashing appeared to be more than 10 ft across, and when that is combined with the 2.75 ft width of slabs, it means multiple adjacent slabs deteriorated similarly. As a result, any consideration of an increase in bridge strength due to distribution of load needs to be evaluated on a span-by-span and slab-by-slab basis.

7.2 – Recommendations for Field Inspection

Based on the field inspection carried out during this research, along with a review of bridge inspection records for the two bridges tested, a number of recommendations are made here for consideration in bridge inspection:

- For structural evaluation purposes, there is no need to record precise sizes of spalls.
- Depth of spalling, on the other hand, is found to be important in this research and has not been recorded uniformly. Depth is frequently difficult to measure in the field using available tools, and instead estimates of spalling are qualitative and should be noted as spalls “*without steel exposed*”, “*to bottom of stirrups*”, “*to bottom layer of strands*”, and “*beyond bottom layer of strands.*” These qualitative depth measurements are useful for load rating purposes.

- In this research, it was observed that the only reliable method to determine the condition of steel above delaminated concrete was to remove the delamination. Delaminated concrete and patching material appear to at times contribute to the corrosion of steel by trapping moisture even as they shield from it. Delaminations should be removed and the underlying condition of the slab documented, assuming exposed steel can be protected promptly.
- Asphaltic wearing surface thickness needs to be estimated at the crown of the roadway. Values recorded at drain holes can substantially underestimate asphalt dead load on a bridge.
- Comparative language is useful in tracking the deterioration and condition of the slabs over time. Attempts should be made to determine whether the condition of a slab is worse than, better than, or different from its condition two years earlier, and deterioration should be noted in a way that makes it possible to make such comparisons in the future. An example of such a statement could be “shallow spall beneath stirrups appears unchanged since 2009.”
- If information about repair methods and procedures is available, the recording of that information would be useful in understanding whether the repair warrants reanalyzing the load rating, and understanding the condition of steel behind the repair.

CITED REFERENCES

- Aktan, H. A. (2009). *Condition Assessment and Methods of Abatement of Prestressed Concrete Box-Beam Deterioration*. Michigan DOT Report, Western Michigan University, Michigan Technological University.
- American Concrete Institute. (2014). *ACI 318*. Farmington Hills, MI: American Concrete Institute.
- ASTM C876. (2009). *Standard Test Method for Corrosion Potentials of Uncoated Reinforcing Steel in Concrete*. West Conshohocken, PA: ASTM International.
- ASTM Standard C42. (2013). *Standard Test Method for Obtaining and Testing Drilled Cores and Sawed Beams of Concrete*. West Conshohocken, PA.
- Attanayake, U., & Aktan, H. (2011, July/August). Capacity Evaluation of a Severely Distressed and Deteriorated 50-Year-Old Box Beam with Limited Data. *Journal of Performance of Constructed Facilities*, 299-308.
- Babaei, K. (1986). *Evaluation of Half-Cell Corrosion Detection Test for Concrete Bridge Decks*. University of Washington. Seattle: Washington State Transportation Center. Retrieved 2015
- Bramblett, R. (2000). *Flexural Strengthening of Reinforced Concrete Beams Using Carbon Fiber Reinforced Composites*. Austin, TX: The University of Texas at Austin.
- Clemeña, G. G. (1992). *Benefits of Measuring Half-Cell Potentials and Rebar Corrosion Rates in Condition Surveys of Concrete Bridge Decks*. Richmond, VA: Virginia Department of Transportation.

- Collins, M. a. (1991). *Prestressed Concrete Structures*. Englewood Cliffs, New Jersey: Prentice Hall.
- Frølund, T. (2003). Pro's and Con's of Half-Cell Potentials and Corrosion Rate Measurements. *Structural Faults + Repairs International Conference*. London, U.K.
- Giatec Scientific. (2015, August 1). *Giatec XCell*. Retrieved from Giatec Scientific:
<http://www.giatecscientific.com/product/giatec-cell/english-cell/>
- Hartle, R. (2008, July). I-70 Overpass Beam Failure: Lakeview Drive Bridge. Pennsylvania.
- Hognestad, E. (1951, November). A Study of Combined Bending and Axial Load in Reinforced Concrete Members. *Bulletin 399, University of Illionis Engineering Experiment Station*.
- Kessler, e. a. (2008). Surface Resistivity as an indicator of Concrete Chloride Penetration Resistance. *CBC*.
- Liu, Y. S.-M. (2010). *Characterization of New and Old Concrete Structures Using Surface Resistivity Measurements*. Tallahassee, FL: Florida Department of Transportation.
- Morales, M. (2015). *Experimental Investigation of the Effects of Embedded Rebar, Cracks, Chloride Ingress and Corrosion on Electrical Resistivity Measurements of Reinforced Concrete*. Oregon State University.
- Muller, D., & Malik, Z. (2015, March 30). Meeting Concerning Deteriorated Cored Slabs Research Project. (Z. Van Brunt, Interviewer) Raleigh, North Carolina.
- Naito, C., Sause, R., Hodgson, I., Pessiki, S., & and Macioce, T. (2010, July/August). Forensic Examination of a Noncomposite Adjacent Precast Prestressed Concrete Box Beam Bridge. *Journal of Bridge Engineering*, 408-418.

- Nakamura, E. e. (2008). Half-Cell Potential Measurements to Assess Corrosion Risk of Reinforcement Steels in a PC Bridge. *Site Assessment of Concrete, Masonry, and Timber*. Como Lake, Italy.
- NCDOT. (2012, October 12). Temporary Bridge in Place on Harkers Island; Weight limit increased to 25 tons. Raleigh, North Carolina. Retrieved from <https://apps.ncdot.gov/newsreleases/details.aspx?r=7146>
- NCDOT. (2013, March 7). *Cored Slab and Box Beam Bridges*. Retrieved from 2013 Construction Training Webinars: <https://connect.ncdot.gov/projects/construction/Structural%20Design%20AGCDOT%20Joint%20Bridge%20Design%20Commi/2013%20Structures%20Webinar%20Structure%20Inspector%20Training.pdf>
- Papè, T. &. (2009). Comparisons Between Two Corrosion Assessment Methods and the Corrosion of Steel in Prestressed Concrete. *Corrosion & Prevention*. Coffs Harbour, Australia.
- Poursaei, A. (2011, May). Corrosion Measurement Techniques in Steel Reinforced Concrete. *Journal of ASTM International*, 8(5).
- Prestressed Concrete Institute. (2010). *PCI Design Handbook, 7th Edition*. Chicago.
- Proceq SA. (2013). *Resipod Family - Operating Instructions*. Retrieved from Proceq SA Website: www.proceq.com
- Ramberg, W. &. (1943). *Description of Stress-Strain Curve by Three Parameters*. Washington, D.C.: National Advisory Committee on Aeronautics.

Rupnow, T. &. (2011). *Evaluation of Surface Resistivity Measurements as an Alternative to the Rapid Chloride Permeability Test for Quality Assurance and Acceptance*. Baton Rouge, LA: Louisiana Transportation Research Center.

Sobanjo, J. M.-R. (2010, November/December). Reliability-Based Modeling of Bridge Deterioration Hazards. *ASCE Journal of Bridge Engineering*, 671-683.

Wikipedia. (2015, August). *Circular segment*. Retrieved from Wikipedia:
https://en.wikipedia.org/wiki/Circular_segment

APPENDICES

Appendix A – Inspection Report Slab Conditions

Inspection Reports discussed in Chapter 2 contained descriptions and photographs of the deterioration of slabs at that time. As a reference for the condition of these slabs as recorded in the field, these are presented here in 4 tables. Slabs in Ward Creek Bridge are described in the first 2 tables, Table A-1 and Table A-2, containing slab descriptions and photographs, respectively. Descriptions and photographs for Oyster Creek Bridge are in Table A-3 and Table A-4. Tables include most, but not all, descriptions of deterioration on slabs. At times deterioration was described for a number of slabs in roughly the same way, in which case efforts have been made to condense the descriptions into one idea, and summarize the extent of deterioration. Photographs selected were those that best showed deterioration for a given year, or photographs that showed slab soffits at all when photographs of deterioration were not taken.

Table A-1 - Ward Creek Bridge slab conditions, 1997-2013

Ward Creek (150035)				
Inspection Year	Superstructure Rating	Descriptions		
		Span 1	Intermediate Spans	Span 9
1997	6	Slabs 2 & 3 are "Spalled and Delaminated"	-	Slabs 7,8,13, & 14 are "Delaminated and/or spalled with rusty exposed steel"
1999	5	Same as previous	-	Same as previous
2001	6	Same as previous	-	Same as previous
2003	6	"Slabs 2 and 3 were spalled and delaminated but are now repaired"	Span 7, Slab 13 has "minor spall"	"Slabs 3, 7, 8, 9, 12, 13, 14, & 15 were delaminated and/or spalled w/ rusting rebars exposed but are also repaired"
2005	6	"Spalled and delaminated area 38" x 28" & up to 0.5" deep in Slab 4" "Spalled area 18" diameter with 8" of exposed rebar in Slab 2"	Span 6, Beams 11 & 14 have delaminated areas	"Slabs 6 & 7 are delaminated"
2007	5	Slab 2 has "a spalled area 18" dia. With 8 in. of exposed rebar" Slab 4 has "A spalled and delaminated area 36" long x 28" wide x up to 0.5" deep"	Span 2, Slabs 7, 11, 13, & 14 have "delaminated areas"	Slab 6 is "cracked and delaminated"
2009	5	"Graded (5)" Slabs 2, 4, 8, 9, 10 note rust stains; Slabs 14, & 15 noted spalls and cracks.	"Graded (5)" Cracks and spalls noted on various slabs in Spans 2, 4, 6, 7, & 8	Slabs 7,8, & 9 "Graded (4)" & "@ Midspan with patches releasing rust stains & corrosion on the steel @ the edges where visible"
2011	4	Slabs 2-4 have rust stains @ previously patched areas; Slabs 8-10 have delam. and rust stains under previous patches	PMs issued for Span 2 Slabs 11 & 14 for spalls w/ exposed steel. Delams noted on 16 slabs overall in Spans 2 - 8.	"Slabs 7 - 9 have new patch material with moderate rust bleed through per previous prompt action last cycle" "Slabs 12 - 15 have large patched areas near midspan w/ some rust bleed through"
2013	4	PMs issued for slabs 2-4, 7-10, 13-15 for various described delamination & deterioration	Extensive notes on patching, PM issued for Span 5, Slab 4 for delam. w/ rust stains	PMs issued for slabs 2, 6-9, 12-15 for various described delamination & deterioration

Table A-2 – Ward Creek Bridge: Select Photos from Inspection Reports - 1997 to 2013

1997



1999



SIMILAR SPALLS AT SLABS, SP 9

2001



2003



REPAIRS @ SLABS 2&3, SPAN 1



REPAIRS @ SLABS 9&10, SPAN 1



REPAIRS IN SLABS 13 - 15 @ SPAN 9

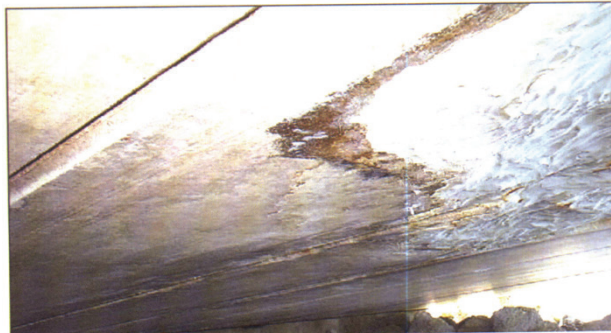


REPAIRS IN SLABS 7&8 @ SPAN 9

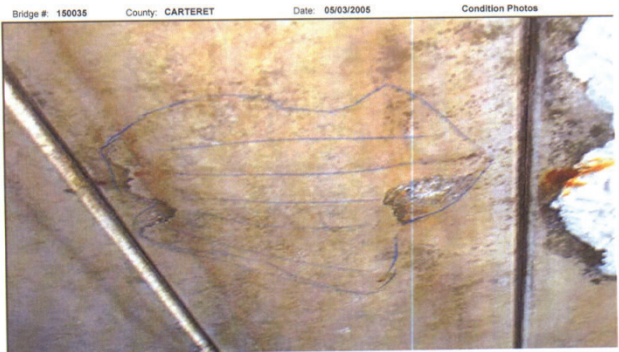
2005



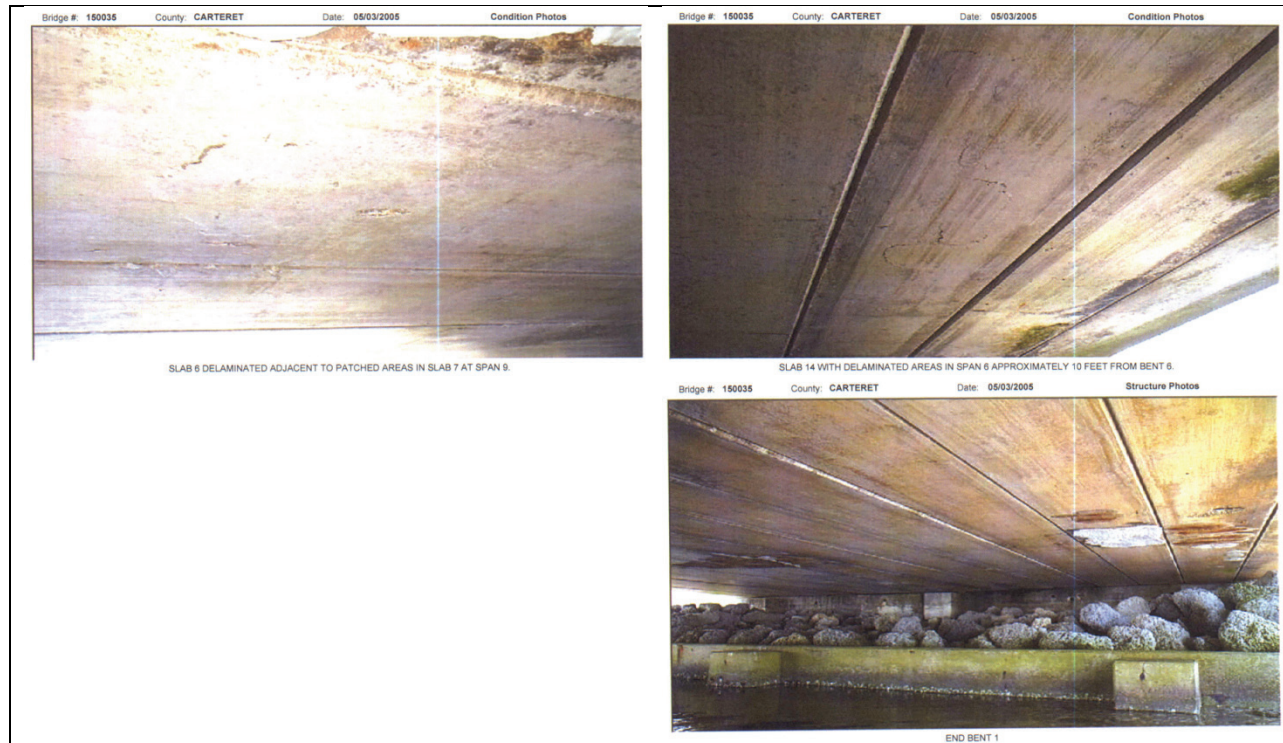
SPALLED AND DELAMINATED AREA 16 INCH DIA. WITH 8 INCHES OF EXPOSED REBAR IN SLAB 2 AT SPAN 1.



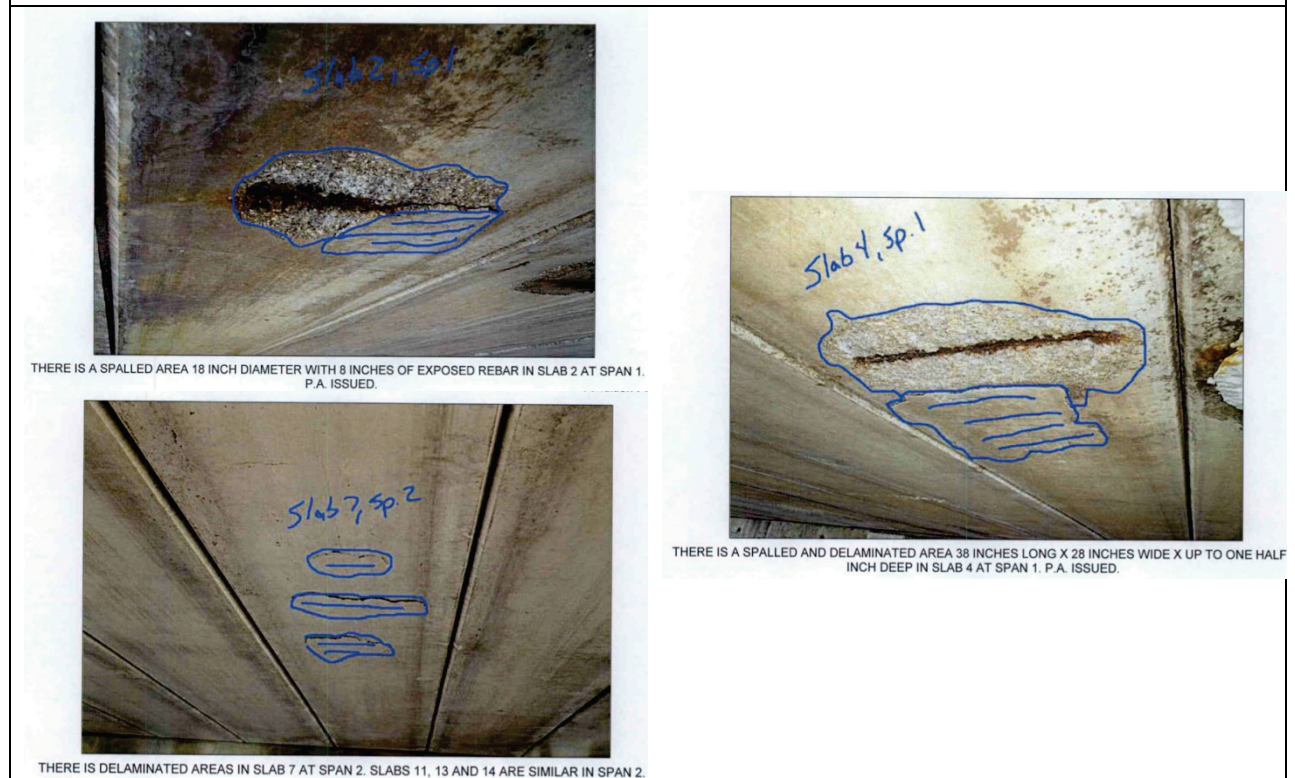
SLAB 7 DELAMINATED AT THE EAST END OF PATCHED AREA IN SPAN 9.

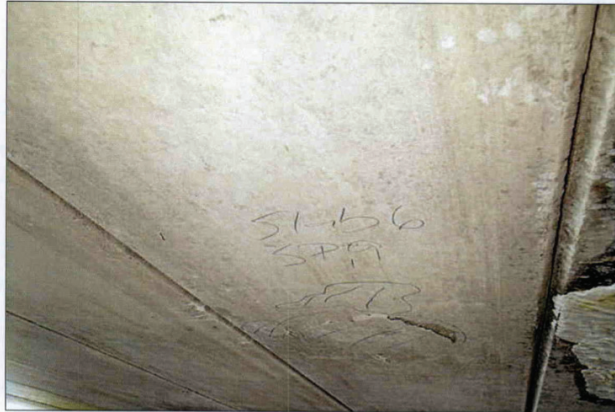


SPALLED AND DELAMINATED AREA 38 INCHES LONG X 28 INCHES WIDE X UP TO ONE HALF INCH DEEP IN SLAB 4 AT SPAN 1.



2007





SLAB 6 IS CRACKED AND DELAMINATED IN SPAN 9.



END BENT 2

2009



SLABS 12- 15 @ MIDSPAN IN SPAN 9 WITH PATCHES & RUST STAINS BLEEDING THRU. SAME AS PHOTO



SLABS 7, 8 & 9 @ MIDSPAN IN SPAN 9 WITH PATCHES RELEASING RUST STAINS & CORROSION ON THE STEEL @ THE EDGES WHERE VISIBLE. (PM ISSUED)



14 IN SPAN 6 WITH SURFACE SPALLS & EXPOSED STEEL WITH COATING APPLIED TO THE SIMILAR AREAS IN SLAB 11, SPAN 6 & SLAB 13, SPAN 7.



7, 8 & 9 @ MIDSPAN IN SPAN 9 WITH PATCHES RELEASING RUST STAINS & CORROSION STEEL @ THE EDGES WHERE VISIBLE. (PM ISSUED)

2011



SLABS 2 THRU 4 IN SPAN 1 HAVE RUST STAINS BLEEDING THRU PREVIOUS PATCHED AREAS ON THE BOTTOM FACE.



SLABS 7 THRU 9 IN SPAN 9 HAVE NEW PATCH MATERIAL WITH MODERATE RUST BLEED THRU PER PREVIOUS PROMPT ACTION LAST CYCLE.



SLABS 8 THRU 10 IN SPAN 1 HAVE DELAMINATION AND RUST STAINS AT PREVIOUS PATCHED AREAS ON THE BOTTOM FACE.

2013



SPAN 8 HAS PREVIOUS PATCH WITH RUST STAINS. THIS REPAIR REPRESENTS THE CATEGORY OF SLABS NOT ITEMIZED FOR PRIORITY MAINTENANCE.







(PM)-SLAB 8 IN SPAN 9

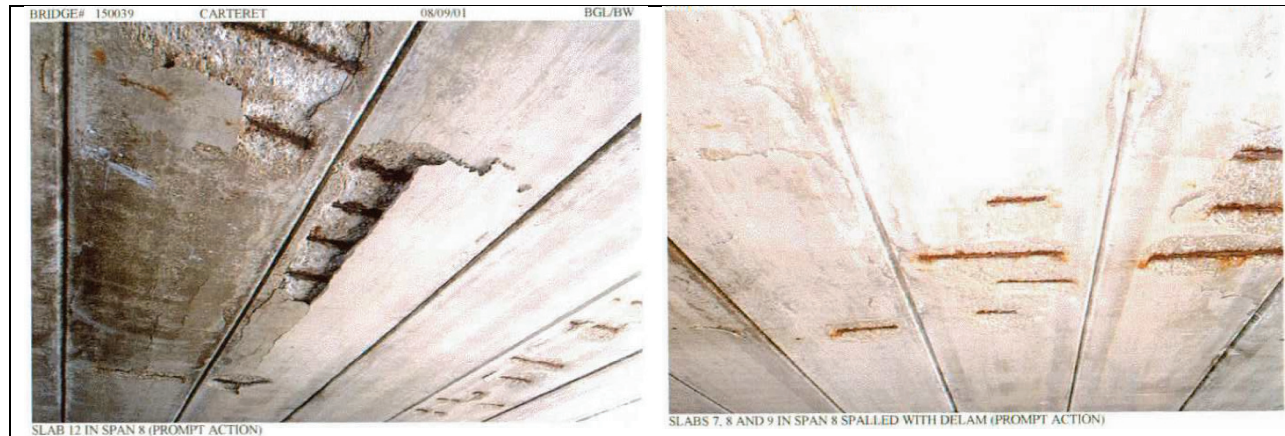


Table A-3 – Oyster Creek Bridge Slab Conditions, 1997 - 2013

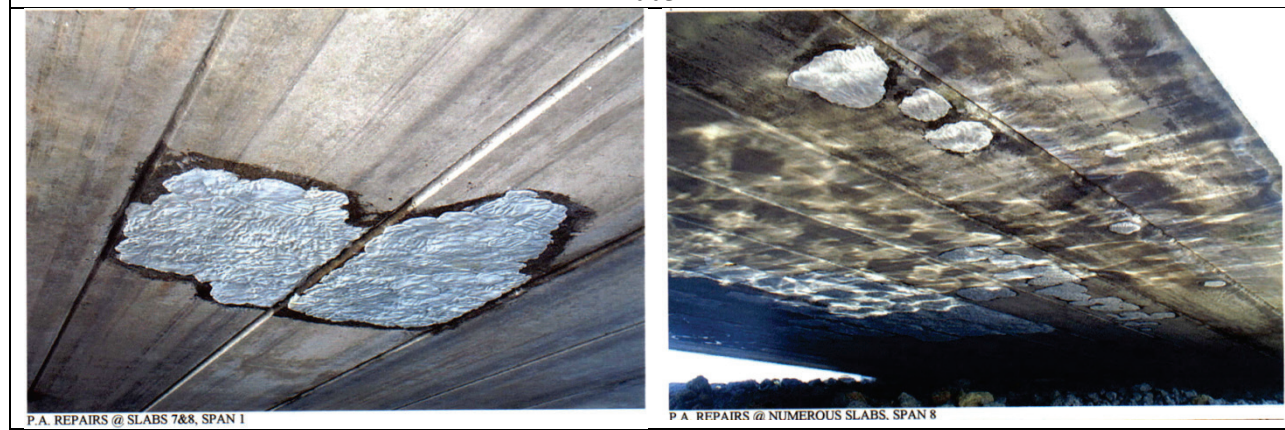
Oyster Creek (150039)				
Inspection Year	Superstructure Rating	Descriptions		
		Span 1	Intermediate Spans	Span 8
1997	6	"Moderate spalling at bottom face of random slabs"		
1999	5	Same as previous		
2001	3	"There are (24) individual cored slabs with moderate to severe spalls with rusty exposed steel showing loss to complete failure of cables. Several have delamination adjacent to spalls. The spalls vary in size from 8" in diameter to 33" wide x 10' long. Most are located at midspan and at 1/3 points along slabs. Slabs still have camber at this time, but exhibit minor to moderate deflection under loads."		
		2, 3, 12, 13, & 14	Span 2: Slabs 2, 3, & 15; Span 5: Slab 3; Span 6: 1,2,4,&15; Span 7: 10	5,6,7,8,9,10,11,12,14,&15
2003	3	"Random minor delamination noted at few slabs"		
2005	6	-	Span 2: "Slabs 11, 12, & 13 are delaminated; two 3" dia. Spalls in Slab 10 (Similar to others)"	"There is a 6" wide x 4" long x 4" high spalled area in Slab 16 over Bent 7"
2007	5	Slabs 3, 4, & 5 have "gunite patches, cracks, delaminated areas, and spalls"	Span 2: Slabs 2, 3, & 4 cracked and delam. and spalls Span 7: Slabs 10 & 11 spalled/delam.	Slab 14 "spalled with exposed steel" Slab 15 has "gunite patch transverse cracked" Slab 16 has "6" x 4" x 4" high spalled area over bent 7"
2009	5	"Patches are ragged with cracks, rust stains throughout. Unable to determine full extent of steel corrosion at these locations."		
		Slabs 3 has "delaminated area and surface spall adjacent to east end of patch to 30" x 6"" Slabs 7 & 8 have "patches with rust stains" & others are similar	"Patches with random delaminated areas in Span 2 cored slabs. Similar at other spans."	Slab 6: Delam. adjacent to patch Slabs 10 - 13 have various delams., rust stains, exposed steel, cracks
2011	5	Slab 4 "is delaminated on bottom face near midspan", Slab 12 "has a large area of delamination adjacent to patch near midspan"	7 slabs in Span 5, 3 in other spans have "surface spall(s) with exposed & untreated steel" In Span 2, "Several surface spalls with the exposed steel being coated since last inspection"	Slabs "have patches, some with rust stains and adjacent delamination"
2013	4	"PM's issued for numerous coured slab units due to failed patches & rust stains bleeding thru. Previously removed icolastic patches revealed stirrups & strands to be in poor condition. Most slabs have an extensive history for patched areas using different materials to cover exposed rust bleed thru." [Followed by itemized PM's for numerous slabs]		

Table A-4 – Oyster Creek Bridge: Select Photos from Inspection Reports - 1997 to 2013

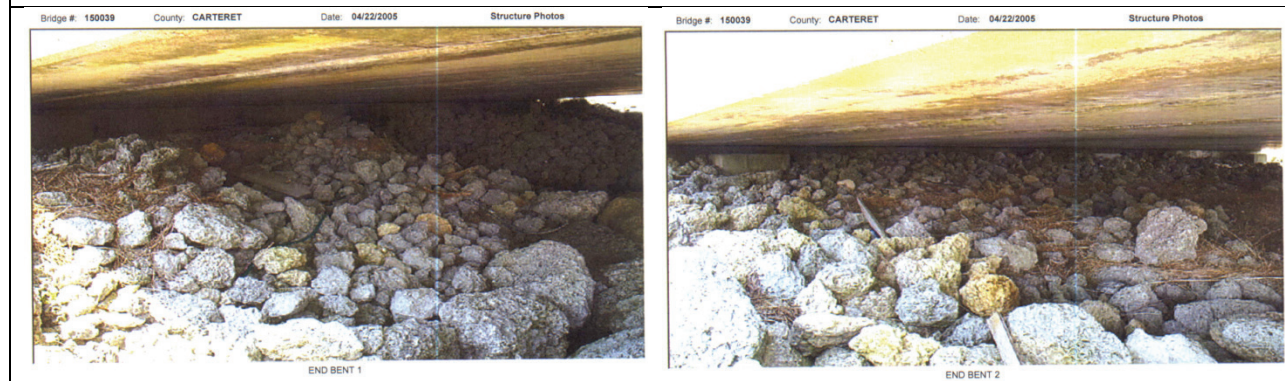
1997	
	
1999	
 <p>SIMILAR SLABS, SP 8</p>	
2001	
 <p>SIMILAR UNDERSIDE (SPAN 8)</p>	<p>BRIDGE# 150039 CARTERET 08/09/01 BGL/BW</p>  <p>SPALLS AT CORED SLABS 12, 13, AND 14 IN SPAN 1 (PROMPT ACTION)</p>



2003



2005





SPAN 2 SIDE OF BENT 2. INTERIOR BENTS 1 3 4 5 6 AND 7 ARE SIMILAR.

2007



GUNIT PATCHES, CRACKS, DELAMINATED AREAS AND SPALLS IN SLABS 3, 4 AND 5 IN SPAN 1.



SLABS 10, 11 AND 12 CRACKED, DELAMINATED AND SPALLED IN SPAN 2.



GUNIT PATCHES IN SPAN 8.



SLAB 14 IS CRACKED, DELAMINATED AND SPALLED WITH EXPOSED STEEL IN SPAN 8.

2009



2011





SPAN 2 HAS SEVERAL SURFACE SPALLS WITH THE EXPOSED STEEL BEING COATED SINCE LAST INSPECTION.



SLABS IN SPAN 8 HAVE PATCHES, SOME WITH RUST STAINS AND ADJACENT DELMINATION.

2013



(PM)-SLAB 13 IN SPAN 1



(PM)-SLAB 7 IN SPAN 5



(PM)-SLAB 6 IN SPAN 8



(PM)-SLAB 14 IN SPAN 8